STUDY REPORT

No. 145 (2005)

Durability of Reinforced Concrete Structures under Marine Exposure in New Zealand

N.P. Lee & D.H. Chisholm

The work reported here was funded by the Building Research Levy and the Foundation for Research, Science and Technology from the Public Good Science Fund

ISSN: 0113-3675

Preface

This report examines the resistance of concrete containing commonly-used SCMs (supplementary cementitious materials) to chloride ingress, based on the results of five years' natural exposure to marine environments of varying severity. The durability design principles for reinforced concrete in these climates fundamentally rely on retarding the rate of chloride-ion migration through the concrete cover, such that the accumulated chloride concentration at the depth of the primary reinforcing will not exceed the threshold required to initiate active corrosion during the intended life of the structure. In this study, particular attention was paid to the contention that concrete made with SCMs demonstrate an improvement in their durability performance over time, distinguished by a measurable reduction in their effective chloride-ion diffusion coefficient. The consequent assumption of a time reduction factor in Fick's Law-derived durability models has a marked affect on the design life calculated for concrete structures, often proving a much more significant control than the degree of chloride resistance measurable in the concrete by early-age testing. It is of some concern that designers, often prompted by SCM suppliers, are willing to take advantage of this phenomenon in their design life calculations, despite a considerable degree of uncertainty remaining about the precise mechanism that drives it. In this study, the magnitude of any temporal improvement in the effective chloride diffusion coefficient, and its associated uncertainty, is determined for the various concrete types investigated and the severity of the chloride load encountered in each environment is tabulated. The potential of simple laboratory tests to serve as early-age durability indices that differentiate the performance of alternative mix designs is also considered.

The aim of the research was to give designers of reinforced concrete structures the confidence to make robust durability predictions, and particularly to validate their inputs to the computerised service-life prediction models that are gaining increased currency for this purpose. The knowledge generated by the programme was also employed to develop the prescriptive durability solutions for 50 and 100 year specified lives in the 2005 revision of NZS 3101 *Concrete structures*.

Acknowledgements

The laboratory and site investigation work reported here was funded by the Building Research Levy and the Foundation for Research, Science and Technology from the Public Good Science Fund. The review of service life prediction models was originally commissioned by Standards New Zealand; their permission to reproduce this material is gratefully acknowledged.

Note

The findings of this research are primarily intended for designers and specifiers of reinforced concrete structures exposed to marine environments. Ready-mix concrete producers, specialist cement suppliers and concrete technologists may also find it of interest.

DURABILITY OF REINFORCED CONCRETE STRUCTURES UNDER MARINE EXPOSURE IN NEW ZEALAND

BRANZ Study Report SR 145 **N.P. Lee & D.H. Chisholm**

REFERENCE

Lee N.P. & Chisholm D.H. (2005). *Durability of Reinforced Concrete Structures under Marine Exposure in New Zealand*. Study Report SR 145, BRANZ Ltd, Judgeford, New Zealand.

ABSTRACT

Large concrete blocks, made with either GP Portland cement or a cement blend incorporating either Duracem blast-furnace slag cement, Microsilica 600 amorphous natural silica, or Micropoz silica fume, were placed on three marine exposure sites of varying severity. The sites equate to the C, B2 and B1 exposure classification categories given in NZS 3101 *Concrete structures*. At periodic intervals over five years, the chloride ingress profile for each combination of cement type and exposure severity was measured. This data was used to calculate notional surface chloride concentrations and effective diffusion coefficients to characterise the performance of each concrete. Particular attention was paid to testing the hypothesis of a temporal dependence in the diffusion coefficient. Actual chloride-ion diffusion coefficients were also determined on virgin concrete from the interior of the blocks to verify whether any observed improvement in resistance to chloride penetration could be attributed to an intrinsic reduction in the pore connectivity within the cement matrix. The applicability of laboratory tests as simple durability indices was also examined.

Keywords: marine concrete, durability, NZS 3101, chloride ions, Fick's law, service-life prediction, models, diffusion coefficients, surface chloride concentration, sorptivity, rapid migration test, rapid chloride test.

Contents

Page

Figures

Page

Tables

1. INTRODUCTION

1.1 Background

Concrete reinforced with carbon steel is widely used for structures in, or in close proximity to, marine environments. Under normal conditions the natural alkalinity of the cement paste generates a tightly-adhering γ-Fe_2O_3 oxide film around that steel, which provides the reinforcing with protection for as long as it remains intact. However, where chloride-ions penetrate the cover concrete to the depth of the reinforcing in sufficient concentration, this passivating layer is destroyed and corrosion is able to occur in the presence of water and oxygen. Chloride-ions have been described as 'a unique and specific destroyer'[1] of reinforced concrete and are undoubtedly the most significant general durability threat to structural concrete in New Zealand.

The impact of chloride-induced corrosion can be described by the familiar initiation-propagation model proposed by Tuutti[2]. In the initiation phase, chloride-ions penetrate the concrete towards the reinforcement with a sufficient accumulation at the depth of the reinforcement ultimately facilitating corrosion. During the propagation phase, active steel corrosion takes place and the dilative pressure generated by the relatively more voluminous corrosion cracks then spalls the cover concrete. In combination with the loss of section from the steel reinforcement, this damage has the potential to seriously compromise the serviceability and, eventually, the structural integrity of the structure.

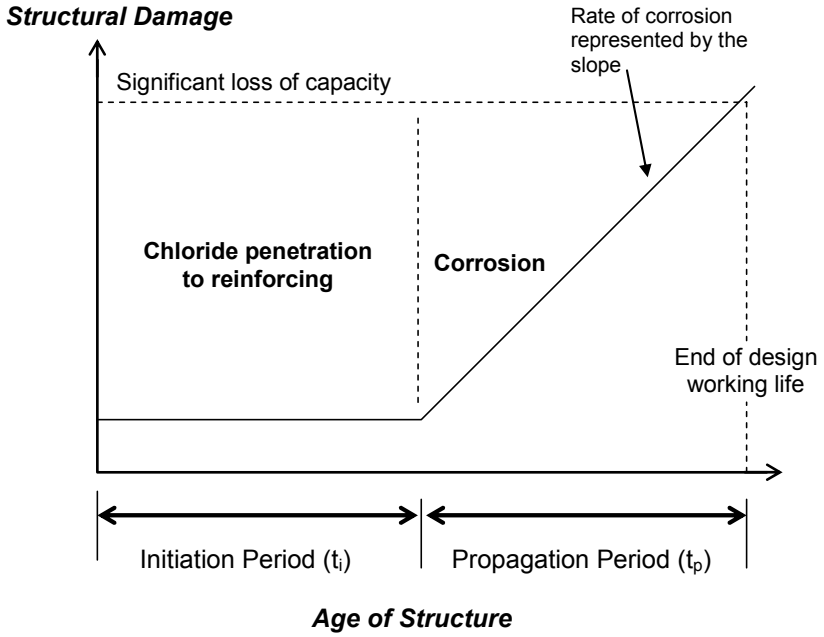

Figure 1: Tuutti's initiation – propagation model

In the design of structures to meet the B2 durability requirements of the NZ Building Code,[3] it is considered that only routine maintenance should be required during the life of the structure. Incidences of cracking or spalling induced by corrosion are presumed unacceptable during the design life unless otherwise specified. In order to provide a sufficient safety margin to guarantee this level of performance, service-life design should be based on the initiation phase alone, i.e.

the time for a critical concentration of chloride-ions (the 'corrosion threshold') to be established at the depth of the primary outer layer of reinforcement. Thus the most important facet of durability prediction for concrete structures is the ability to model the rate of ingress of chloride-ions for the encountered range of concrete quality and exposure conditions.

Concrete technologists have long recognised the significant benefit of incorporating supplementary cementitious materials (SCMs) such as fly-ash, ground granulated blast-furnace slag and amorphous silica or silica fume in concrete to extend the life of reinforced concrete structures in severe environments. Durability design provisions under the current concrete design standard NZS 3101:1995[4] do recognise that SCMs can enhance concrete durability, but saw their use as an alternative to the prescriptive solutions specified for concrete produced with ordinary Portland cement.

The BRANZ marine durability research programme was established to provide specific data on the chloride ingress of concretes made with New Zealand cement and aggregates that incorporated locally available SCMs. As part of the research, a number of test methods capable of measuring durability more directly than by inference from compressive strength were also evaluated. This research programme was timed to enable the results to be utilised for the 2005 revision of NZS 3101. It was envisaged this revision would allow for specific durability solutions taking advantage of concretes incorporating SCMs.

1.2 Overview of research programme

There were two main objectives to the research programme reported here:

- To quantify appropriate input values for prediction of time to corrosion initiation, using the 'Fick's Law' type models that are gaining increasing currency for this purpose within the concrete industry.

- To identify practical laboratory tests that can characterise the expected durability of a particular concrete mix.

1.2.1 Preliminary laboratory studies

The initial BRANZ research in this area concentrated on developing test methods that directly measure the transport properties of concrete linked to ingress of chloride-ions under field exposure. These purely laboratory-based studies included four different cementitious binder types: one concrete made with purely GP cement and three concretes where the cement was supplemented with fly-ash, slag or silica fume.

Tests carried out included the determination of capillary water absorption using the ISAT (Initial Surface Absorption) technique in accordance with BS 1881 Part 5, electrical conductivity tests using the ASTM C1202 'rapid chloride' permeability technique, and the measurement of steady-state chloride-ion diffusion coefficients using a conventional split-cell diffusion apparatus. A description of these test methods and the detailed findings are given by Chisholm.[5] From these studies, a number of difficulties were apparent:

- The ISAT test was both very dependent on the initial moisture content of the concrete and also somewhat awkward in practice. A simpler and more robust means of determining absorption was required that also included a standardised sample preconditioning routine to guarantee a consistent internal moisture content in the concrete specimen.

- The ‘split-cell’ diffusion test was not able to adequately discriminate between the various high-performance concrete mix designs tested. These incorporated blended cements and low water-to-binder (w/b) ratios. Test periods ranging from months to years were necessary to establish steady-state diffusion conditions, limiting the practicality of this method for determining chloride-ion diffusion coefficients for concretes of this quality, even in laboratory studies.

- The ASTM C 1202 conductivity results did not always correlate well with the reference diffusion coefficient measurements, particularly across differing cement types, which can significantly alter the pore solution chemistry within the concrete. While its performance was acceptable as a rapid quality control check where expected conductivity parameters have already been established, it was found too unreliable for use in mix qualification purposes or as a specification tool. Clearly there was a need for a more robust electrically-accelerated chloride-ion migration test.

Based on these issues, and a realisation of the need to correlate laboratory tests with the actual performance of well-characterised concrete placed in environments of known severity, BRANZ embarked on a more extensive programme in which the monitoring of concrete under natural exposure was the most significant component.

1.2.2 Studies of chloride ingress into concrete

The BRANZ exposure site programme was established primarily to measure chloride ingress in a variety of concrete grades, produced with cement incorporating SCMs, and placed in three environments with different degrees of exposure to marine aerosols. The programme is described in Section 2. It was believed that sufficiently detailed monitoring of chloride ingress over time would allow prediction of the theoretical service life of each concrete, assumed to be the time to corrosion initiation at typical reinforcement cover. With adequate characterisation of both the concrete and the environment this can be generalised into a methodology for service-life prediction. To explain how this is achievable, a brief treatise on chloride-ion penetration into concrete is required.

Penetration of the cover concrete occurs because chloride-ions are transported through the porous concrete matrix by a variety of different physio-chemical processes. An often cited example considers a seawall: below the low tide mark, where the concrete is permanently submerged, chloride-ions diffuse through the water-saturated pore structure of the concrete in response to concentration gradients. In the zone dominated by tidal and wave action, concrete is intermittently exposed to both seawater and air so chloride ingress occurs via a combination of diffusion and capillary absorption. Above the high tide mark, where waves irregularly splash relatively dry concrete, absorption due to capillary suction predominates. Behind the seawall, brackish groundwater may permeate the concrete driven by hydrostatic pressure. For structures located further inland, salt is deposited on concrete surfaces from marine aerosols carried on the wind, and is similarly absorbed through capillary action.

Thus chloride-ions can penetrate towards the reinforcing steel by a number of mechanisms including diffusion (movement under a concentration gradient), permeation (movement by hydrostatic pressure) and absorption (capillary uptake). An ideal model of chloride penetration should include all these factors to define the chloride concentration in the pore solutions of the concrete.

Fick's Law

Despite the variety of possible transport mechanisms, chloride penetration into concrete has been conventionally analysed by borrowing from the language and mathematics of classical diffusion, in particular Fick's 2nd Law which relates the temporal variation in chloride-ion concentration, C, to the spatial distribution of the ions by means of the diffusion coefficient, D:

$$\frac{\partial C}{\partial t} = D\frac{\partial^2 C}{\partial x^2} \qquad [1\text{-}1]$$

Crank[6] provides an analytical solution to this differential equation for the simple case of diffusion into a semi-infinite two-dimensional slab driven by a constant concentration gradient:

$$C_{(x,t)} = C_i + (C_s - C_i)\left(1 - erf\left(\frac{x}{2\sqrt{Dt}}\right)\right) \qquad [1\text{-}2]$$

where $C_{(x,t)}$ is the chloride-ion concentration at depth x and time t

C_s is the surface chloride-ion concentration

C_i is the initial chloride concentration in the concrete

D is the chloride-ion diffusion coefficient of the concrete, and

erf is the Gaussian error function.

Adoption of Fick's Law is largely a matter of pragmatism: plots of chloride concentration vs depth for concrete structures can often be reasonably described by equation [1-2]. This offers the possibility of a predictive model because, provided D and C_s are adequately known, chloride penetration profiles can be calculated for any subsequent time interval.

Figure 2 shows a hypothetical example assuming a constant surface chloride load and an unchanging diffusion coefficient.

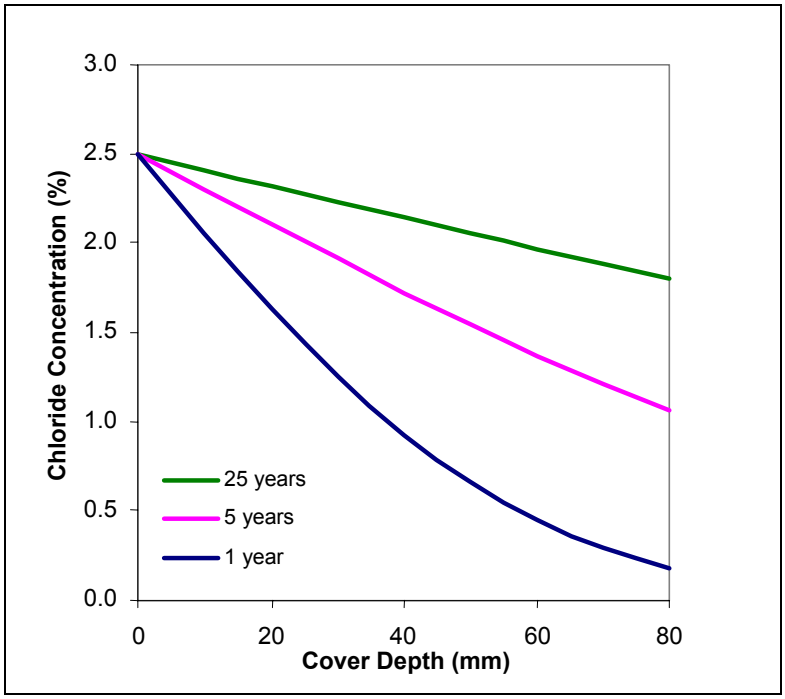

Figure 2: Example of chloride depth profile development with time

Measuring diffusion coefficients

To determine surface chloride concentrations (C_s) and diffusion coefficient (D) values it is necessary to have a 'chloride profile', i.e. experimental data for C vs x at any time t, for concrete exposed to a chloride-laden environment. In practice, such a profile is obtained by incrementally drilling into the concrete, perpendicular to the exposed surface. The powdered concrete collected from each depth interval is collected and analysed for chloride content by x-ray fluorescence or an equivalent convenient technique.[7] An example of a typical profile is shown in Figure 3.

The values of C_s and D are determined by fitting equation [1-2] to the chloride profile through non-linear regression using least squares, i.e. minimising the sum S given by equation [1-3]:

$$S = \sum_{n=1}^{N} \Delta C^2(n) = \sum_{n=1}^{N} \left(C_m(n) - C_c(n)\right)^2 \qquad [1\text{-}3]$$

where N is the number of concrete layers sampled

$C_m(n)$ is the measured chloride concentration in the nth layer (% by mass)

$C_c(n)$ is the calculated chloride concentration in the middle of the nth concrete layer (% by mass)

Diffusion coefficients are conveniently expressed in units of mm^2/year, although the SI dimensions of m^2/s are also commonly encountered (30 mm^2/year ≈ 1.0 x 10^{-12} m^2/s). Chloride concentrations are determined on mass percent of concrete or cement binder. The latter is more correct, the former more convenient, and the conversion between the two is simple where density and cement content of the concrete are known.

The first point of the chloride profile is often omitted from the regression analysis because of a variety of possible interferences close to the outer surface of the concrete.[8] Ideally the profile should include at least six individual measurements, covering the full range of chloride concentrations encountered in the sample.

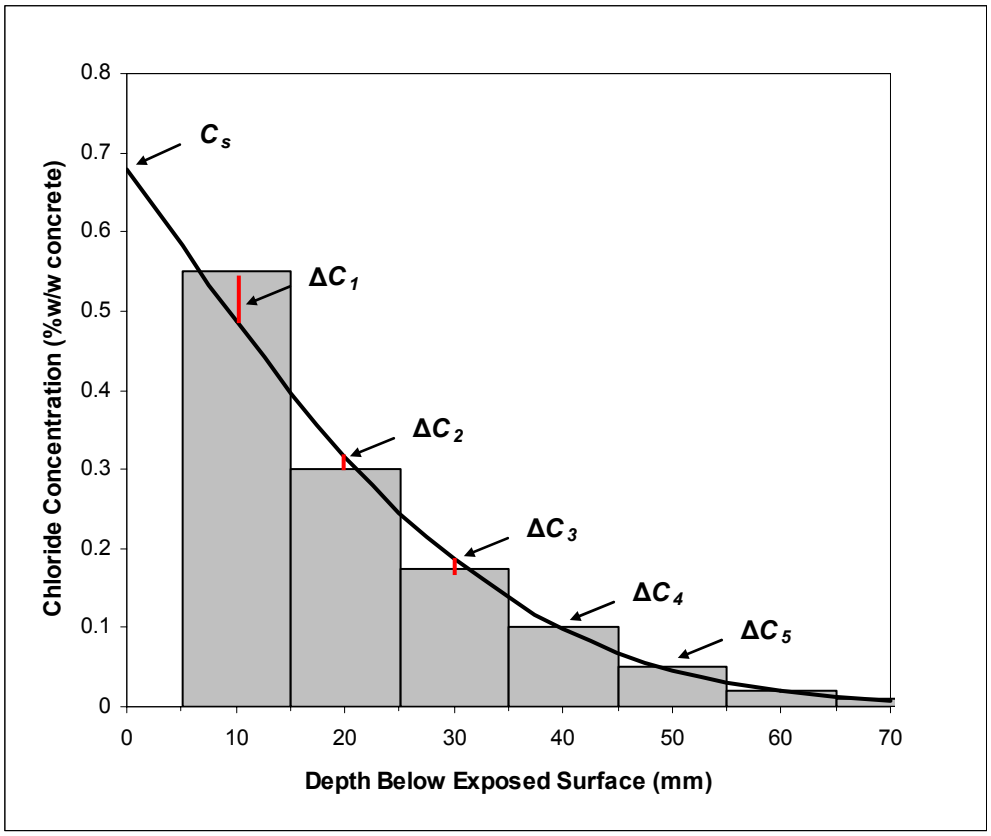

Figure 3: An example of a chloride profile from a concrete structure. The bars represent the measured chloride concentrations and the curve is the optimised Fick's Law model given by equation [1-2] after optimisation of the C_s and D parameters. The minimised differences are indicated in red

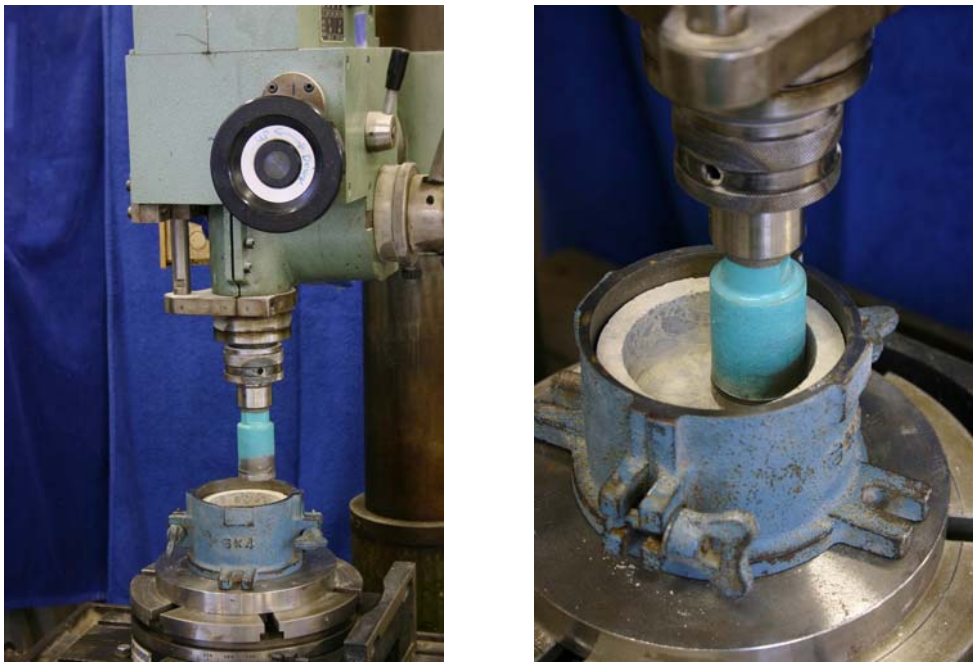

Figure 4: Profile grinding of a concrete core using a vertical mill

The surface chloride concentration, C_s, therefore does not represent a physical measurement on the concrete, but rather the extrapolation of the idealised Fick's Law model profile back to the y-axis intercept ($x = 0$). It can be visualised as the concentration determined in the analysis of an infinitely thin depth increment of concrete, sampled infinitesimally close to the exposed surface. The D_{ce} value expresses the resistance of the concrete to penetration and controls the curvature, (more precisely the second derivative) of the concentration vs depth curve.

The procedure described can be employed both for short-term laboratory-based testing to characterise the durability of new concrete and also to interpret and predict the performance of existing structures from field data. However, neither C_s or D are intrinsic material properties of a given concrete i.e. the surface chloride concentrations and diffusion coefficients obtained would not necessarily be comparable if they result from different conditions of exposure, even with the same concrete.

Crank's solution is routinely applied to the analysis of concrete in two ways which, although superficially similar, are quite distinct in meaning and need to be carefully distinguished.

The first application is to determine the 'actual diffusion coefficient', D_{ca}. This attempts to measure the intrinsic diffusivity of concrete as correctly as possible via a bulk immersion test. One example of such a test is NT Build 443,[9] in which a completely saturated concrete specimen is immersed in a synthetic chloride solution for around 35 days. A diffusion coefficient is calculated from the developed chloride profile by applying the non-linear regression analysis described above, which yields best-fit values for D_{ca} and C_s. This procedure is normally carried out on early-age (28 or 56 day old) specimens to yield a characteristic chloride-ingress based material factor, but can also be usefully performed on core samples (uncontaminated with chloride) from existing structures to determine the current diffusivity of the interior concrete. The similar American methodology ASTM C 1556[10] refers to this property as D_a, the apparent chloride diffusion coefficient.

The second is to use equation [1–2] and the same curve-fitting procedure to determine the 'effective diffusion coefficient', D_{ce}, of existing structures where a near-surface chloride ingress

profile has already developed in the concrete through natural exposure. This provides a means of characterising the historical performance of a particular concrete or structure and can also be used for predicting future performance.

D_{ce} and D_{ca} can both be used to predict the corrosion initiation. Corrosion is possible when the concentration of chloride at the depth of the reinforcement exceeds the critical threshold value required for de-passivation of black steel, typically estimated at 0.4 – 1% w/w of chloride on cement.[11] This age can be calculated simply by solving equation [1-2] for t, using the appropriately derived values of D_{ce} or D_{ca} and C_s, with the shallowest reinforcement cover depth representing x. Less easy, and of critical importance to the accuracy of this technique, is the choice of appropriate C_s and D values. It is with this problem that the research described in this report is mostly concerned.

D_{ce} is distinct from D_{ca}, both because it reflects the influence of all the possible transport mechanisms acting on the concrete that have contributed to establishing the chloride profile, and also because it does not yield an instantaneous measure of the current resistance to chloride penetration. Instead, it reflects the 'time-averaged' performance of the concrete over the period between first exposure of the structure and the time when the chloride profile was determined.

Arguments against this approach

It should be emphasised that the justification for adopting diffusion theory is primarily convenience and empiricism: the mathematics of Crank's solution are straightforward, it can be cast in terms that are familiar to structural engineers – an imposed environmental load, C_s, and a resistance to that load, D_{ce} – and it models the chloride profiles observed to develop in concrete with at least some degree of fidelity. However, except for the always submerged parts of marine structures, the pore system of concrete is rarely under complete saturation when exposed to chlorides. Consequently convective transport mechanisms, such as permeation, capillary absorption and wick action, are likely to be significant contributors to the chloride flux in addition to pure ionic diffusion. Even a completely water-saturated concrete violates the conditions necessary for the compliance with the assumptions of classical diffusion theory. In particular, the hydrated cement matrix is not an inert material and will partially immobilise chloride-ions, primarily through reaction of the tri-calcium aluminate phase to form Friedel's salt ($3CaO.Al_2O_3.CaCl_2.10H_2O$). The extent of this chloride binding is known to be, at the very least, a complex function of chloride concentration, the cement binder composition and pore solution pH.[12] For this reason, the value of D_{ce} depends on the environmental chloride load, a clear violation of one of the central tenets of classical diffusion.

It is not clear to what extent ignoring these theoretical considerations might compromise the integrity of service life prediction. A number of researchers have developed multi-mechanistic transport models for partially-saturated concrete from first principles.[13] Unfortunately, their meaningful application requires an extensive knowledge of a wide variety of material properties and site-specific conditions that are not usually available. Simply describing the spatial moisture distribution within a concrete structure sufficiently well to use such a model currently represents a formidable technical (and economic) barrier.

Equally, the importance of attempting to account for chloride binding remains contentious. There is little doubt that the removal of chloride-ions from the pore solution of the cement matrix via binding reduces the free chloride concentration and therefore the quantity of mobile chloride at all depths within the concrete. However, modelling of chloride binding isotherms[14] demonstrates that an increased chloride binding capacity also serves to maintain higher concentration gradients for extended periods in the near-surface concrete, thereby increasing the velocity and quantity of the chloride-ions entering the concrete through diffusion. Experimental evidence[15] also seems to demonstrate that the corrosion risk presented by bound chloride at the

steel-concrete interface may be very similar to that presented by free chlorides. This is contrary to a long-standing view that only the free chloride concentration is important and that the relative aggressiveness of a particular chloride-contaminated concrete is best expressed by the pore solution concentration of chloride and hydroxyl ions.[16] The potential importance of the bound ions justifies the simple analysis of concrete in terms of total chloride per unit of mass, as described above, rather than extraction and analysis of pore fluids. However, this procedure does produce some not entirely intuitive consequences. For example, the boundary C_s value of concrete completely submerged in seawater is not equal to the chloride concentration of the brine but also depends, because of binding effects, on the chemistry of the cement, the concrete's total porosity and even surface finishing and curing.

At the present time, the simplicity and practicality of the empirical Fick's Law approach described appears to outweigh any theoretical disadvantage over a more complex multi-mechanistic treatment of unsaturated flow. It should always be borne in mind, however, that the necessary surface chloride concentrations and diffusion coefficients for input to these models are bundled parameters, reflecting a variety of physical, chemical and environmental variables. They need to be collected and interpreted with great care, especially when trying to correlate laboratory test results with field data.

Field studies and observed temporal dependence of D_{ce}

The application of the error-function solution to the characterisation and prediction of concrete durability in the field dates back to the 1970s.[17] Initially, D_{ce} was treated as a constant for any particular concrete type. However, extensive observations of marine structures in Japan led Takewaka et al[18] to propose a modified equation allowing for an apparent temporal (time-related) dependence of the diffusion coefficient. The resistance of concrete to chloride-ions, as determined by ingress profiles, is therefore seen to improve with age according to a simple power function:

$$D_{ce}(t) = D_{ce0} \cdot \left(\frac{t_0}{t} \right)^m \qquad [1\text{-}4]$$

where $D_{ce}(t)$ is the average effective diffusion coefficient representing the observed chloride profile at any time, t

D_{ce0} is a reference diffusion coefficient at some specified time t_0 (often chosen to be 28 days, D_{28}, simply for consistency with standard concrete tests), and

m is a 'time-reduction index', quantifying the temporal dependence of the diffusivity.

Both m and D_{28} (or any other convenient reference diffusion value) are mathematically fitted parameters, derived by plotting experimental data for D_{ce} vs t in a logarithmic coordinate system: m is the (negative) gradient of the resulting best-fit line. Equation [1-4] can simply be substituted into Crank's solution to Fick's Law to take account of the temporal dependence, as shown below. The meaning of the terms remain as previously defined.

$$C_{(x,t)} = C_i + \left(C_s - C_i\right)\left(1 - erf\left(\frac{x}{2\sqrt{D_{ce0}\left(\frac{t_0}{t}\right)^m t}}\right)\right) \qquad [1\text{-}5]$$

Equation [1-5] is valid for a range of m values between 0 and 1 only; the lower limit implies a constant chloride-ion diffusivity with time and the higher limit a state where the concrete is completely blocked to further chloride ingress. Values of $m > 1$ have no physical meaning because they imply a chloride-ion front that recedes out of the concrete with time.

Other researchers[19,20] have confirmed this apparent time dependence of diffusivity appears to hold for both laboratory specimens and aged concrete in the field. The value of m is known to be influenced by, at the very least, the cement type and w/b (water to binder) ratio of the concrete under consideration. The literature[19,21] indicates that concrete incorporating blast-furnace slag, fly-ash or silica fume can demonstrate substantial reductions in effective diffusivity over time, corresponding to m values of approximately 0.6 – 0.8. Plain Portland cement concretes by contrast show much smaller reductions; Bamforth indicates an m value of 0.25 while Takewaka's original figure was $m = 0.1$.

Any temporal dependence to the chloride-ion diffusivity has the potential to impact enormously on the predicted service life for marine concrete. Figure 5, Figure 6 and Figure 7 demonstrate the effect of systematically varying m, C_s and D_{28} respectively on the time to corrosion initiation for reinforcement at various depths, calculated using equation [1-5]. The range of input parameters used encompasses the typical spectrum of values encountered in the literature, as shown in Table 1. The 'reference concrete' chosen, shown in red, has values of C_s = 3.0 %w/w on cement, D_{28} = 100 mm^2/yr and m = 0.1, intended to represent a high quality unadulterated Portland cement concrete in a sea splash or tidal zone. It is obvious that varying m, the time-reduction index for the effective diffusion coefficient, is a much stronger control on the corrosion initiation time than either C_s, the environmental chloride load, or $D_{28,}$ the initial resistance of the concrete to chloride penetration. Possessing accurate values for m for each concrete type therefore becomes a matter of critical importance. Modelling a constant chloride-ion diffusivity potentially underestimates durability but, equally, severe over-estimates in predicted service life are also possible if unwarrantedly large reduction indices are assumed.

Table 1: Typical input parameters for modelling concrete service life with Fick's Law

Fick's Law Calculation Inputs		Typical Range of Values Encountered			Units
C_s	surface chloride concentration	0.7	to	5	%w/w on cement
D_{28}	reference diffusion coefficient at 28 days	10	to	1,000	mm^2/year
m	time-reduction index	0.0	to	0.7	dimensionless

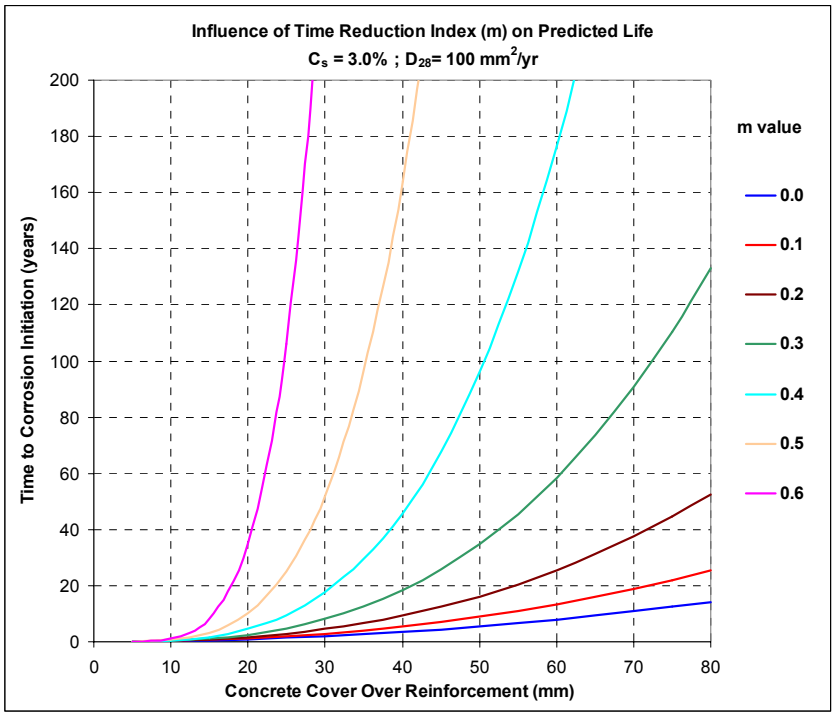

Figure 5: The effect of various values of the 'time-reduction index', *m*, on predicted service life

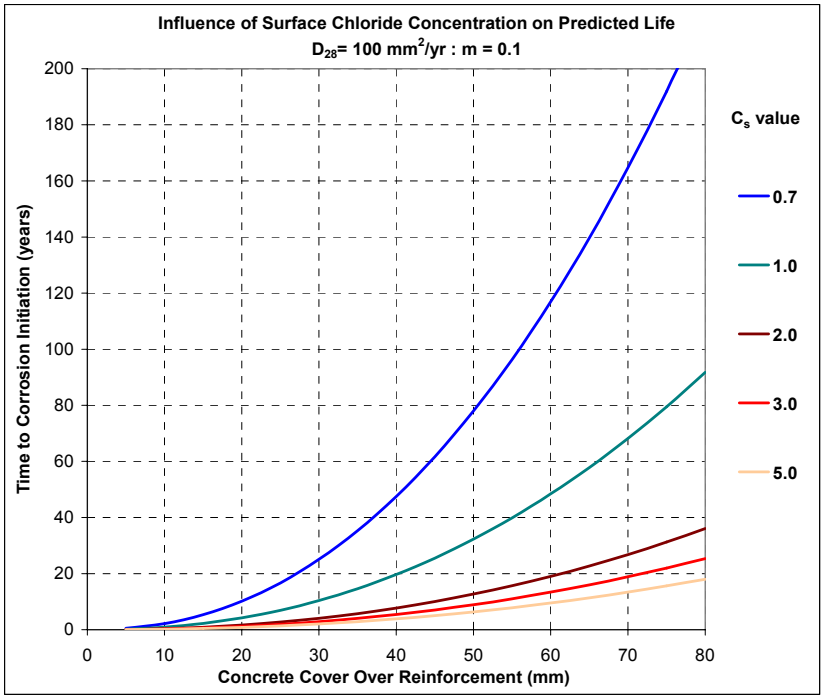

Figure 6: The effect of surface chloride concentration, C_s, on predicted service life

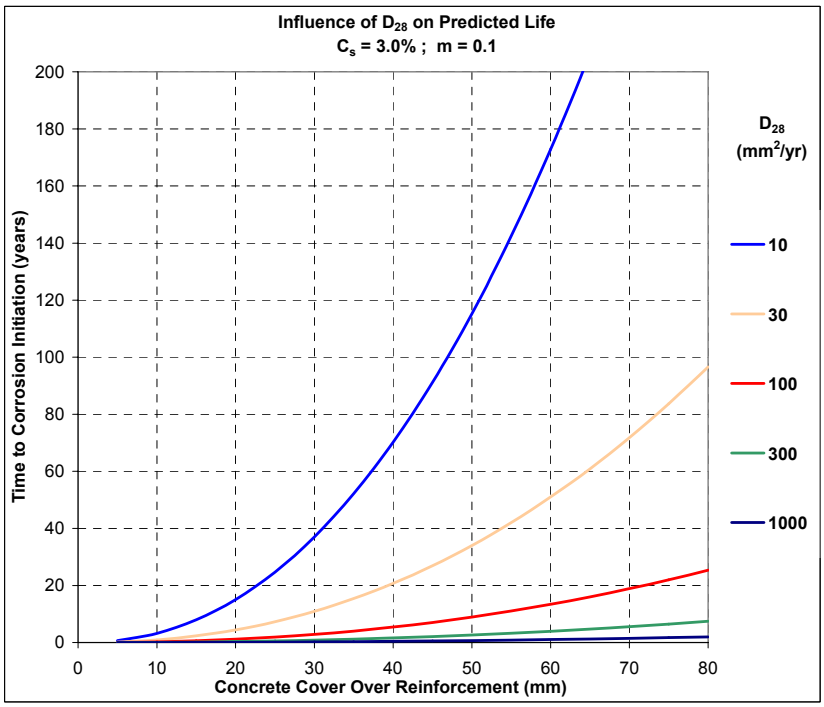

Figure 7: The effect of variable initial effective diffusion coefficients at 28 days, D_{28}, on predicted service life

Consequently, one of the key objectives of the BRANZ exposure site programme was to quantify the surface concentration C_s, the effective chloride diffusion D_{ce} and any associated temporal dependence in the diffusion coefficient, for each of the concrete types investigated. These are the critical input values for predicting time to corrosion initiation using a Fick's Law type model.

1.3 Development of durability indices

The other key objective of the programme was to validate laboratory-based test methods that could adequately characterise the expected durability performance of a given concrete but are still simple enough to use as quality control tests during construction. Ideally these durability indices would demonstrate a correlation with chloride ingress observed in the field, giving them the potential to be incorporated as direct inputs into service-life predictions models. Because of the lengthy test duration for a bulk immersion test to determine D_{ca}, it was also desirable to identify a rapid method for determining chloride-ion diffusion coefficients, if this parameter is ever going to be routinely called-up in quality specifications for concrete placed in marine environments.

1.4 Scope of BRANZ Study Report 145

This report presents the information derived from five years' natural exposure of the test concrete, a review of extant service life prediction models and the results of the ancillary laboratory programme. The topics addressed include:

- Establishing the appropriate surface chloride concentrations, C_s, and effective chloride-ion diffusion coefficients, D_{ce}, that should be used for life prediction. This was achieved by modelling of the chloride ingress data for different concrete types and exposure zone classifications using Crank's solution to Fick's 2nd Law.

- Determining if the specialised marine concrete formulations available in New Zealand (Duracem slag cement, Micropoz silica fume and Microsilica 600 natural silica pozzolan at the commencement of the programme) demonstrate a temporal dependence to their effective chloride-ion diffusivity.

- Establishing whether temporal dependencies in D_{ce} are statistically significant and to what, if any, extent they should be allowed for in service-life prediction.

- If a temporal improvement is observed, what are the appropriate time-reduction indices, m, necessary to characterise the performance of these concretes with Crank's equation?

- Can any observed improvement in the effective diffusivity of the concrete be explained by intrinsic refinements in the connectivity of the pore network of the concrete by continued hydration? If so, the reduction in diffusivity might confidently be expected to occur always; if not, the phenomenon may depend on some specific chemical or physical interaction with the external environment and appear with less reliability.

- A comparison of the currently-available service-life prediction models for concrete in marine environments.

- An investigation of the benefits and limitations of hydraulic sorptivity as a concrete durability parameter.

- An examination of electrically accelerated chloride-ion migration tests as a quicker alternative to natural diffusion tests.

The report is structured as three largely independent sections:

- Section 2 describes the exposure site testing and the derivation of appropriate input data for Fick's Law-based service life prediction models from the collected data.
- Section 3 reviews the readily-accessible models of this type available for service life design of marine concrete structures based on resistance to chloride-ion penetration.
- Section 4 examines early-age laboratory tests that may be suitable to act as simple durability indices i.e. methods of characterising the expected in-service durability performance of a particular concrete mix design.

2. BRANZ EXPOSURE SITE PROGRAMME

2.1 Manufacture of samples

In late 1998, thirty six 1.0 m x 0.75 m x 0.35 m blocks of structural quality concrete were cast at BRANZ's Judgeford laboratory. As the establishment of chloride profiles was expected to be relatively slow, particularly for the blended cement concretes, sufficient blocks were made to enable a pair of each mix type to be placed at the environmental exposure site, ensuring adequate material for repeated sampling visits.

The concrete was produced by Ready Mixed Concrete's Dry Creek Quarry plant under the supervision of BRANZ personnel. Four series of mixes were produced, consisting of a control series containing only type GP cement and three further series in which a quantity of the cement was replaced with three common SCMs then available on the New Zealand market (Table 2). Each series included mixes at three different levels of total cementitious material: 280 kg/m^3, 325 kg/m^3 and 400 kg/m^3, as appropriate for the severity of the exposure environment for which they were intended. The mix designs were developed by BRANZ, but were intended to be representative of commercial ready-mixed concrete. Each mix type is identified by a five character code that consists of the total cementitious binder content followed by the two-letter abbreviation from Table 2, e.g. 325 DC is a concrete with a 325 kg/m^3 total binder content in which 65% of the Portland cement has been replaced by blast-furnace slag furnished by Duracem cement (note the latter figure is the total percentage replacement of undiluted slag not the percent Duracem). Twelve concrete mixes were produced in total.

Table 2: Concrete mix types used

Mix Code	Unique SCM	Description	Cement Replacement (%)
GP	Golden Bay GP	Type GP cement	100
DC	Duracem	Blast-furnace slag cement	65 #
MP	Micropoz	Silica fume	8
MS	Microsilica 600	Natural amorphous silica	8

percent replacement by undiluted slag; 50% replacement was used for the 280 kg/m^3 mix

The concrete was made with crushed 19 mm and 13 mm greywacke coarse aggregate from Winstone Aggregate's Belmont site and natural river sand from the Rangitikei River at Kakariki. The target w/b ratio of the mixes was designed to be kept constant at each cement factor and the workability was adjusted by the addition of super-plasticiser, targeting a slump of

100 mm. Mixes with straight GP cement were not super-plasticised. In practice, some variation of water content was unavoidable due to the difficulty of precisely batching small quantities of materials at the ready-mix plant, which resulted in small deviations from the intended w/b ratios. Mix design details, including the measured fresh concrete properties, are shown in Table 3.

Twenty-four hours after casting, each block was stripped, turned bottom form-face uppermost and wet-cured for seven days using soaker hoses. The blocks were then stored outside before being placed at one of three exposure sites, chosen to be representative of the range of hazardous marine environments as classified in NZS 3101:1995. These exposure classification categories (C, B2, B1) are unchanged in the 2005 revision of the standard.

Table 3: Mix proportions and fresh concrete properties

Mix Proportions (Quantities per m^3)		GP Concrete				Micropoz Concrete			Microsilica Concrete			Duracem Concrete		
		250GP	**280GP**	**325GP**	**400GP**	**280MP**	**325MP**	**400MP**	**280MS**	**325MS**	**400MS**	**280DC**	**325DC**	**400DC**
***19mm** (kg)*	Belmont Chip	762	762	763	761	765	764	764	765	761	763	764	765	759
***13mm** (kg)*	Belmont Chip	316	316	326	320	323	325	318	317	320	317	316	319	322
***Sand** (kg)*	Puketapu	913	886	844	778	893	846	781	890	842	803	872	832	749
***GP Cement** (kg)*	Golden Bay*	260	280	326	399	276	302	370	269	306	373	93	45	50
***Duracem** (kg)*		*	*	*	*	*	*	*	*	*	*	186	279	350
***Microsilica** (kg)*		*	*	*	*	*	*	*	14	26	32	*	*	*
***Micropoz** (kg)*		*	*	*	*	14	26	32	*	*	*	*	*	*
***Total binder** (kg)*		260	280	326	399	290	328	402	283	332	405	279	324	400
***Water reducer** (l)*	Sika BV40	0.7	0.7	0.8	1.0	0.5	0.8	1	0.8	0.8	1.1	1.2	0.8	1.0
***Super-plasticiser** (l)*	Sika 1000N	*	*	*	*	1.3	2.7	3	1.3	0.6	2.5	2.3	1.6	0.6
***Total water** (l)*		160	161	159	160	160	159	183	161	169	157	176	160	175
Target w/b ratio		*0.62*	*0.57*	*0.49*	*0.40*	*0.57*	*0.49*	*0.40*	0.57	0.49	*0.40*	*0.57*	*0.49*	*0.40*
Achieved w/b ratio		0.62	0.57	0.49	0.40	0.55	0.51	0.45	0.57	0.51	0.39	0.63	0.49	0.44
***Slump before S.P.** (mm)*		70	60	60	70	40	80	70	60	80	40	50	50	80
***Slump after S.P.** (mm)*		*	*	*	*	120	100	100	140	100	150	170	110	100
***Air content** (%)*		1.9	1.4	1.8	1.3	0.8	1.2	1.5	2.0	2.50	1.5	1.2	2.2	1.7
Measured yield		1.003	0.996	1.003	1.000	0.998	1.002	1.017	0.997	1.01	0.995	0.994	0.986	0.994
Theoretical yield		1.005	0.999	1.003	0.999	0.987	1.011	1.026	1.011	1.01	1.001	1.018	1.013	1.022
***Fresh density** (kg/m^3)*		2395	2411	2403	2421	2405	2419	2406	2418	2403	2434	2435	2442	2442

*Milburn GP cement was used for mixes including Duracem

The blocks were placed at each exposure site approximately one month after casting and orientated such that the 1.0 m x 0.75 m formed face was exposed to chloride ingress. The sites were as follows:

Weka Bay (C Zone): Weka Bay is located within the confines of the Wellington urban area in the southwest of the city's harbour. The blocks are placed above high tide level; however, the bay is exposed to the predominant northerly winds and the fetch across the harbour means the blocks are regularly splashed with salt water on breezy days. The resultant periodic wetting and drying is generally regarded as being one of the vulnerable conditions for reinforced concrete structures because chlorides are concentrated by evaporation and both water and oxygen are available to facilitate corrosion. The blocks are lying on their flat on a ledge adjacent to a sea wall, with the formed 1.0 m x 0.75 m face uppermost. Figure 8 shows the blocks being installed on site and Figure 9 illustrates the less benign conditions that can occur.

Figure 8: Installation of concrete blocks on Weka Bay C zone exposure site

Figure 9: Weka Bay C Zone exposure site on a stormy day. The arrow indicates the position of the blocks (photograph courtesy of the *Dominion Post* newspaper)

Oteranga Bay (B2 Zone): Oteranga Bay is situated on Wellington's windswept southern coast. The blocks are placed on a private exposure site, within 100 m of the shore, standing on their end with the formed face facing the open sea. The blocks are never directly splashed by wave action, but rates of salt deposition due to wind-blown aerosols are extremely high. The site is considered a severe example of the B2 coastal frontage zone and is used by BRANZ for studies of marine-derived metallic corrosion.

Judgeford (B1 Zone): Located approximately 20 km north of Wellington harbour at the BRANZ research station, this private site is 5 km distant from the nearest salt water, a tidal estuary, situated across flat farmland and further protected from the open sea by gently rolling hills. The NZS 3101 exposure classification maps place the Judgeford site in the B1 coastal perimeter zone.

The blocks were distributed across the exposure sites according to the severity of exposure and the concrete grade, discriminated by total cement content, as shown in Table 4. Thus, the 400 kg/m^3 mixes were restricted to the most severe C Zone site (Weka Bay), while 325 kg/m^3 were placed at both C and B2 (Oteranga Bay) sites. This was intended to reflect the likely use of these concrete grades in actual construction practice. For the same reason, no mixes containing SCMs were placed on the less exposed Judgeford site because it seemed unlikely that such high quality concrete would be specified for use in the relatively undemanding B1 environment.

.

Table 4: Distribution of mixes on exposure sites

Mix Type cement blend	kg/m^3	Weka Bay	Oteranga Bay	Judgeford
GP	280		●	●
	325	●	●	●
	400	●		
Slag [DC]	280	●	●	
	325	●	●	
	400	●		
Micropoz [MP]	280		●	
	325	●	●	
	400	●		
Microsilica [MS]	280		●	
	325	●	●	
	400	●		

2.2 Mix characterisation testing

Simultaneously with the block production, sets of 200 mm x 100 mm test cylinders and 285 mm x 75 mm x 75 mm beams were cast to characterise the quality of the concrete produced. The tests chosen were compressive strength, sorptivity, actual chloride diffusion coefficient, 'rapid chloride' ion conductivity and drying shrinkage. The methods employed are shown in Table 5. Figure 10 demonstrates how the test specimens were cut from the test cylinder.

Table 5: Methodologies for characterisation testing

Concrete Property	**Test Method**	**Test Date** (days after casting)
Compressive strength and density	NZS 3112: Part 2:1986[22]	7, 28, 56
Drying shrinkage	AS 1012.13-1992[23]	7
Sorptivity	Hall (1989)[24]	56
Actual chloride diffusion (D_{ca})	BRANZ in-house test	56
Chloride-ion penetration (rapid chloride)	ASTM C1202-97[25]	56

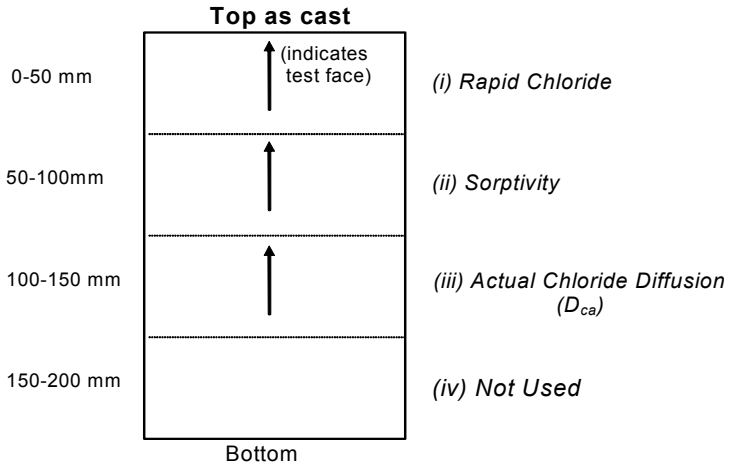

Figure 10: Location of test specimens taken from characterisation cylinders

The characterisation tests are described below, with results given in Table 6. Section 4 examines the role of sorptivity and 'rapid chloride' type permeability tests as indices of concrete durability.

2.2.1 Compressive strength and density (NZS 3112: Part 2: 1986)

Compressive strength and density were determined on cylinders under saturated surface-dry conditions after wet curing at 23ºC and 100% R.H. Densities were determined by Archimedes' Principle and compressive strength by using a 1,800 kN capacity Avery testing machine.

2.2.2 Drying shrinkage (AS 1012.13 – 1992)

After de-moulding, the beams were cured in lime-saturated water maintained at 23º ± 2ºC. Seven days after casting, the initial length of each specimen was determined to a precision of 0.001 mm using a purpose-designed horizontal comparator equipped with a calibrated Mitutoyo digital gauge. The beams were subsequently placed on racks in a controlled climate drying room operating at 23º ± 2ºC and 50% ± 5% RH. Systematic checks are made on the temperature, humidity and water evaporation rate within the drying room during the course of the test. The shrinkage of the test specimens in this environment was measured over a 56 day exposure period using the horizontal comparator. The final drying shrinkage, in microstrain, is calculated from the difference between the initial and final lengths divided by the effective gauge length in the samples.

2.2.3 Sorptivity (Hall's method)

The penetration of chloride deposited on the surface of the concrete exposed to atmospheric conditions is thought to be controlled initially by absorption[26] with the highest chloride concentration occurring at some small depth into the concrete. Consequently, capillary absorption is a property which does have at least some influence on chloride ingress near the surface. Sorptivity is a well-defined and highly reproducible hydraulic property, and is preferred to other tests for characterising the water absorption of concrete because it is not empirical and is independent of sample geometry.

To perform the test, a cut cross-section of the concrete cylinder, conditioned by drying to constant weight as described below, is immersed in shallow water. The change in mass of the sample is monitored at 10 or 20 minute intervals over two hours. Assuming that the water

ingress can be modelled as simple one-dimensional absorption into a porous solid, the volume of water per unit area of absorbed surface, i, is related to the elapsed time, t, by:

$$i = St^{1/2}$$

where S is the sorptivity of the concrete expressed in units of mm/min$^{1/2}$.

For the characterisation tests, the test specimens were conditioned at 100ºC. This temperature was subsequently reduced to 50ºC to provide greater test sensitivity, as a result of experimental trials described in Section 4.2. Consequently, the results given in Table 6 are not directly comparable with the results presented in that section.

2.2.4 Actual chloride diffusion

For determination of the 'actual chloride diffusion coefficient', D_{ca}, a thoroughly water-saturated concrete specimen is exposed on a single cut face to artificial seawater (see below). After a specified period of time, t (here 35 days), thin layers of concrete are ground off parallel to the exposed face and the total chloride content of each layer determined by X-Ray Fluorescence Spectroscopy (XRF). The original (background level) chloride content of the concrete is measured at a suitable depth below the exposed surface. The actual chloride-ion diffusion coefficient, D_{ca}, and the boundary condition of the chloride profile at the exposed surface, C_s, are then calculated. This is achieved by modelling the chloride concentration vs depth profile with Crank's solution to Fick's 2nd Law of diffusion.

The test method is modelled on NT BUILD 443 and differs primarily in the use of synthetic seawater as the immersion medium, rather than a 165 g/dm^3 aqueous NaCl solution, which is approximately five times as concentrated in chloride-ions. The use of a synthetic seawater solution, compliant with the specifications of ASTM D1141 minus the heavy metal ions, was intended to facilitate comparison of the D_{ca}-type diffusion coefficients obtained in the laboratory with the D_{ce} values measured on site.

2.2.5 Rapid chloride test (ASTM C1202)

ASTM C1202 essentially measures the electrical conductivity of concrete. It reflects not only pore tortuosity and connectivity, which are the important influences on durability, but also the concentration of the pore solution electrolytes. Thus it may give misleading results for SCMs that react with sodium and potassium ions liberated into the concrete pore solution through cement hydration. Although it is not a scientifically rigorous test, it was included because its relative convenience means it is often used as a specifying/quality control test despite shortcomings, which are widely recognised.[27,28] The 'rapid migration test' outlined in section 4.3.3 is a significant improvement on ASTM C 1202 in this regard; however, it had not been published when the exposure blocks were cast.

Table 6: Summary of characteristic hardened concrete properties

Property	GP Concrete				Micropoz Concrete			Microsilica Concrete			Duracem Concrete		
	250GP	**280GP**	**325GP**	**400GP**	**280MP**	**325MP**	**400MP**	**280MS**	**325MS**	**400MS**	**280DC**	**325DC**	**400DC**
7 day compression *(MPa)*	31.5	39.5	49.5	53.5	30.0	44.5	50.5	28.5	33.0	41.5	20.0	24.5	29.0
28 day compression *(MPa)*	38.0	43.5	53.5	60.5	46.5	66.0	69.5	39.0	51.0	61.5	31.0	39.0	42.5
56 day compression *(MPa)*	42.0	46.0	58.0	65.0	47.5	65.0	71.5	42.0	56.0	66.0	42.5	44.0	49.5
S.S.D. density *(kg/m^3)*	2430	2440	2440	2460	2440	2460	2430	2430	2430	2450	2440	2440	2450
56 day shrinkage *(microstrain)*	580	570	570	600	650	630	650	630	660	620	680	630	630
Sorptivity index *($mm/min^{1/2}$)*	0.14	0.13	0.12	0.11	0.12	0.07	0.08	0.11	0.10	0.06	0.10	0.09	0.10
Rapid chloride permeability *(Coulombs)*	3860	3061	2906	2265	1473	541	576	1515	915	529	1300	792	788
Chloride diffusion coefficient D_{ca} *(10^{-12} m^2/s)*	18.9	22.0	11.4	10.7	14.1	3.4	4.1	15.7	5.3	2.3	6.9	2.9	1.9

2.3 Exposure site testing

The exposure site testing schedule undertaken is summarised in Table 7. The programme was developed to allow a range of tests to be carried out on specimens cut from 100 mm diameter cores, taken at periodic intervals perpendicular to the exposed face of the blocks. Figure 11 demonstrates how the cores were sectioned to yield the test specimens.

The periodic sorptivity, compressive strength and electrically-accelerated migration measurements were not able to discern any statistically significant changes in the material properties of the exposed concrete with time and are consequently not discussed further. This was attributable to either the poor reproducibility of the test results, particularly true for compressive strength measurement on cores, or refinements to the test methodology gained through experience negating the ability to validly compare the data from each sampling interval. An example of the latter was the lowering of preconditioning temperatures for sorptivity testing.

Chloride penetration into the blocks was measured at regular intervals, with surface chloride profiles determined between 6 and 60 months exposure on five occasions for the C Zone, three occasions in the B2 Zone, and twice for the B1 Zone. The modelling of effective diffusion coefficients and surface chloride concentrations from this data, together with the changes observed in the actual diffusion coefficients of the interior concrete, are the focus of the following discussion.

Table 7: Durability research test programme

Property	Test Method	Sampling Age
Compressive strength and density	NZS 3112: Part 2:1986	3, 6, 60 months
Sorptivity	BRANZ in-house test	3, 6, 30, 60 months
Rapid chloride	ASTM C1202	3, 60 months
Rapid migration (RMT)	NT BUILD 492[29]	48, 60 months
Actual chloride diffusion (D_{ca})	BRANZ in-house test	3, 6, 18, 30, 48, 60 months
Effective chloride diffusion (D_{ce})	BRANZ in-house test	3, 6, 12, 18, 30, 48, 60 months

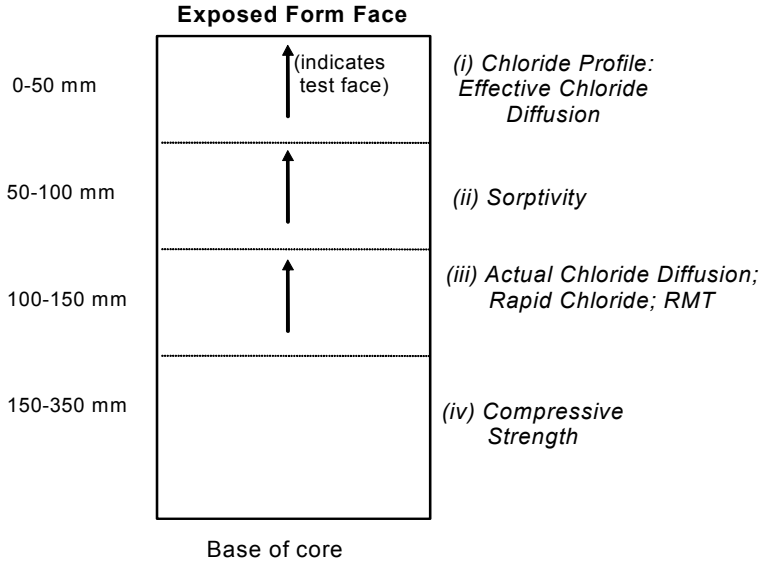

Figure 11: Test specimen location in cores taken from the exposure site concrete

2.4 Modelling of chloride ingress data collected from exposure sites

2.4.1 C Zone severe marine exposure – Weka Bay

The chloride profiles determined on the concrete specimens in the severe marine (NZS 3101 C Zone) exposure site are shown in Figure 12 and Figure 13. Multiple 100 mm diameter cores were taken from each specimen at the indicated time intervals using a water-cooled diamond coring bit and subsequently dry milled in-depth increments of 2 – 5 mm to provide powder samples for analysis by x-ray fluorescence. The average chloride concentration from each set of analyses is plotted in the figures. The analytical data used to construct each profile are reproduced in the Appendix.

For both the 400 kg/m^3 and 325 kg/m^3 mixes it is noticeable that a significant profile was established very quickly for all of the concrete types, with measurable chloride-ion penetration to as deep as 15 mm occurring after six months of exposure. The profiles for the Portland cement (type GP) concrete subsequently flatten, as proportionally larger concentrations develop in the deeper depth increments at later times, i.e. there is clear progress towards an equilibrium state with a uniform chloride concentration as a function of depth. In contrast, the more chloride-resistant concretes, especially the Duracem mixes and the Microsilica mix at the 400 kg/m^3 binder level, maintain a steep and relatively static profile with little further chloride penetration below 15 – 20 mm, despite higher concentrations present in the near-surface concrete.

Note that after five years of exposure the chloride profile in the GP concrete mixes, when extrapolated to the typical reinforcing cover depth of 50 mm, would be approaching the corrosion threshold for black steel (0.4% by mass of cement). This supports the position taken by the durability sub-committee responsible for the 2005 revision of NZS 3101 not to permit concrete without SCMs in the C Zone exposure category.

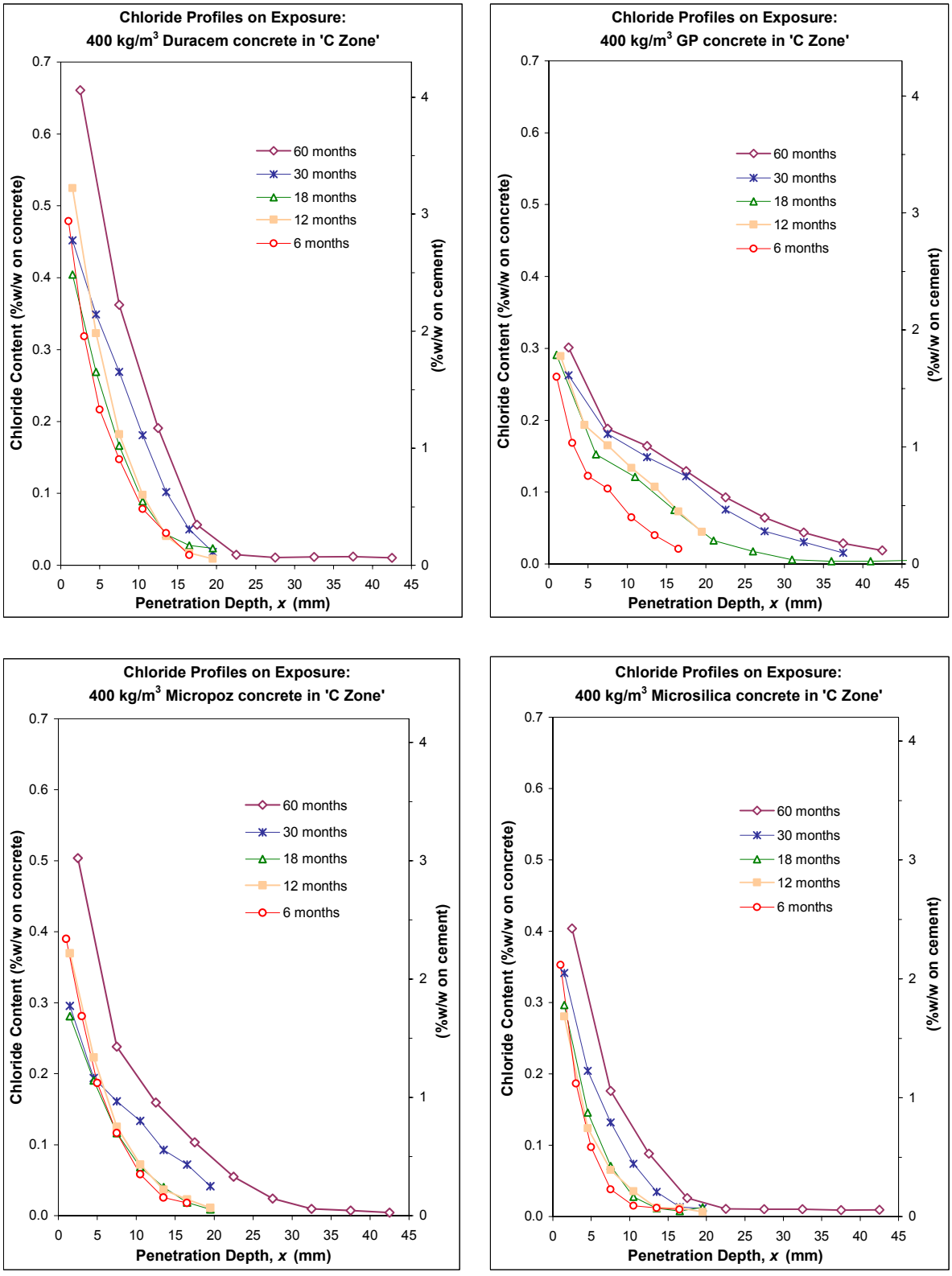

Figure 12: Chloride profiles for the 400 kg/m^3 total binder content concrete mixes after five years of natural exposure on the Weka Bay C Zone site

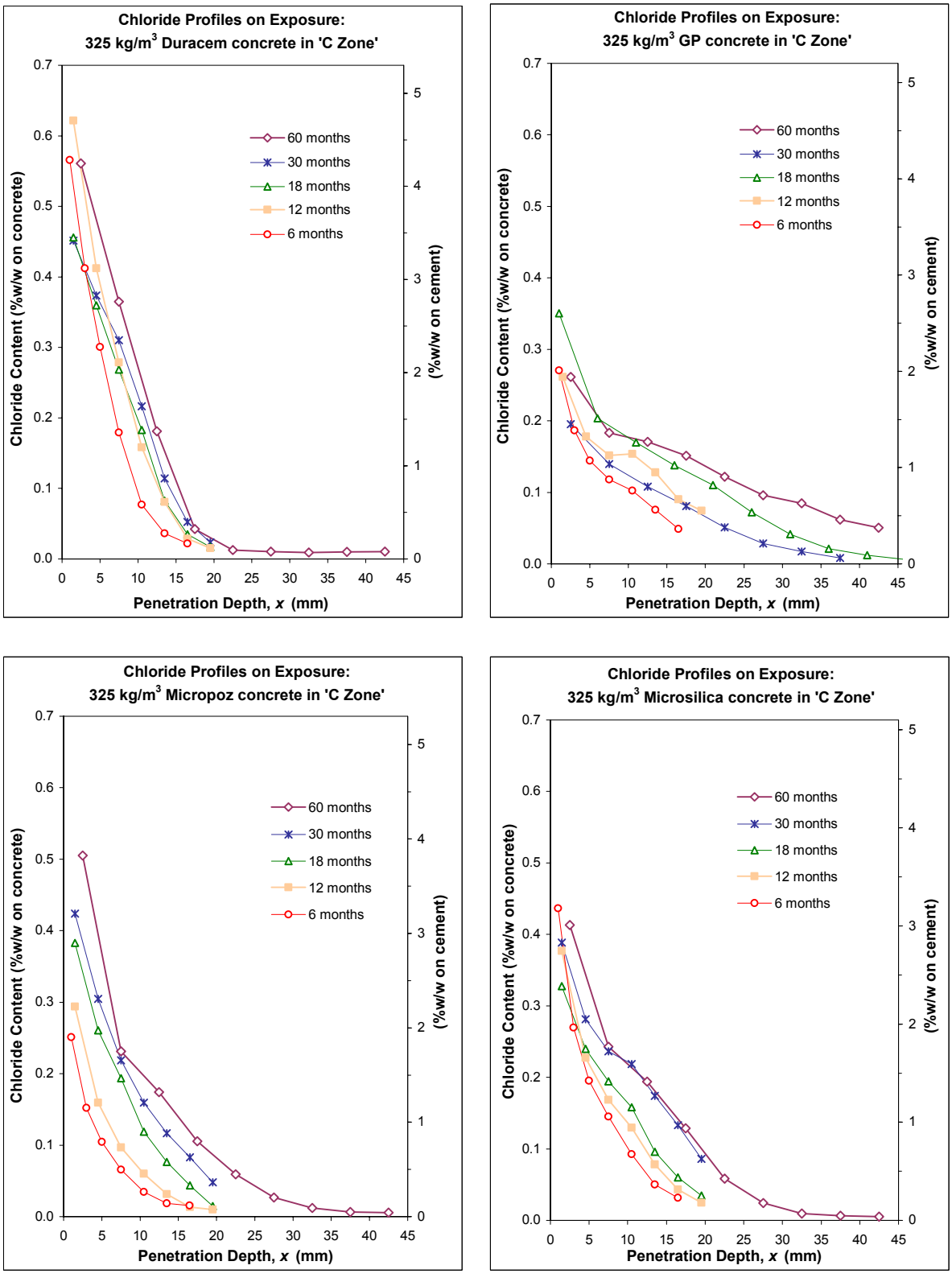

Figure 13: Chloride profiles for the 325 kg/m^3 total binder content concrete mixes after five years of natural exposure on the Weka Bay C Zone site

As an approach to quantifying the durability performance of the concretes, the surface chloride concentration, C_s, and the effective diffusion coefficient, D_{ce}, were calculated for each concrete mix at each sampling age. The procedure used a least-squares best-fit analysis for Crank's solution to Fick's Law (equation [1-2]) as previously described. For maximum accuracy each individual profile was fitted, rather than just the average plotted in Figure 12 and Figure 13.

2.4.2 Surface chloride concentration

The mean C_s values derived from the C Zone chloride profiles are plotted against the period of exposure in Figure 14. There is a significant degree of random fluctuation in the derived values that possibly reflects the climatic conditions immediately before the sampling, e.g. the amount of rain-washing the surface of the blocks received. This is an unavoidable consequence of choosing a wave splashed exposure environment above the mean high tide level, rather than an inter-tidal site where the imposed environmental chloride load is more consistent. To a broad approximation, however, the surface chloride concentrations under the site's spray/splash conditions appear to be (i) relatively constant and (ii) fixed early in the life of the concrete. Thus there is some experimental justification for adopting the simplifying assumption of a time-independent C_s that is a necessary condition for applying Crank's solution. Also, as noted previously, predicted initiation times for corrosion calculated with this equation are relatively insensitive to small changes in chloride load. Table 8 gives the mean derived C_s values for each concrete type, assuming independence with time. The calculated upper 90% confidence limits on these values, assuming a normal distribution, are also given. Examination of the individual replicate chloride profiles tabulated in the Appendix indicates that significant variations in C_s are possible, even on concrete cores taken adjacent to each other in the sample. Accordingly the upper 90% limits may be more suitable values for design purposes, offering a safety factor for the environmental loading.

The surface chloride concentration is very obviously a function of concrete type, with the Duracem slag cement specimens demonstrating approximately double the C_s values of the GP concretes. This effect has been noted by other authors and has been explained as a combination of enhanced chemical binding capacity, a higher pore-wall surface area capable of physi- and chemi-sorption, and increased refinement of the concrete pore structure preventing chloride removal through washout. The clear implication is that these differences in C_s must be taken into account when predicting rates of chloride ingress.

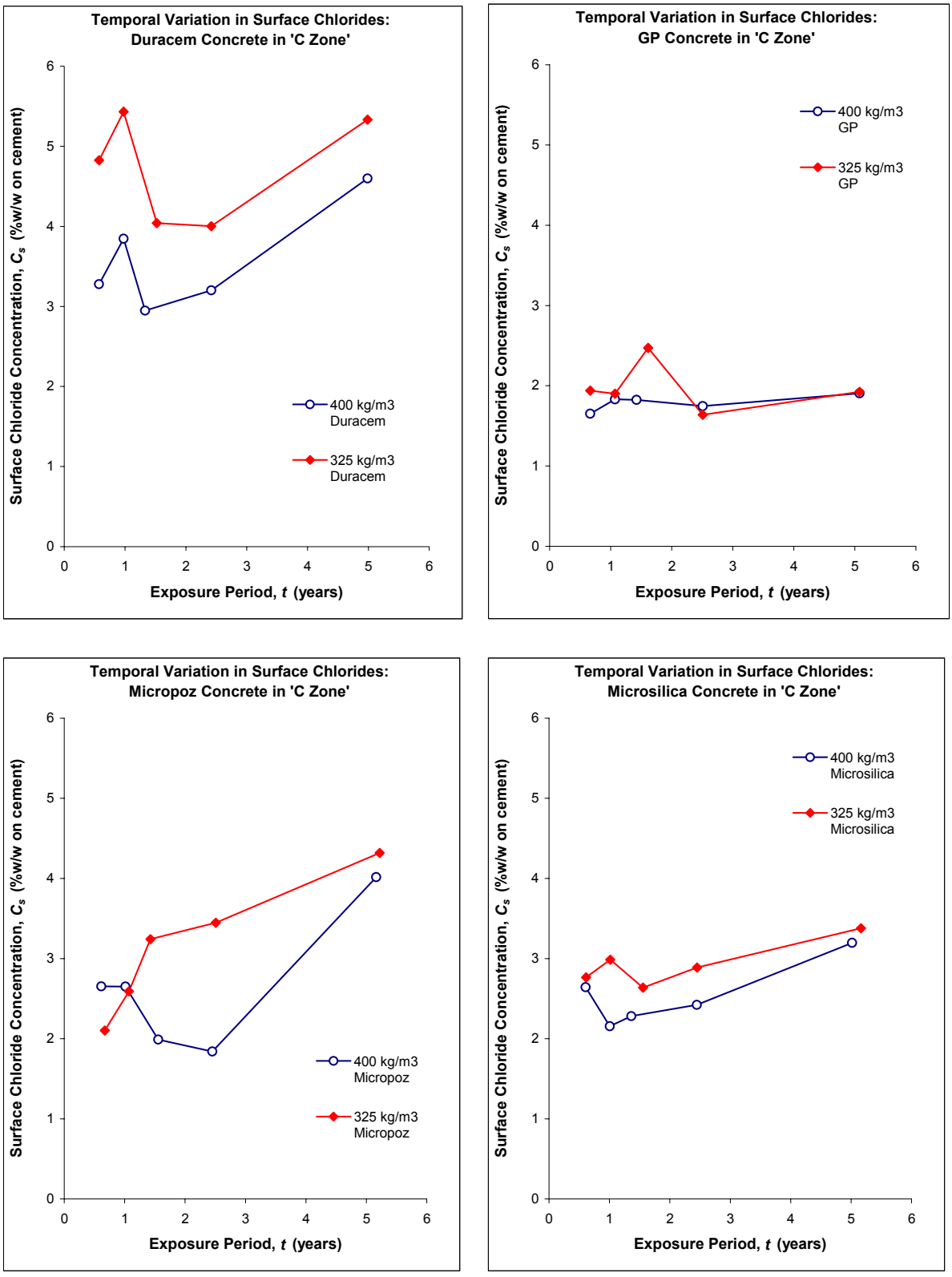

Figure 14: Variation in the calculated surface chloride profile, C_s, with period of exposure for concretes on the Weka Bay C Zone severe marine site

Table 8: Mean values and upper 90% confidence limits for derived Cs values from the severe marine C Zone exposure site

	Surface Chloride Concentration, C_s			
	% by weight of concrete		% by weight of cement	
	mean	upper 90% confidence limit	mean	upper 90% confidence limit
325 kg/m³ mixes				
Duracem	0.60	0.78	4.7	5.9
GP	0.13	0.41	2.0	2.6
Micropoz	0.32	0.54	3.2	4.8
Microsilica	0.33	0.57	3.0	3.8
400 kg/m³ mixes				
Duracem	0.50	0.70	3.5	4.6
GP	0.10	0.38	1.8	2.1
Micropoz	0.47	0.71	2.6	3.9
Microsilica	0.31	0.43	2.5	3.3

2.4.3 Temporal dependence of effective diffusivity

Figure 15 and Figure 16 plot the individual D_{ce} values determined from the chloride profiles for each concrete type against the corresponding period of exposure. The plots are in a double logarithmic coordinate scale and include the best-fit line arising from a linear regression of $\log(D_{ce})$ vs $\log(t)$ to verify whether the relationship given by equation [1-4] holds. Also included are 90% confidence limits for the values of D_{ce}, derived from the uncertainty in the slope (i.e. the time-reduction index, m) and intercepts of the log–log plots. Of particular significance are the possible boundaries for the value of the effective diffusion coefficients after 28 days exposure, D_{28}, which is a usual input into empirical Fick's Law models.

The Fick's Law input parameters derived from regression analysis of the diffusion coefficient data are given in Table 9 and a summary of the statistical quality of the fit to a linear relationship between $\log(D_{ce})$ and $\log(t)$ is given in Table 10. The effective diffusion coefficients for the Duracem slag concrete show both the strongest temporal dependence (mean m values of 0.5 – 0.6) and the best correlation to the predicted logarithmic relationship. For all of the Duracem, Micropoz and Microsilica mixes, it was statistically possible to reject the null hypothesis (that there is no relationship between effective diffusivity and time) at the 90% confidence level, although the scatter in the data is high and the relationship is not especially convincing for the 325 kg/m^3 Micropoz and Microsilica concretes. In contrast, both the GP concretes demonstrate very small mean time-reduction indices that are not statistically separable from a constant effective diffusivity (i.e. $m = 0$).

With appropriate values of C_s, D_{28} and m derived for a particular concrete type and exposure environment, prediction of service life simply becomes a case of solving equation [1-5] for t, knowing the designed reinforcing cover, x, and assuming a corrosion initiation threshold, usually taken to be $C_{(x,t)} = 0.4\%$ chloride by weight of cement. Table 11 demonstrates the calculated life for the concrete specimens, supposing 50 mm of cover to the steel reinforcement.

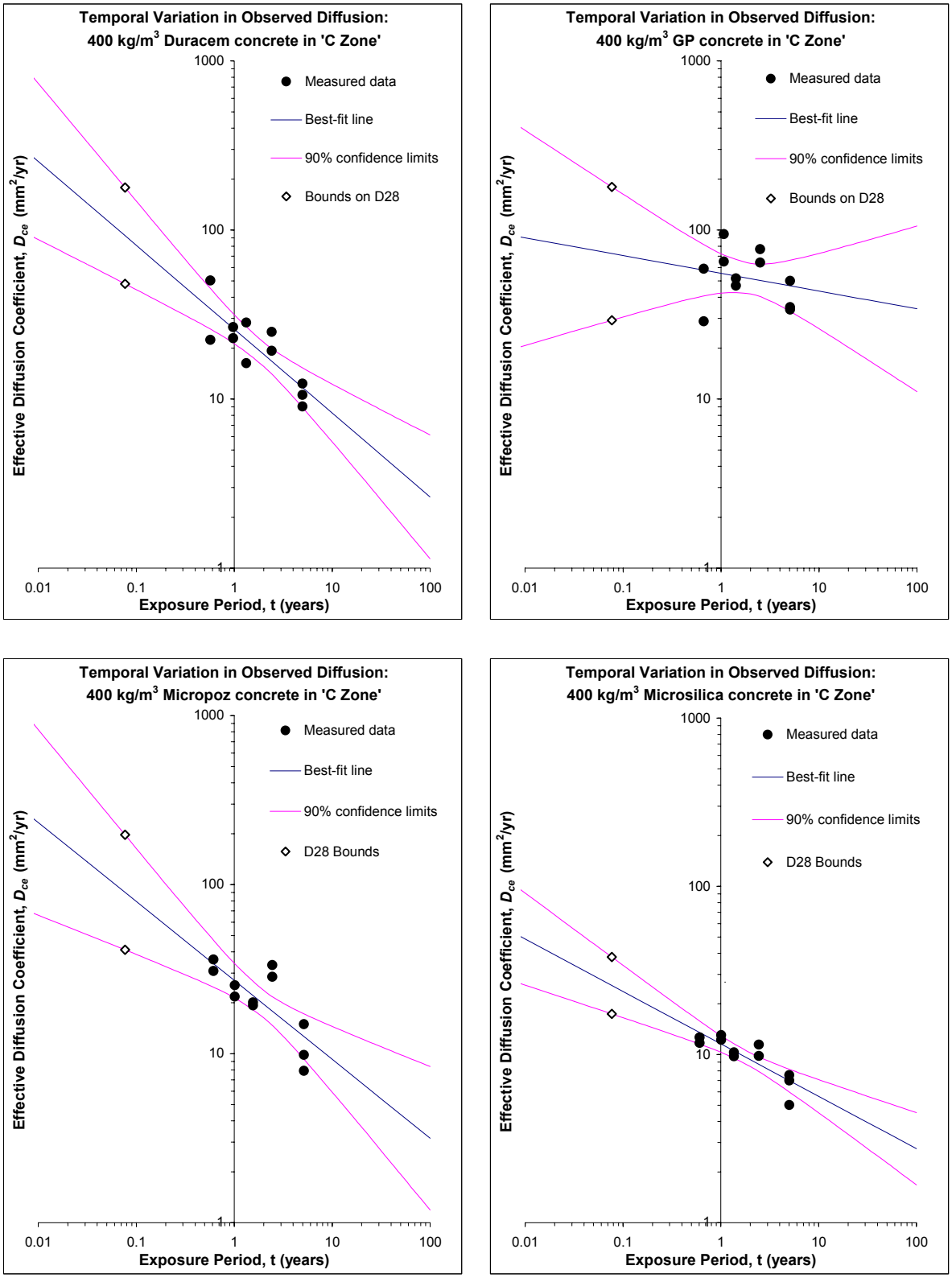

Figure 15: Variation in the effective diffusion coefficient, D_{ce}, with age for the 400 kg/m^3 total binder concretes on the Weka Bay C Zone severe marine exposure site. The best fit linear regression line and standard error curves for a 90% confidence level are shown

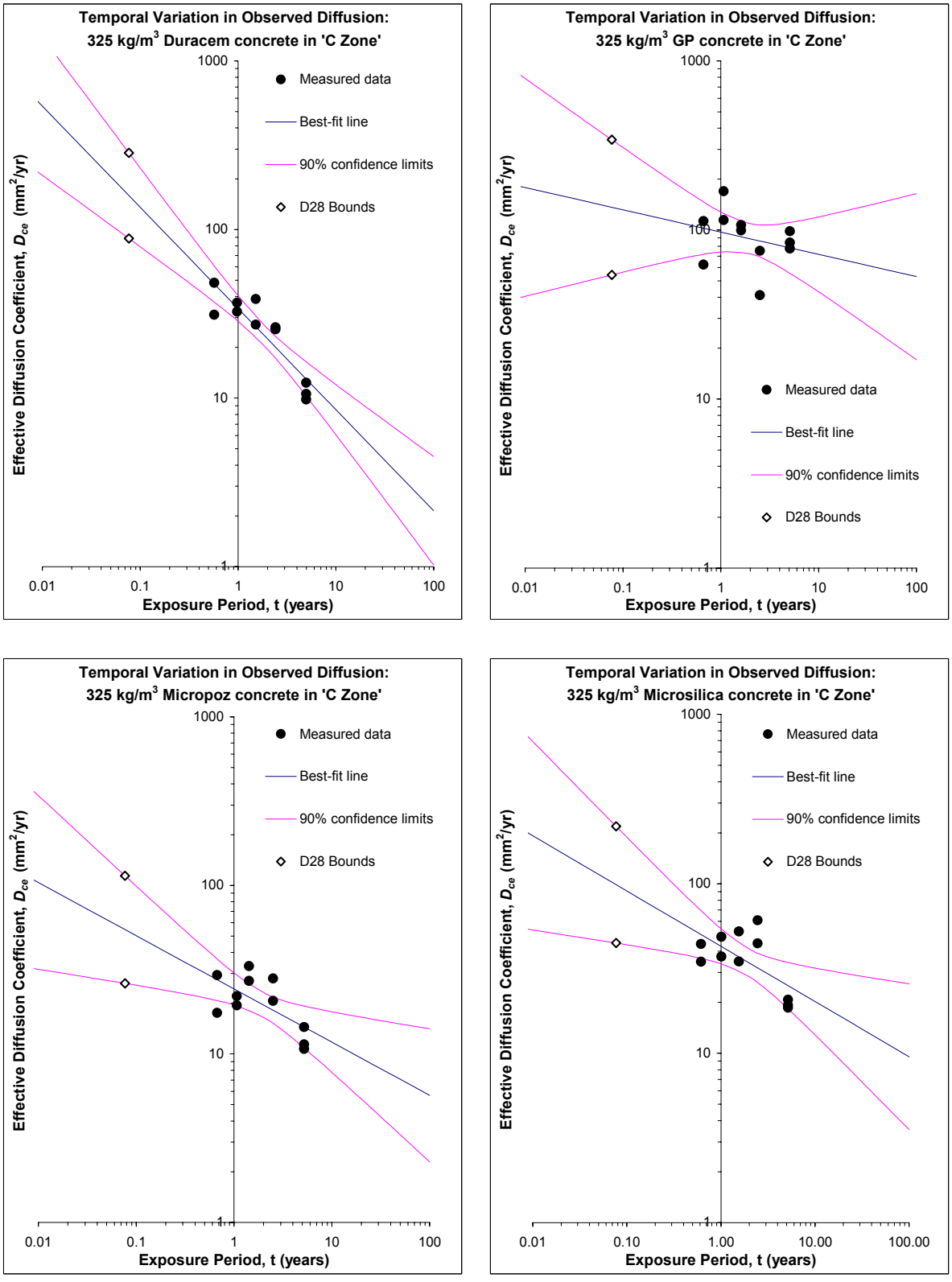

Figure 16: Variation in the effective diffusion coefficient, D_{ce}, with period of exposure for the 325 kg/m^3 total binder concretes on the Weka Bay C Zone severe marine exposure site. The best fit linear regression line and standard error curves for a 90% confidence level are shown

Table 9: Derived time-reduction indices and 28 day effective diffusion coefficients calculated from regression analysis of exposure site data

Concrete Type	Time Reduction Index, m			Effective Diffusion Coefficient, D_{28}		
		90% confidence limits			90% confidence limits	
	mean	upper	lower	mean	upper	lower
325 kg/m^3 mixes						
Duracem	0.60	0.78	0.42	159	285	89
GP	0.13	0.41	-0.15	136	342	54
Micropoz	0.32	0.54	0.09	55	114	26
Microsilica	0.33	0.57	0.08	99	219	45
400 kg/m^3 mixes						
Duracem	0.50	0.70	0.29	93	178	48
GP	0.10	0.38	-0.17	73	180	29
Micropoz	0.47	0.71	0.23	90	197	41
Microsilica	0.31	0.43	0.19	26	38	17

Table 10: Statistical fit of the experimental data to equation [1-4] linking effective diffusivity with time

Concrete Type	$\log D_{ce} - \log t$ Correlation	Accept temporal diffusivity?
	r^2 value	(rejection of null hypothesis)
325 kg/m^3 mixes		
Duracem	0.81	Yes
GP	0.08	No
Micropoz	0.42	Yes
Microsilica	0.40	Yes
400 kg/m^3 mixes		
Duracem	0.69	Yes
GP	0.05	No
Micropoz	0.59	Yes
Microsilica	0.71	Yes

Table 11: Predicted mean and worst case (90% confidence limit) times to corrosion initiation, from initial exposure to chloride-ions, for concrete on the severe marine exposure site. These figures presuppose 50 mm of cover over the reinforcing

Concrete Type	Predicted Service Life (years to corrosion initiation with 50 mm rebar cover)	
	mean value	upper 90% confidence limit
325 kg/m^3 mixes		
Duracem	555	29
GP	11	5
Micropoz	90	12
Microsilica	46	7
400 kg/m^3 mixes		
Duracem	346	25
GP	21	10
Micropoz	325	18
Microsilica	341	76

The absence of any temporal improvement in effective diffusivity is reflected by very short predicted lives for both of the GP concrete mixes. This reality is already evident in the 60-month chloride profiles, where the chloride concentration in the 40 – 45 mm depth increment is already approaching corrosion threshold values. Note that this is despite the GP concrete having a slightly better mean D_{28} value than the much better performed Duracem mix, again reinforcing the sensitivity of life prediction to the chosen reduction index for the effective diffusion coefficient.

The 400 kg/m^3 mixes containing SCMs all have similar mean predicted lives in the vicinity of 325 – 350 to years. Interestingly, the relatively small time-reduction index for the Microsilica concrete is compensated for by its very low initial effective diffusivity (Table 9) and also to some extent by the smallest surface chloride levels developed on the blended cement concretes. The Microsilica mixes' low D_{28} value is seen to advantage in the calculated 'worst-case' life where the Microsilica performance is less affected than the other mixes by the large amount of scatter in the derived m values. This reduces the contribution of temporal improvements in chloride resistance.

It is unclear why the 325 kg/m^3 Duracem concrete should appear to perform better than the equivalent 400 kg/m^3 mix; given the scatter in, and high sensitivity of the life calculation to, effective diffusion coefficients. This may simply be a statistical aberration. It is generally assumed that increasing the binder content, and hence lowering the w/b ratio, of a concrete will reduce the initial value of D_{ce} but not significantly change its temporal dependence (i.e. m). This seems to be confirmed by the derived values for the Microsilica and GP concrete, and to a lesser extent the Duracem concrete also. The performance of concrete containing silica fume, such as Micropoz, under aging has been the matter of some debate, with a wide range of differing time-reduction indices reported. A synthesis of published literature results suggests the temporal improvement of diffusivity in silica fume concrete strongly depends on w/b ratios,[30] possibly explaining why the mean Micropoz m value increases more than that of the other SCMs with an increase in binder content from 325 kg/m^3 to 400 kg/m^3.

The high variability of the collected effective diffusion coefficient data from the idealised $\log(D_{ce}) - \log(t)$ linear relationship apparent in Figure 15 and Figure 16 is reflected in the very large differences between the mean predicted time-to-corrosion initiation and the life that can be guaranteed with 90% confidence (Table 11). This uncertainty is almost entirely due to the variability of the chloride penetration of the concrete itself, rather than imprecision in the techniques used; analysis suggests the experimental inputs for determining the chloride profile (depth, concentration) have associated uncertainties of < 1%.

While the results obtained provide some degree of confidence that the apparent chloride resistance of Duracem, Microsilica and Micropoz does improves with time, the data is not precise enough to be useful for design purposes. The degree of imprecision is a concern, considering that the results were obtained from a very idealised situation; i.e. well-compacted and well-cured 'lab-crete' samples of simple geometry that were not subject to significant mechanical or thermal stress. The variables influencing chloride ingress in a real structure would reasonably be expected to be more numerous and more complex. Accordingly this observed improvement in chloride diffusivity should not be used as a justification for reducing cover depths, or lowering binder content, or increasing w/b ratios for durability design of marine concrete.

2.4.4 The relationship between actual and equivalent diffusivity

In addition to sampling the concrete to determine its chloride profile, the 'actual diffusion coefficient', D_{ca}, of the concrete was measured in the laboratory. This was an attempt to assess any temporal dependence in the 'pure' diffusivity of the concrete, isolated from any interfering effects of the environment or non-diffusion transport mechanisms. Changes in D_{ca} should solely reflect the connectivity of the concrete's pore structure. To make these measurements, virgin sections of concrete (taken from sufficiently deep in the test cores to be uncontaminated with chloride) were carefully water-saturated, sealed to ensure only uniaxial diffusion through a single surface was possible and exposed to a synthetic seawater solution for 35 days at 23ºC. The resulting profiles were then analysed as previously described. Figure 17 and Figure 18 show the variation of D_{ca} with exposure time.

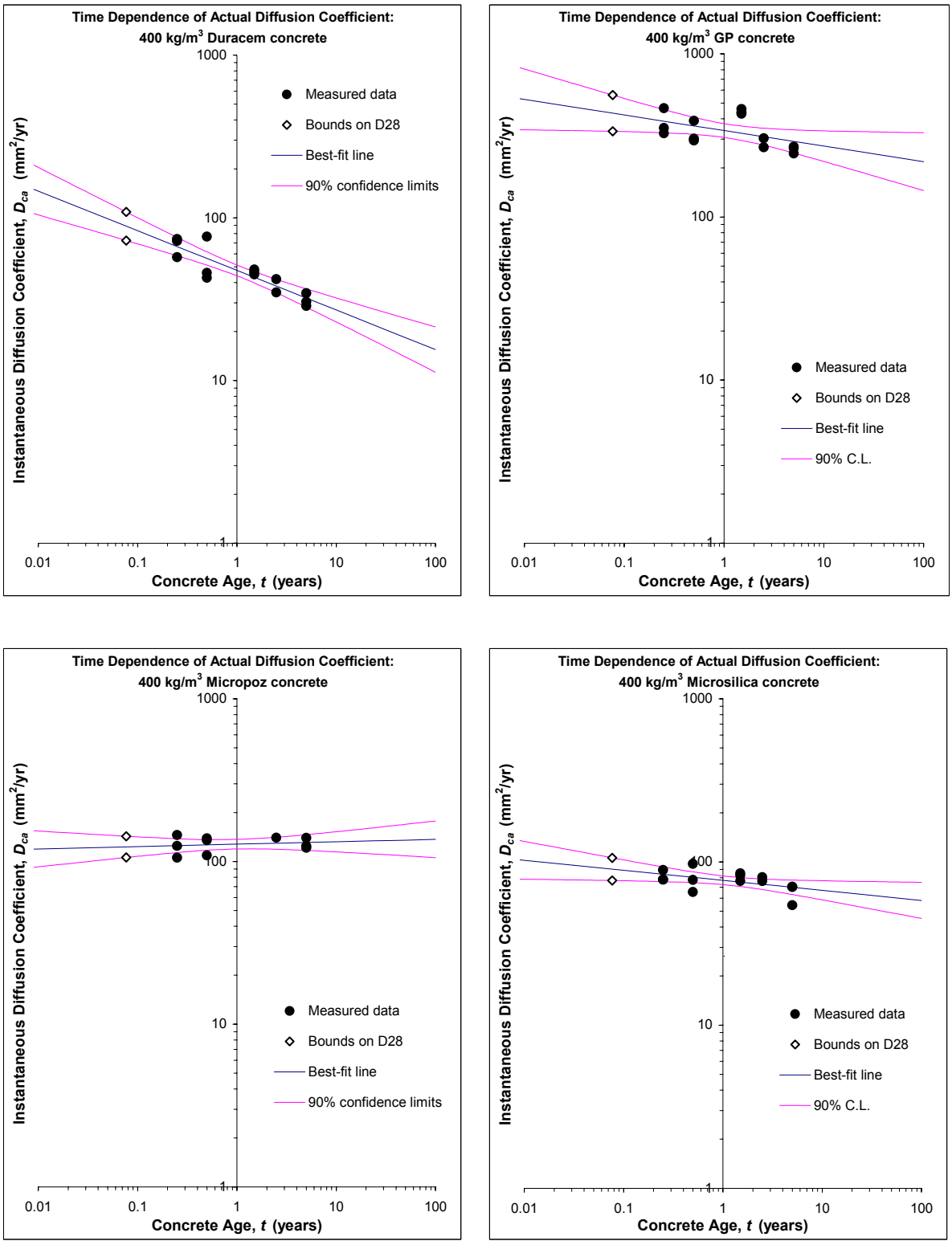

Figure 17: Variation in the actual diffusion coefficient, D_{ca}, with age for the 400 kg/m^3 total binder concretes, measured on uncontaminated cores. The best fit line and standard error curves for a 90% confidence level are shown

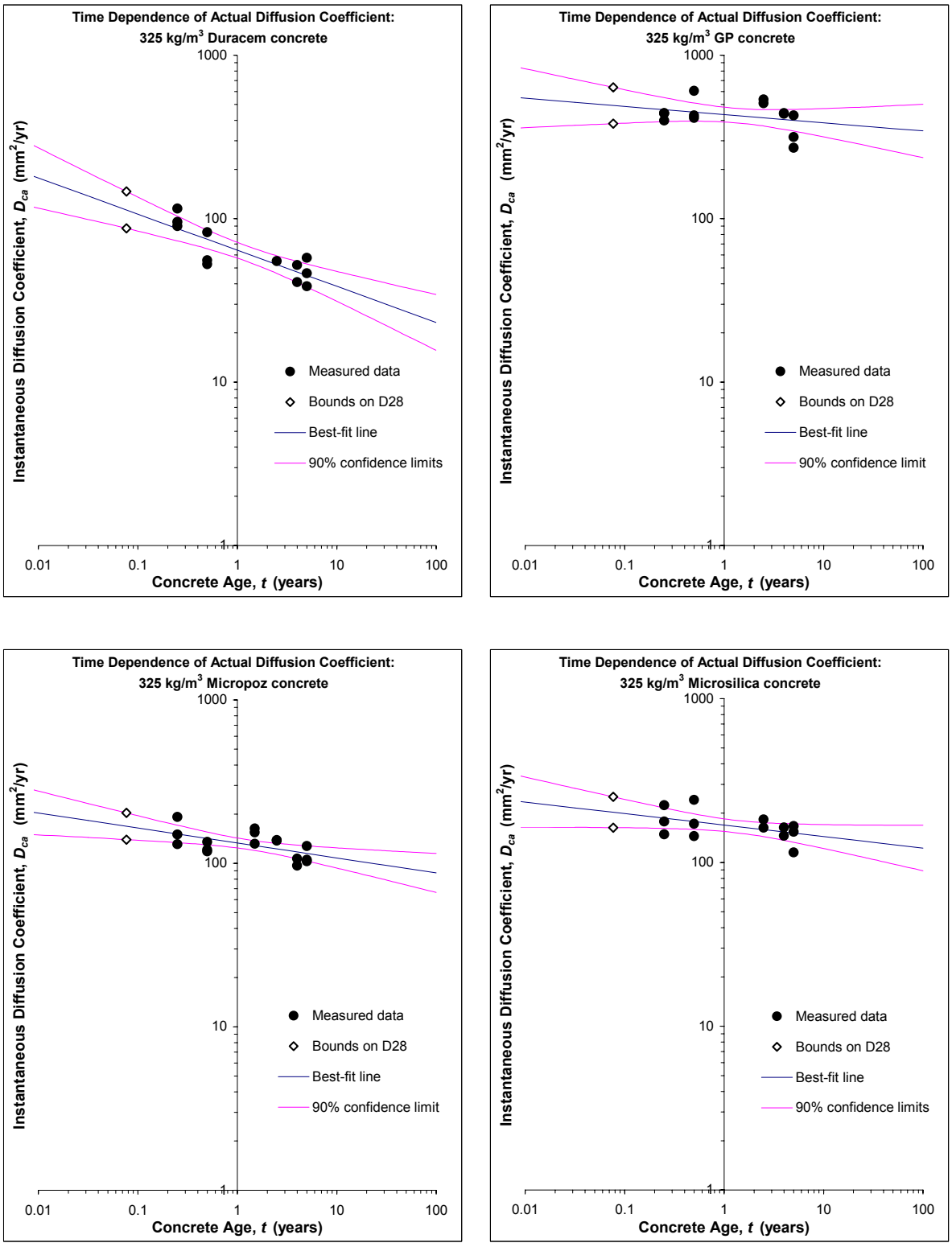

Figure 18: Variation in the actual diffusion coefficient, D_{ca}, with age for the 325 kg/m^3 total binder concretes, measured on uncontaminated cores. The best fit line and standard error curves for a 90% confidence level are shown

The primary purpose of this testing was to verify whether the change in diffusivity with time is related to continued hydration of the cement phases within the concrete. Hydration of the cement phases, supplemented by pozzolanic reaction for mixes containing SCMs, refines and tightens the pore structure of the hydrated cement gel, thereby increasing its resistance to chloride ingress over time. This is the usual explanation given for the temporal dependence of diffusion coefficients.[31]

If this hypothesis is correct, and is solely responsible for the temporal changes in effective diffusion coefficients observed on the exposed concrete, then there should be a relationship linking D_{ca} and D_{ce}. Such a relationship is of great potential value. While only effective chloride diffusivity is ultimately important for service life, this information can only be determined 'after the fact' from field measurements or by analogy with existing concrete in a similar environment. This is information that may not be conveniently available at the design stage. In contrast, actual diffusivity is a material property that could be readily determined in the laboratory on trial mixes.

Existing information on the relationship between the two different diffusivity determinations is somewhat contradictory. Maage et al present data that suggests D_{ca} approximates D_{ce} shortly after exposure and that the ratio $D_{ce}(t)$ / $D_{ca}(t)$ decreases with age in a predictable way. Mathematically if the temporal reduction in effective diffusivity solely reflects a genuine improvement in the intrinsic resistance of the concrete to chloride diffusion then:

$$D_{ce}(t) = \frac{\int_{t_{ex}}^{t} D_{ca}\left(\frac{t_0}{t}\right)^n dt}{\int_{t_{ex}}^{t} dt} \qquad [2\text{-}1]$$

where t_{ex} is the time of exposure to the initial chloride environment.

The key point of equation [2-1] is that D_{ce} should, theoretically, represent a *time-averaged* value of the actual diffusivity, D_{ca}. If any temporal dependence is present in these diffusion coefficients, D_{ce} will change more slowly than D_{ca}, an instantaneous parameter, and correspondingly have a smaller time-reduction index. Figure 19 compares the variation of the idealised (best-fit) D_{ca} and D_{ce} values for the concrete mixes on the severe marine exposure site. Two points are immediately clear from this graphic: first, there is not necessarily a single time during the exposure period where $D_{ca} \approx D_{ce}$ and, even where such an intersection exists, it appears to be unique to each concrete type (this clearly eliminates the hope of a simple relationship between the two diffusivity measurements). Secondly, the time-reduction indices observed for D_{ca} (i.e. the slope of the best-fit line) are, in all cases, smaller than those for D_{ce}. Thus it is not possible for the hypothesis of continued hydration to completely explain the reduction in effective diffusivity observed for the exposure site concrete. This mechanism must make a partial contribution in some cases – both Duracem concretes show small but statistically significant reductions in D_{ca} for example – but is not evident at all for the 400 kg/m^3 Micropoz concrete, despite its significant improvement in chloride resistance with aging.

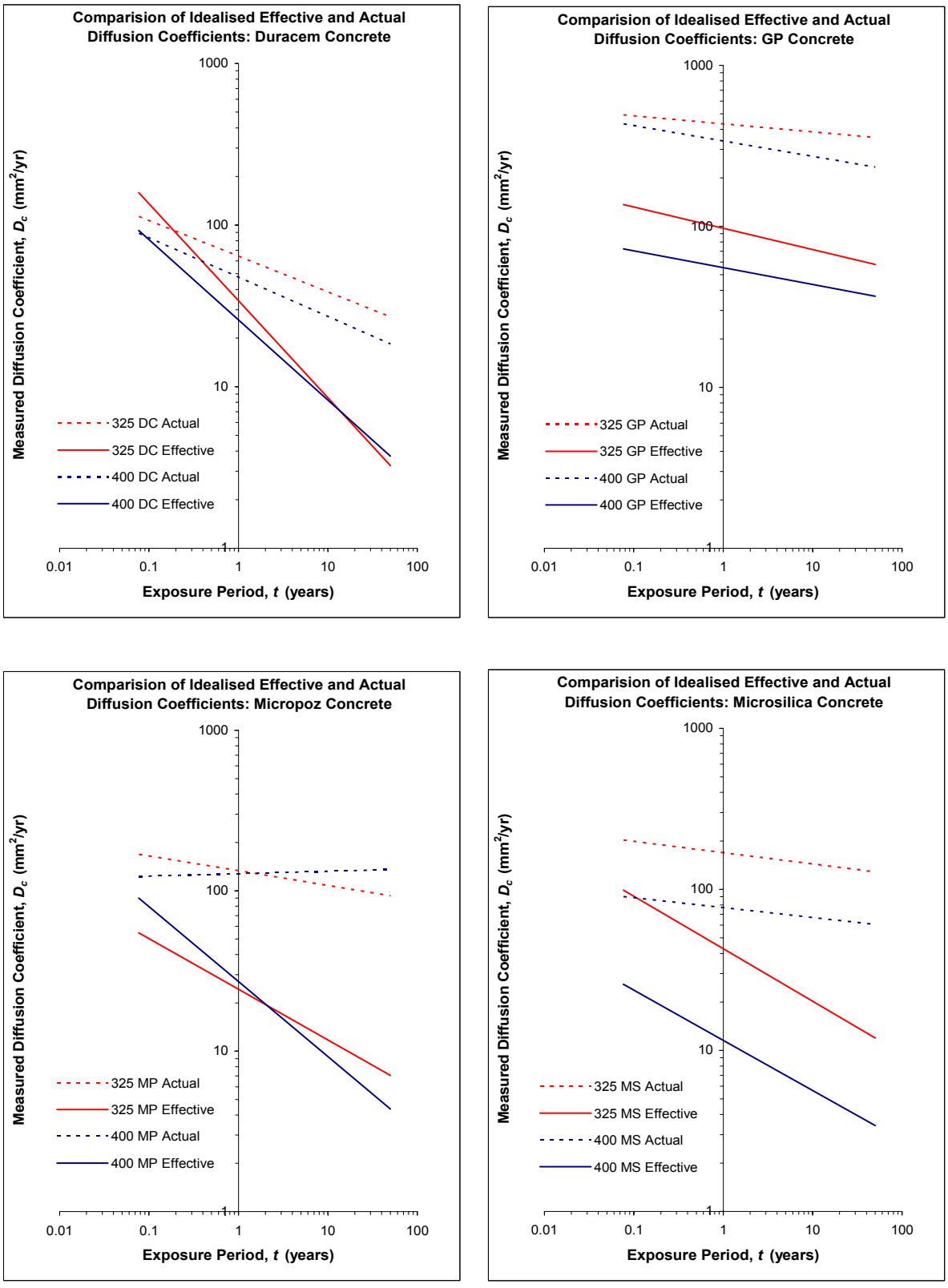

Figure 19: Comparison of the temporal variation of idealised actual and effective diffusion coefficients

Another physical explanation of the apparent temporal dependences in diffusivity is the formation of brucite [$Mg(OH)_2$] and calcite [$CaCO_3$] as a consequence of ion exchange between the cement paste and seawater. This pore-blocking reaction can result in the gradual development of a surface skin on the concrete with a significantly reduced permeability.[32] The optimal condition for improvements in intrinsic diffusion are constant immersion, providing an abundance of water for both ion-exchange and continued hydration. Therefore, hydration and self-sealing reactions are less likely to have developed on the test specimens because they were only subjected to intermittent wetting by wave action. As previously noted, however, these 'splash-zone' conditions are a worst-case for the risk of chloride-induced corrosion.

Other possible reasons for the temporal dependence of effective diffusivity are not linked with an inherent material improvement with time, and hence could not be guaranteed to occur for every structure, casting some doubt on the reliability of incorporating this factor into design tools. Evident improvement in chloride resistance may simply reflect:

Misinterpretation of a spatial variation as an apparent temporal variation: While D_{ce} is frequently assumed to be a function only of time, it is probable that it is also spatially dependent. The exposed surface of most concrete is likely to have a diffusion coefficient significantly inferior to that of its interior. For example, Higgins[33] has shown that the cement-to-aggregate ratio is much higher in the 10 – 15 mm of concrete immediately adjacent to a cast face than in the main body. The surface is also likely to be less well-cured and more extensively carbonated, thereby reducing chloride binding ability, and to have connected capillary pores directly in contact with the environment. All these factors serve to increase diffusivity. Computer simulations by Bentz et al[34] have demonstrated that if the diffusivity of the surface concrete exceeds that of the interior, a conventional Fick's Law analysis will predict a power law type behaviour for D_{ce} with time even when no such relationship actually exists. This arises from the fact that the higher-diffusivity outer layer is traversed earlier in time than the bulk concrete by the penetrating chloride front.

Misinterpretation of a change in the predominant transport mechanism with an apparent temporal variation: As previously noted, D_{ce} is a 'bundled' parameter that measures the combined effect of all possible chloride transport mechanisms without distinction. It seems reasonable that for concrete that is only infrequently splashed by waves, initial ingress is dominated by absorption due to capillary action, as the relatively dry near-surface pores are wetted by chloride solutions. However, once a concentration is established in this zone, and at greater depths where the pores are more likely to be saturated, diffusion will play a far greater role. A numerical simulation of chloride transport in non-saturated concrete indicates that absorption gives rise to more rapid ingress than diffusion.[35] The one-off transition in transport mechanisms (from absorption to diffusion) would appear as a temporal improvement in D_{ce}. Extrapolating this short-term behaviour of D_{ce} over the projected life of a concrete structure risks an unduly optimistic assessment of potential life.

2.4.5 B2 Zone exposure conditions – Oteranga Bay

In addition to the severe marine exposure site, BRANZ also placed lesser grades of concrete on two additional natural exposure sites subjected to milder conditions, zoned B2 and B1 under the durability classification of NZS 3101.

The chloride profiles determined on the B2 Zone samples, located in Oteranga Bay approximately 100 m above the high tide mark on a wind swept southerly coast, are shown in Figure 20 and Figure 21. The concrete on this site is never directly splashed by wave action but is subjected to some of the highest chloride deposition rates in New Zealand. Despite this, the extent of the chloride ingress is significantly less advanced than in the C Zone, almost certainly

due to a combination of no direct imbibing of brine through capillary absorption and drier internal concrete reducing the potential for diffusion.

As with the C Zone site the environmental chloride load, quantified as the regression fitting parameter C_s, is established quickly and remains relatively constant thereafter, as seen in Figure 22. The C_s values are typically around one-third of those seen for the concrete directly wetted with seawater. The surface chloride concentrations of the 280 kg/m^3 Duracem concrete appear to show an exception to this pattern, with a continuous rise in the C_s value. This is, in fact, largely an artefact of the fitting procedure used to model the chloride profiles. The later profiles demonstrate a 'skin effect' wherein the chloride concentrations are locally depleted, i.e. the maximum concentration occurs as a peak some distance below the concrete's surface. The curve-fitting omits those experimental points that obviously deviate from the idealised Fick's Law behaviour, resulting in an exaggeratedly high C_s parameter as depicted in Figure 23. The chloride peak is commonly observed in profiles from field structures. It is usually ascribed to the progress of atmospheric carbonation reactions converting hydrated cement phases to calcium carbonate, thus both reducing the chloride binding capacity of the affected surface and liberating the previously bound chlorides to deeper into the concrete. Carbonation has not been measured on the exposure site concretes; however the relative depletion of free lime in slag cements is known to increase their susceptibility. It is unsurprising that the chloride profile of the lower grade Duracem concrete would be affected first.

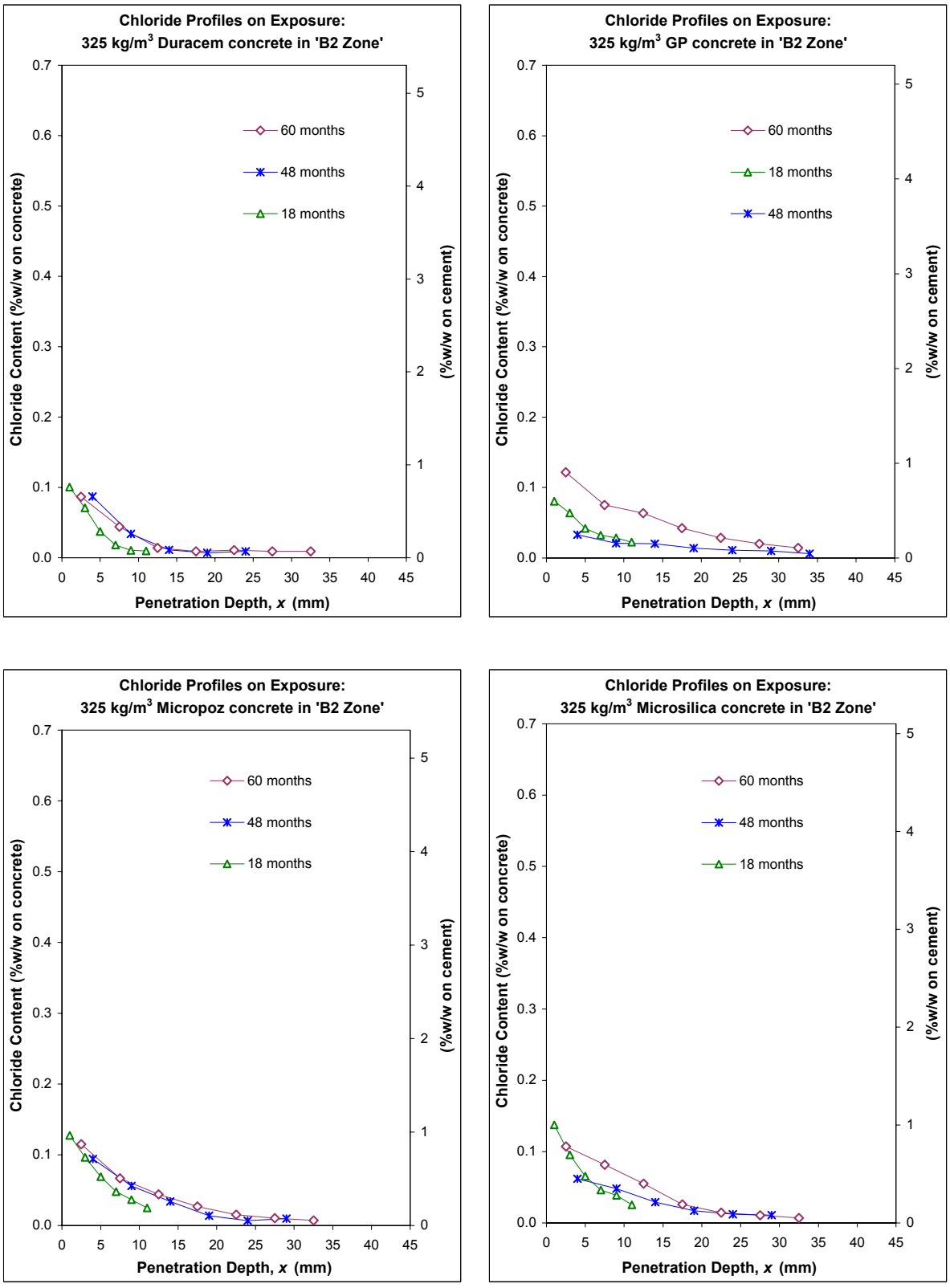

Figure 20: Chloride profiles for the 325 kg/m^3 total binder content concrete mixes after five years' natural exposure on the Oteranga Bay B2 Zone site

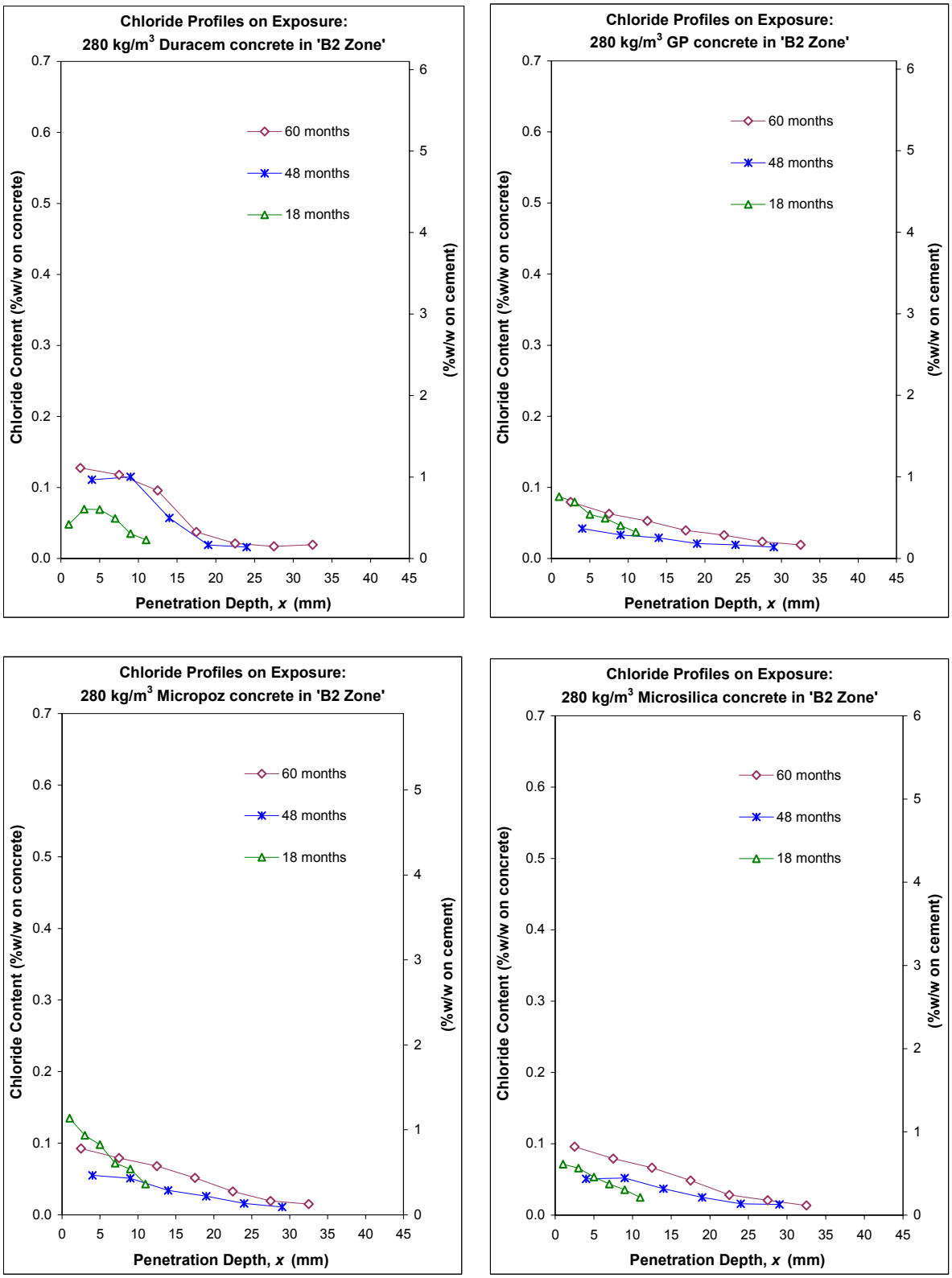

Figure 21: Chloride profiles for the 280 kg/m^3 total binder content concrete mixes after five years' natural exposure on the Oteranga Bay B2 Zone site

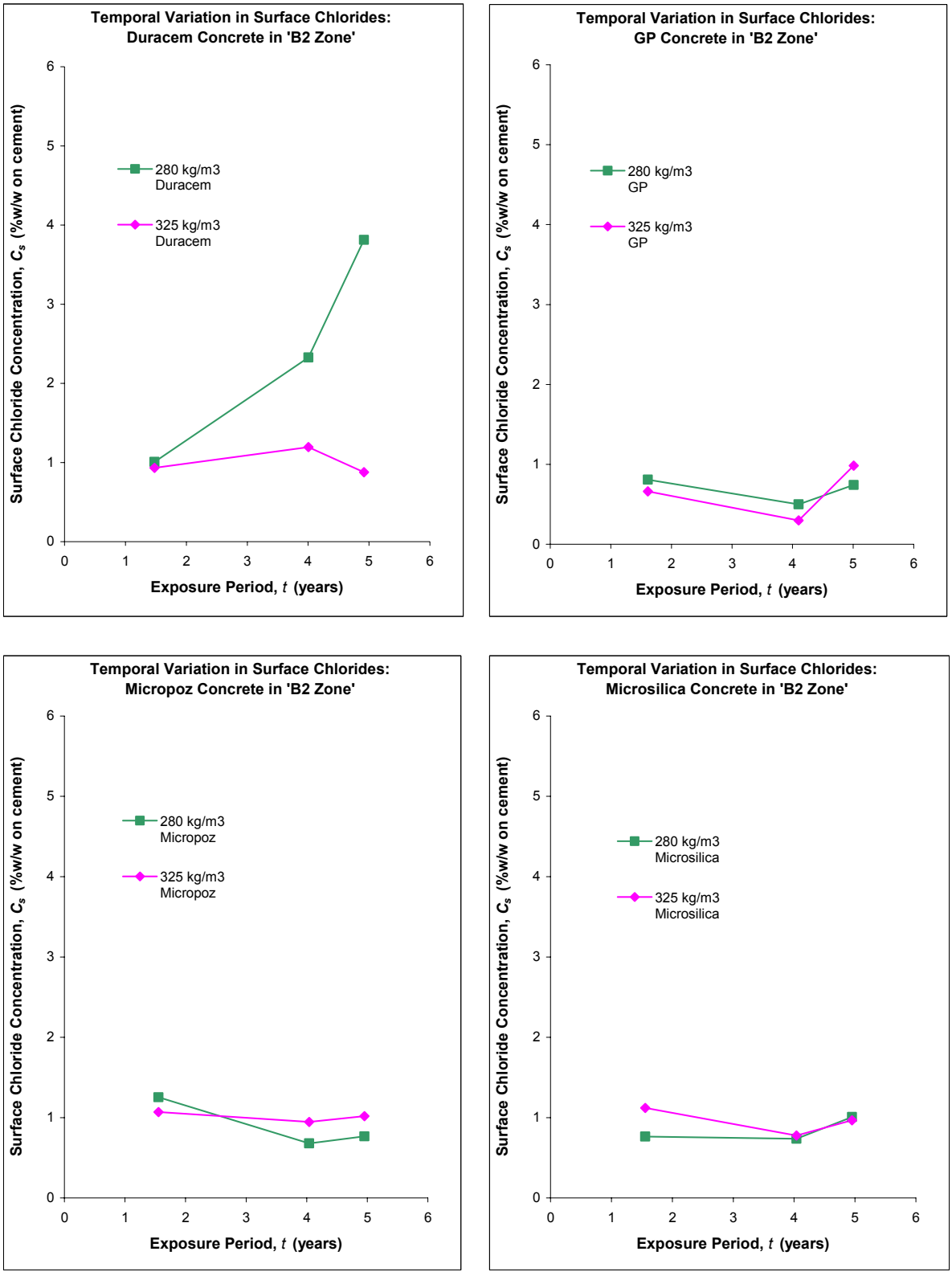

Figure 22: Variation in the calculated surface chloride concentration, C_s, with period of exposure for concretes on the Oteranga Bay B2 Zone site

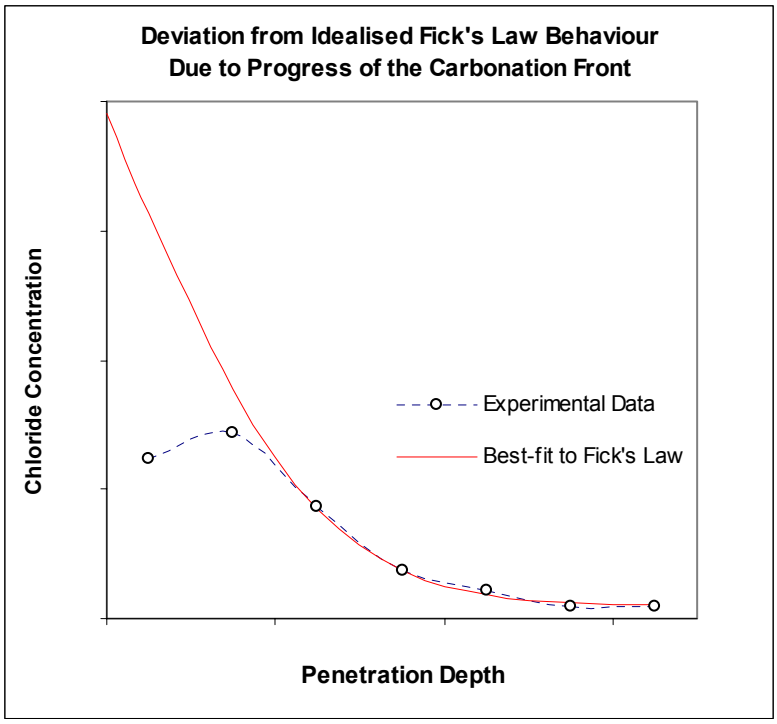

Figure 23: Where measured chloride profiles deviate from the idealised solution to Fick's Law exaggerated regression parameters for the surface chloride concentration can result

Thee effective diffusion coefficients determined for concrete on the B2 exposure site are shown in Figure 24. They must be regarded with a degree of caution because the amplitude of the chloride profiles from which they were derived is relatively small. However, it appears that unlike the directly wetted concrete on the severe marine site, there is no evidence for a temporal component to D_{ce}. This further supports the contention that any age-related improvement in resistance to chloride ingress is the result of interaction with a specific environment rather than an inherent material property of concrete containing SCMs. The apparent exception of the 280 kg/m^3 Duracem concrete performance is again a consequence of the potentially erroneous C_s values: a constant rate of chloride ingress under an (apparently) increasing environmental load appears as in improvement in effective diffusion when analysed with a simple Fick's Law model.

The lack of temporal component to D_{ce} may reflect that the transport mechanisms for the concrete on the B2 site are likely dominated by absorption rather than diffusion because of the dry or only partially-saturated capillary pore network. This may vary, depending on, for example, how rain-washed the exposed face of the concrete is. It is likely that local micro-climates will strongly influence the appropriate inputs (C_s, m, D_{28}) required for the use of Fick's Law type models in the less severe exposure zones where the environmental chloride load is less predictable.

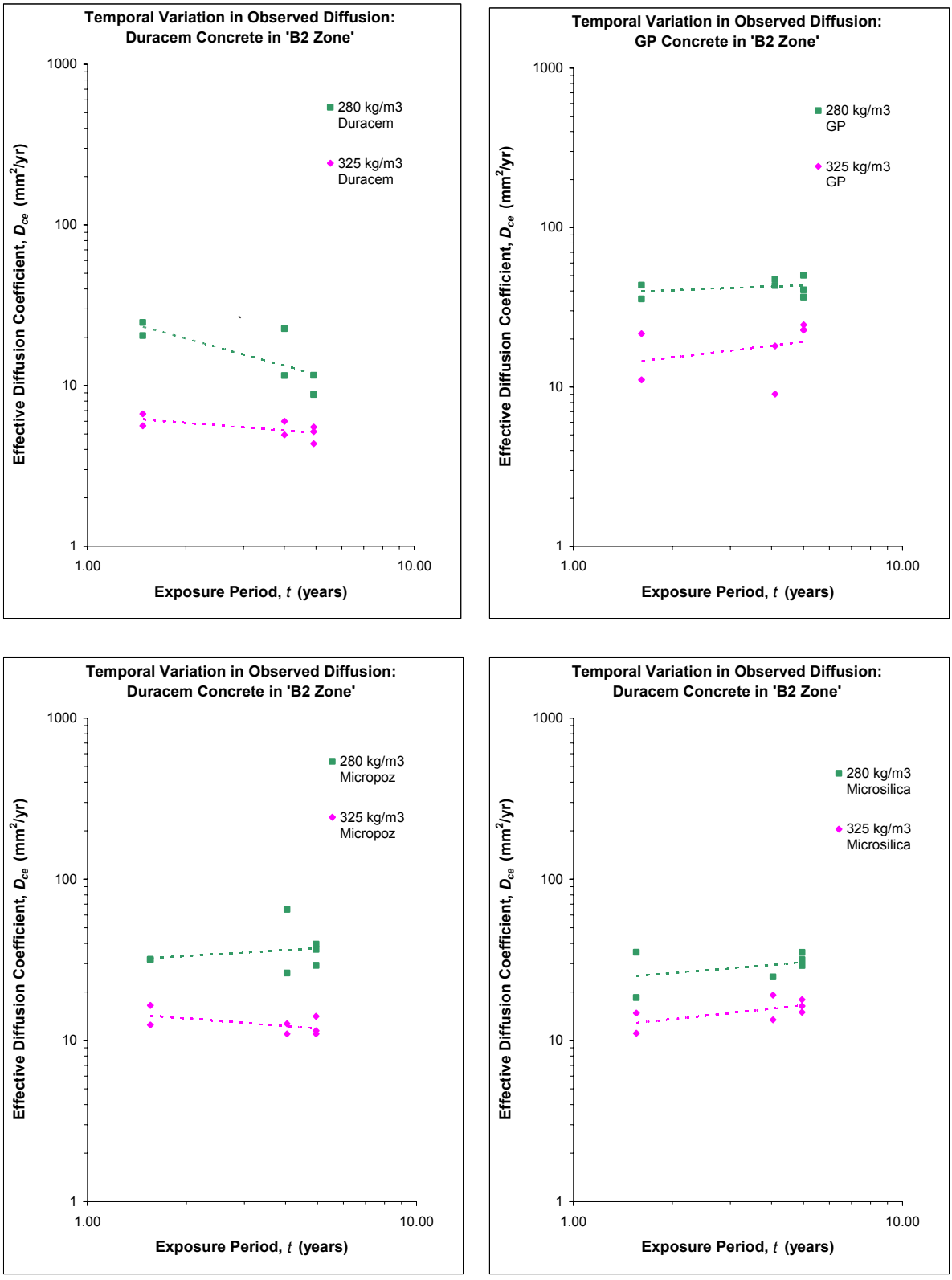

Figure 24: Variation in the effective diffusion coefficients with age for concretes on the Oteranga Bay B2 Zone exposure site

The durability performance of the Oteranga Bay site concrete is summarised in Table 12. The combination of reduced environmental chloride load and very small effective diffusion coefficients results in significantly extended corrosion initiation times for the 325 kg/m^3 concretes compared with the equivalent mixes on the C Zone site, assuming adequate cover and quality of construction. The lesser grade 280 kg/m^3 total binder content concrete should readily meet the 50 year durability requirements of the NZBC with respect to the risk of chloride ingress. Without any temporal improvement in diffusivity evident, there is little reason to favour concrete containing SCMs over standard Portland cement concrete for durability purposes. Only the Duracem concrete offers a significantly better diffusivity and this advantage appears to be potentially offset by its tendency to develop larger environmental chloride loads.

Table 12: Performance summary for concrete on the B2 Zone natural exposure site

Concrete Type	**Surface Chloride Concentration, C_s**	**Effective Diffusion Coefficient, D_{ce}**	**Predicted Time to Corrosion Initiation**
	%w/w on cement	mm^2/year	years
280 kg/m^3 mixes			
Duracem	2.4	17	40
GP	0.7	42	99
Micropoz	0.9	38	57
Microsilica	0.8	28	89
325 kg/m^3 mixes			
Duracem	1.0	6	317
GP	0.6	18	279
Micropoz	1.0	13	135
Microsilica	1.0	15	126

2.4.6 B1 exposure conditions – Judgeford

Concrete was exposed to the mildest level of chloride load at the BRANZ research station site in Judgeford. The nearest salt water is a tidal estuary, approximately 5 km distant which is itself protected from the open sea by gently rolling hills. The NZS 3101 exposure classification maps place the Judgeford site in the B1 coastal perimeter zone. Even at shallow depths in the lowest grade concrete, the chloride levels after five years' exposure did not significantly exceed the background concentrations of 0.010 – 0.015 %w/w initially present in the uncontaminated concrete (Figure 25). This confirms that electrolytic depassivation of reinforcement through carbonation is a more likely durability threat than chloride-induced corrosion for these moderate environments.

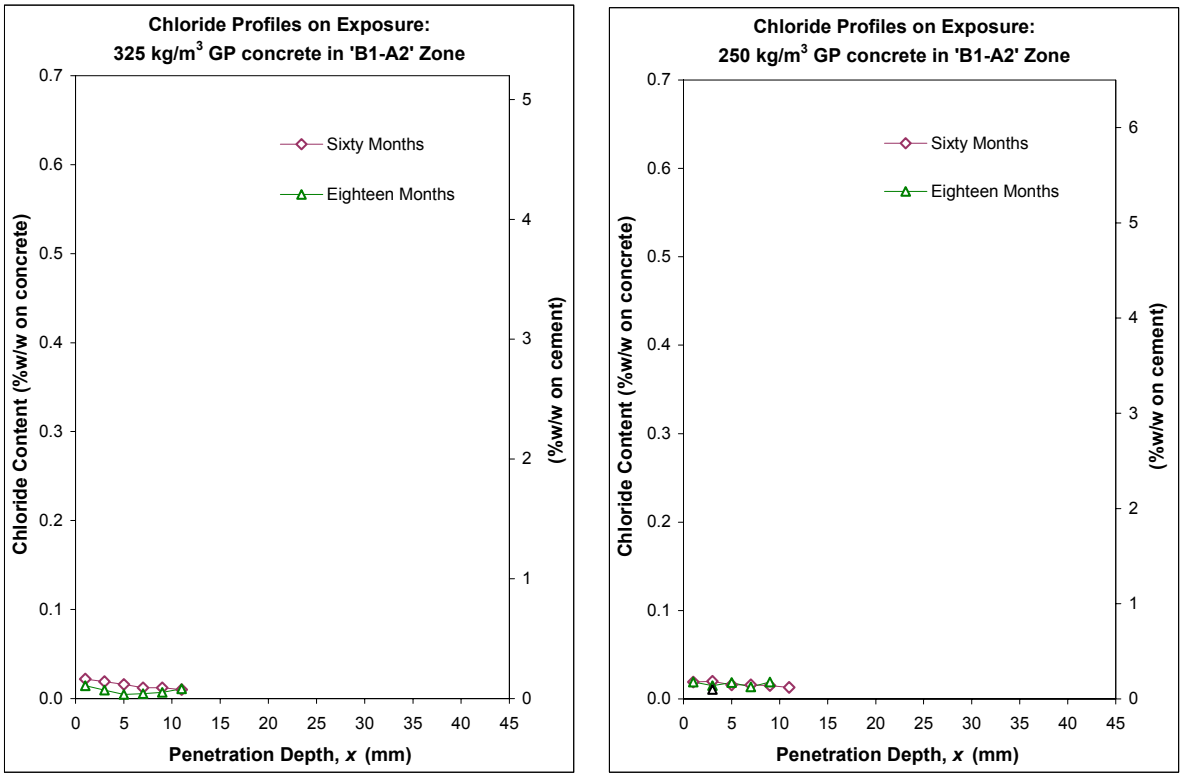

Figure 25: Chloride profiles after five years' exposure on the inland Judgeford B1 site

2.5 Conclusions from chloride ingress modelling

Experimental chloride profiles from a series of concrete blocks placed in environments corresponding to the NZS 3101 C, B2 and B1 exposure classifications for up to five years have been fitted to the error-function solution to Fick's 2nd Law. The curve-fitting has resulted in three parameters: a surface chloride concentration, C_s, quantifying the stress imposed by the environment and an effective diffusion coefficient, D_{ce}, characterising the concrete's response to the environmental stress, and an index, m, representing an apparent improvement in the diffusivity of the concrete with time. There is a large amount of scatter in this data, but a number of trends are evident:

- Concrete containing Duracem slag cement, Micropoz silica fume and Microsilica natural pozzolan all showed a statistically significant reduction in effective diffusion with time, indicating an improved resistance to chloride ingress.

- Of all the four binders tested, Duracem demonstrates the strongest temporal variation in diffusivity and seems the least sensitive to the proportion of binder in the concrete.

- The decrease in diffusivity with time cannot be completely explained by continued hydration reducing the connectivity of the pore structure in the cement, but does seem to require direct contact with seawater (rather than just exposure to chloride-laden aerosols) to occur. Therefore the apparent temporal dependence probably results from a complex interaction of distinct phenomena, which may not all be time-related.

- To a first approximation, C_s values appear to be established quickly and remain fairly uniform thereafter, justifying the use of a constant chloride concentration in life prediction calculations based on Fick's Law.

- The magnitude of D_{ce} and C_s both decrease substantially with reducing severity of the exposure environment.

- An appropriate C_s, a reference diffusion coefficient (D_{28} or equivalent) and a time-reduction index m, describing the rate of improvement in the diffusivity, are all needed to characterise the performance of a particular concrete in a particular environment. Most implementations of Fick's Law models offer guidelines for appropriate input values (refer Section 3 for more detail). Modelling of chloride ingress data from BRANZ's exposure studies suggests the following values may be reasonable inputs for durability prediction of concrete in the C Zone exposure classification:

Table 13: Suggested input values for service-life prediction in the C Zone

Binder Type	C_s (%w/w on cement)	D_{28} (mm^2/year)		m (time-reduction index)
		0.5 w/b ratio	0.4 w/b ratio	
Duracem	3.5 – 6.0	160 – 300	100 – 200	0.4 – 0.6
GP	2.0 – 2.5	140 – 350	75 – 200	0.0 – 0.15
Micropoz (silica fume)	3.0 – 5.0	50 – 120	90 – 200	0.1 – 0.3 (0.5 w/b) 0.2 – 0.5 (0.4 w/b)
Microsilica	2.5 – 4.0	100 – 220	25 – 40	0.2 – 0.3

The GP values are included for comparative purposes only. Plain GP concrete should not be used with mild steel reinforcement in the C Zone.

For service-life modelling of concrete in the B2 Zone, the following values may be suitable:

Table 14: Suggested input values for service-life prediction in the B2 Zone

Binder Type	C_s (%w/w on cement)	D_{28} (mm^2/year)		m (time-reduction index)
		0.6 w/b ratio	0.5 w/b ratio	
GP Concrete	0.8 – 1.2	15 – 50	5 – 20	No allowance for time-dependent diffusivity ($m = 0$)
SCM Concrete	1.0 – 1.5			

- There is no simple relationship between effective diffusion coefficients (D_{ce}) measured on field samples after long-term exposure and actual diffusion coefficients (D_{ca}) determined by early-age testing in the laboratory. This lack of correlation means the approach to service-life prediction typified by Fick's Law type models is only feasible if an extensive database of the model input parameters C_s, D_{28}, and m exists for well-characterised concrete under realistic exposure conditions.

- Until more rigorous theoretical models of chloride ingress are available, the empirical application of the error-function solution to Fick's 2nd Law offers a simple method for comparing and predicting durability performance in marine environments. However, this approach should not be used uncritically, particularly for the choice of input parameters. In the absence of an extensive database of chloride profiles determined on known concrete under natural conditions from which suitably comprehensive and statistically-reliable input data could be generated, any prediction of corrosion initiation time will necessarily be subject to a degree of uncertainty. Consequently, values produced by these models should not be used as justification to reduce reinforcement cover or w/b ratios when dealing with structures in marine environments.

3. AN EXAMINATION OF EXISTING SERVICE-LIFE PREDICTION MODELS FOR CONCRETE IN MARINE ENVIRONMENTS

3.1 Introduction

The review presented in this section was commissioned by Standards New Zealand for the sub-committee responsible for the 'Design for Durability' chapter of the 2005 revision of NZS 3101 *Concrete structures*. Standards New Zealand's generosity in allowing this information to be made freely available is gratefully acknowledged.

The brief for the review included:

- A comparative critique of the marine concrete service-life prediction models readily accessible by New Zealand designers of reinforced concrete structures.
- A comparison of the input values used by the various models, such as surface chloride concentrations, characteristic diffusion coefficients, time-reduction indices and any other relevant factors.
- The development of 50 and 100 year durability solutions for concrete containing blast-furnace slag cement, fly-ash or amorphous silica SCMs for the NZS 3101 C Zone exposure classification, based on model-calculated corrosion initiation periods of 40 and 80 years respectively.
- A review of existing cover – concrete strength solutions for 50 year service-life for pure GP cement concrete in the NZS 3101 B2, B1, A2 and A1 exposure classifications, as specified in Table 5.5 of the existing standard. Covers for the B2 Zone were based on model-calculated times for chloride-induced corrosion initiation; in the other zones it was assumed carbonation would be the dominant deterioration mechanism.

It was anticipated that Standards New Zealand would endorse suitable models as an alternative to prescriptive cover and strength requirements in the durability provisions of the revised standard. The review document is included in this work because it provides a valuable insight into the variability associated with the assumptions made by these relatively simple tools. The review was originally published in August 2003 and only minor editorial changes have been made here. Some of the information presented is no longer current, for example:

- The *'AGEDDCA'* model has now been formally published by the UK Concrete Society as TR61 'Enhancing Reinforced Concrete Durability', available as a book plus CD-ROM package from www.concreteinfo.org.
- The *'Diffuse6-13MS'* (*'Microsilica'*) model may no longer be accessible. Prospective users should contact Microsilica New Zealand for technical advice.

There may be other issues that the author is unaware of.

3.2 Scope

The particular models examined are detailed in Table 15. It was understood that the comparison would be based upon the initiation phase of the deterioration process only. In all of the models, the initiation phase is primarily based on a solution to Fick's 2nd Law of diffusion, incorporating temporal dependence in the chloride-ion diffusion coefficient.

Table 15: Service-life prediction models examined in the review

Name of Model	Version No	Supplier
AGEDDCA	10	UK Concrete Society / Taywood Engineering
CIM (Chloride Ingress Model)	2.2 (October 2002)	Holcim (New Zealand) Ltd / Concrete Consultancy Services
CIKS 'Computer Integrated Knowledge System for High Performance Concrete'	Website accessed August 2003	NIST (US National Institute of Standards and Technology)
Life-365™	1.1.0 (December 2001)	Grace, MBT, Silica Fume Association (US)
GBC / Microsilica NZ Model	Diffuse6-13MS	Microsilica NZ / ANCON Beton Pty Ltd

3.3 Nomenclature

Abbreviations used in this report are defined in Table 16.

Table 16: Definition of abbreviations

GP	Portland cement without SCMs
FA	Pulverised fly-ash
MK	Metakaolin
MS	Microsilica
SF	Silica fume
SL	Granulated blast-furnace slag
SCM	Supplementary cementitious material
HRP	High reactivity pozzolan (SF, MS, MK)
f′c	Specified strength (28 days)
C_s	Surface chloride concentration
C_t	Corrosion threshold chloride concentration
D_{ce}	Effective diffusion coefficient
D_{28}	Effective diffusion coefficient after 28 days exposure
m	Time reduction index for D_{ce}

For consistency, and to remain uniform with New Zealand usage, 'GP' signifies Portland cements without addition of pozzolanic or latent hydraulic supplementary additions. Research suggests that incorporation of inert fillers such as limestone does not significantly affect the diffusion of chloride-ions.[36]

3.4 Range of model applicability

Given that the assumptions implicit in each model are not necessarily shared between them, it seems desirable that any model endorsed by Standards New Zealand should be applicable to as wide a range of cement blends as possible. That is, it should be possible to compare a fly-ash concrete solution with a slag solution (say) without using separate models that may not share the same assumptions. Most of the models' input values are sufficiently customisable that this can be achieved by an operator with the knowledge to supply appropriate parameters for different cement types. However, only *AGEDDCA* and to a lesser extent *Life-365* fulfil this criteria by default, as demonstrated in Table 17.

Table 17: Applicability of the models to different cement blends

Model	Cement Type					
	GP	FA	MK	MS	SF	SL
AGEDDCA	Y	Y	Y		Y	Y
CIKS	Y				Y	
CIM	Y		(y)	(y)	(y)	Y
Life-365	Y	Y			Y	Y
Microsilica	Y			Y		

Y = specific incorporation, i.e. the model contains a selectable default for that cement type
(y) = treated together as HRP (high reactivity pozzolan)

3.5 General observations

A specific point-by-point comparison of the models is undertaken in Section 3.7. That examines: How surface chloride concentrations are defined; how the reference diffusion coefficient is established; the nature of any time reduction in the diffusion coefficient; whether any temperature corrections are made; the corrosion threshold values adopted; and any factors of safety included. More general observations about the nature and useability of the models are incorporated in Sections 3.5.1 to 3.5.5.

3.5.1 CIM

Holcim's *CIM* model offers a straightforward graphical solution to Fick's 2nd Law incorporating a time-dependent diffusion coefficient. The reference diffusion coefficient is linked to concrete design strength, modified appropriately for cement type. The time-reduction index reflects the percentage of blended cement (slag or 'high reactivity pozzolan' – a catch-all term for silica fume, metakaolin etc) incorporated.

The model is simple to use, well documented through its help screens, and strikes a reasonable balance between presenting default values and allowing user customisation of input parameters. One possible improvement would be linking the default C_s value to predefined exposure classes.

The model predicts extremely good performance for slag concrete with maximum time-reduction indices around 0.7. The default parameters largely derive from real exposure data[37] and have been independently verified as fairly reflecting that data set.[38] *CIM*'s major limitation would seem to be restricted applicability; there are no default values provided for fly-ash concrete for example. The default values are also probably overly conservative for assessment of silica fume concrete, with a low maximum composite time-reduction index of 0.20. This is less than the default for undiluted GP cement in the *AGEDDCA* model, for example. The temporal dependence of diffusion coefficients in silica fume concrete has admittedly been contentious; a small allowance for aging is consistent with some researchers' data, whereas others have recorded large reductions with age.[19]

3.5.2 AGEDDCA

The UK Concrete Society's *AGEDDCA* model shares some similarity with *CIM* in essential philosophy, i.e. the reference diffusion coefficient and time reduction derive from the analysis of chloride profile data over extended periods of observation. *AGEDDCA*'s database for deriving the parameters is more extensive, however, and encompasses the broadest range of cement types of the models reviewed. Mix characterisation is also by cement content and w/b ratio rather than strength, which has a consequence for silica fume concrete as discussed below.

Long initiation times are predicted for fly-ash and slag blends at typical incorporation levels, with very high maximum time-reduction indices of 0.62 for 60% slag cement and 0.7 for 30% FA. The model resolves the contradictory reports of silica fume performance by linking the time-reduction index to w/b ratio for this concrete type only. Thus a value of m > 0.7 as reported in Maage et al is achievable at very low w/b ratios (< 0.4). To some extent, silica fume is therefore penalised by specifying concrete by strength classes, since any given f'c is likely to be achievable at a relatively higher w/b ratio than with the other cement types.

Diffusion coefficients within the model are temperature adjusted, although this is probably less significant in this model, where defaults are determined through natural exposure, than in others (*Life-365*, *Microsilica*) in which the reference coefficient is measured in a lab at 23ºC.

AGEDDCA includes a number of refinements to the Fick's Law prediction model, including taking account of additional durability enhancement measures such as surface coatings, controlled permeability formwork and corrosion and corrosion inhibitors. These are all accommodated by varying one or other of the fundamental parameters within the model (C_s, C_t, D_{ce} and cover). For example, a surface coating is treated as acting to reduce the surface chloride concentration. While the model is comprehensive it is one of the more inflexible in use; it is not possible to manually adjust the time-reduction index for example. It is also the least user-friendly with no in-built prompts or help screens. However, it is understood that the version examined was still in draft form; the finished product, released in 2005, may differ in this regard but has not been reviewed. The derivation of the model was also well described in Bamforth's NZ Concrete Society 2002 conference paper.[30]

3.5.3 Life-365

The *Life-365* model is generally simple to use and flexible. The predefined exposure conditions and temperature settings are tied to US geographic locations and need to be over-ridden with suitable New Zealand data, but this is easily accomplished. The model is the only one examined which specifically calculates the case of two-dimensional ingress, i.e. into columns. The default time-reduction indices are more conservative than the other models with $m < 0.6$ for slag and fly-ash and fixed at 0.2 for GP. Silica fume has no effect on the time-reduction index, but does reduce the reference diffusion coefficient, which other SCMs do not. These diffusion coefficients are based on laboratory measurements using a non-steady state immersion test (e.g. NT Build 443) and are consequently lower than those interpolated from natural exposure in *CIM* and *AGEDDCA*. The predicted initiation period is generally shorter than in these models because this is more than balanced by the smaller m value and the application of a safety factor which assumes that any reduction in the diffusion coefficient halts after 30 years.

Of particular note is the excellent manual, describing both the operation of the model, the assumptions behind it and the test methods used to derive the input parameters.

3.5.4 Microsilica model

It is difficult to evaluate the *Microsilica* model fairly under the terms of reference for this review because, unlike the other candidates, the assumptions underpinning its service-life prediction favour the importance of the propagation phase at the expense of initiation period. For example, while the use of Microsilica significantly reduces the reference diffusion coefficient, the time-reduction index is very conservatively set at 0.25 and a factor of safety is applied dependent on the environment, giving relatively short initiation times. To a degree this is compensated for by basing the reference diffusion coefficients on steady-state laboratory tests which typically give values significantly lower than natural exposure in splash zones or immersion tests. The model also has the unique concept of a zone of cover dominated by sorptivity effects, in which a constant chloride concentration is developed quickly after exposure depending on average times of wetting. For the most extreme case of submerged

concrete, the chloride threshold at the reinforcing is exceeded immediately i.e. there is no concept of an initiation period.

For this reason, a judicious assessment of the value of this model needs to be made by a corrosion specialist, competent to evaluate the assumptions made about the propagation phase, which includes the resistivity and potential difference values given and particularly the assumptions about macro- and micro-cell corrosion and anode/cathode geometries.

3.5.5 CIKS

Unlike the other models, which are either stand-alone applications or Microsoft Excel worksheets, the *CIKS* consists of multiple internet web forms, accessible at *http://ciks.cbt.nist.gov/~bentz/welcome.html*. Note that the form specifically tailored to service life prediction is rudimentary, consisting of the straightforward solution of Fick's 2nd Law with no inclusion of a time-dependent diffusion coefficient. However, the underlying finite difference calculation engine is quite sophisticated and associated forms allow for the prediction of chloride profiles considering such features as chloride binding isotherms, variation in C_3A content of cement, time and spatial dependence of the diffusion coefficient, and yearly cycles for both temperature and chloride load. A program is also available to theoretically predict diffusion coefficients from a given mix design (currently limited to GP and SF concrete). Despite these features it is difficult to recommend *CIKS* for routine use. There is no automation linking the time-reduction index or the reference diffusion coefficient with simple mix parameters, for example, or predefined defaults for particular exposure conditions. Furthermore there is limited 'sanity-checking' on the inputted data. Thus obtaining credible results is very dependent on the competency of the operator.

3.6 Model calculations for 40 and 80 year initiations

The models, with the exception of *CIKS*, were used to estimate covers necessary to achieve 40 and 80 year initiation times for 40, 50, 60 and 70 MPa grade concrete in the NZS 3101 C and B2 zones. To do this it was necessary to assume a number of input parameters. Surface concentration values were based upon those achieved in the BRANZ Weka Bay and Oteranga Bay marine exposure sites (Table 18), plus a small increase (0.5 percentage points) for conservatism in the C Zone. Cement contents and w/b ratios to achieve a particular strength grade were estimated as shown in Table 19. Chosen values reflect that relatively higher strengths are achievable with silica fume at a given w/b ratio, but lower strengths usually result with slag or fly-ash. The chloride threshold was set at 0.4% by mass of cement if the model did not supply an automatic value based on the reinforcing type (black steel). Mean annual temperature was set to 14ºC (approximating Wellington) where required.

3.6.1 C Zone

The necessary covers calculated by the models for 40 and 80 year initiation periods in the C Zone are given in Table 20 and Table 21 respectively.

Table 18: Model input parameters for C and B2 Zone calculations

Cement Binder	C Zone C_s (mass % on cement)	B2 Zone C_s (mass % on cement)
GP	2.0	1.0
SF	2.5	n/a
SL & FA	3.0	n/a

Table 19: Model input parameters (continued)

Concrete Grade	GP		SF		SL & FA	
	w/b	kg/m^3	w/b	kg/m^3	w/b	kg/m^3
40 MPa	0.45	350	0.65	270	0.5	325
50 MPa	0.40	400	0.55	325	0.4	400
70 MPa	0.35	500	0.45	400	0.3	530

Table 20: Calculated cover (mm) required for a 40 year initiation phase in the C Zone. X = no solution with less than 100 mm cover; [(1)]cover > 75 mm not available in model

AGEDDCA				
Cement Binder	Specified Compressive Strength f'c			
	40 MPa	**50 MPa**	**60 MPa**	**70 MPa**
GP	55	45	40	30
30% FA	30	25	20	20
60% SL	30	25	20	20
7% SF	X	65	50	40

CIM				
Cement Binder	Specified Compressive Strength f'c			
	40 MPa	**50 MPa**	**60 MPa**	**70 MPa**
GP	X	100	75	60
30% FA				
60% SL	45	35	30	20
7% SF	X	85	65	50

Life-365				
Cement Binder	Specified Compressive Strength f'**c**			
	40 MPa	**50 MPa**	**60 MPa**	**70 MPa**
GP	X	X	X	95
30% FA	100	75	65	60
60% SL	80	60	55	45
7% SF	X	X	100	85

Microsilica				
Cement Binder	Specified Compressive Strength f'c			
	40 MPa	**50 MPa**	**60 MPa**	**70 MPa**
GP	X	X	X	X
30% FA				
60% SL				
7% SF	X	X	X	60

Table 21: Calculated cover (mm) required for an 80 year initiation phase in the C Zone. X = no solution with less than 100 mm cover; [(1)] cover > 75 mm not available in model

AGEDDCA				
Cement Binder	Specified Compressive Strength f'c			
	40 MPa	**50 MPa**	**60 MPa**	**70 MPa**
GP	70	60	50	40
30% FA	35	30	25	20
60% SL	35	30	25	20
7% SF	X	> 75[(1)]	60	50

CIM				
Cement Binder	Specified Compressive Strength f'c			
	40 MPa	**50 MPa**	**60 MPa**	**70 MPa**
GP	X	X	100	80
30% FA				
60% SL	55	45	35	25
7% SF	X	X	90	70

Life-365				
Cement Binder	Specified Compressive Strength f'c			
	40 MPa	**50 MPa**	**60 MPa**	**70 MPa**
GP	X	X	X	X
30% FA	X	100	90	80
60% SL	X	80	70	60
7% SF	X	X	X	X

Microsilica				
Cement Binder	Specified Compressive Strength f'c			
	40 MPa	**50 MPa**	**60 MPa**	**70 MPa**
GP	X	X	X	X
30% FA				
60% SL				
7% SF	X	X	X	X

The differences in cover requirements predicted by the models are largely explained by their different assumptions for the initial diffusion coefficients (D_{28}) of the various concrete types and the appropriate time-reduction indices (m). The values of these variables assumed by the models for the calculations of required covers for 40 and 80 year initiation periods are tabulated in Table 23. For illustrative purposes, Figure 26 and Figure 27 demonstrate the sensitivity of the general Fick's 2nd Law solution at the heart of all the models considered to these two factors. It is clear that the predicted initiation time is very sensitive to the time-reduction index, especially for values of m greater than 0.1 – 0.2. It follows that care must be exercised in choosing the appropriate value of m for a given binder type. It should also be noted that while there appears to be a large volume of data from which a definite temporal dependence of diffusion can be interpolated, there is also a considerable amount of scatter in this data, illustrated by Figure 28. This suggests a cautious approach should be taken towards models that assume large time-reduction indices.

Other points of variance worth noting include that the *AGEDDCA* model automatically adjusts the corrosion threshold dependent on w/b ratio and cement type, whereas *CIM* and *Life-365* have constant default values. More details of this are given in the 'point-by-point' comparison in Section 8. The *AGEDDCA* model also takes account of the background chloride concentration of the concrete mixes, effectively deducting this value from the critical chloride threshold necessary to initiate corrosion.

Table 22: Comparison of the time-reduction indices assumed by each model in generating the initiation time predictions given in Table 20 and Table 21

Comparison of Time-reduction Indices, m				
Model	**40 MPa**	**50 MPa**	**60 MPa**	**70 MPa**
GP				
AGEDDCA	0.26	0.26	0.26	0.26
CIM[1]	0.08	0.08	0.08	0.08
Life-365	0.20	0.20	0.20	0.20
Microsilica	0.25	0.25	0.25	0.25
FA				
AGEDDCA	0.69	0.69	0.69	0.69
CIM[1]				
Life-365	0.44	0.44	0.44	0.44
Microsilica				
SF				
AGEDDCA	0.28	0.36	0.41	0.45
CIM[1]	0.14	0.14	0.14	0.14
Life-365	0.20	0.20	0.20	0.20
Microsilica	0.25	0.25	0.25	0.25
SL				
AGEDDCA	0.62	0.62	0.62	0.62
CIM[1]	0.60	0.60	0.60	0.60
Life-365	0.54	0.54	0.54	0.54
Microsilica				

[1]CIM value quoted is the composite index, i.e. N=m′n′

Table 23: Comparison of the diffusion coefficient at 28 days assumed by each model in generating the initiation time predictions given in Table 20 and Table 21 (when given the inputs in Table 19)

Comparison of Initial Diffusion Coefficient, D_{28} (mm^2/yr)				
Model	**40 MPa**	**50 MPa**	**60 MPa**	**70 MPa**
GP				
***AGEDDCA*[1]**	83	65	52	41
CIM	170	100	58	34
Life-365	331	250	190	144
Microsilica	170	114	88	79
FA				
***AGEDDCA*[1]**	240	166	120	120
CIM				
Life-365	435	250	190	144
Microsilica				
SF				
***AGEDDCA*[1]**	216	154	134	118
CIM	170	100	58	34
Life-365	315	181	137	104
Microsilica	240	101	28	20
SL				
***AGEDDCA*[1]**	158	109	79	79
CIM	430	260	150	89
Life-365	435	250	190	144
Microsilica				

[1]AGEDDCA values are at 20ºC; all others are for 14ºC

Diffusion Coefficient Conversion Guide	
mm^2/yr	**m^2/s**
30	~ 1 x 10^{-12}
100	~ 3 x 10^{-12}
300	~ 1 x 10^{-11}
1000	~ 3 x 10^{-11}

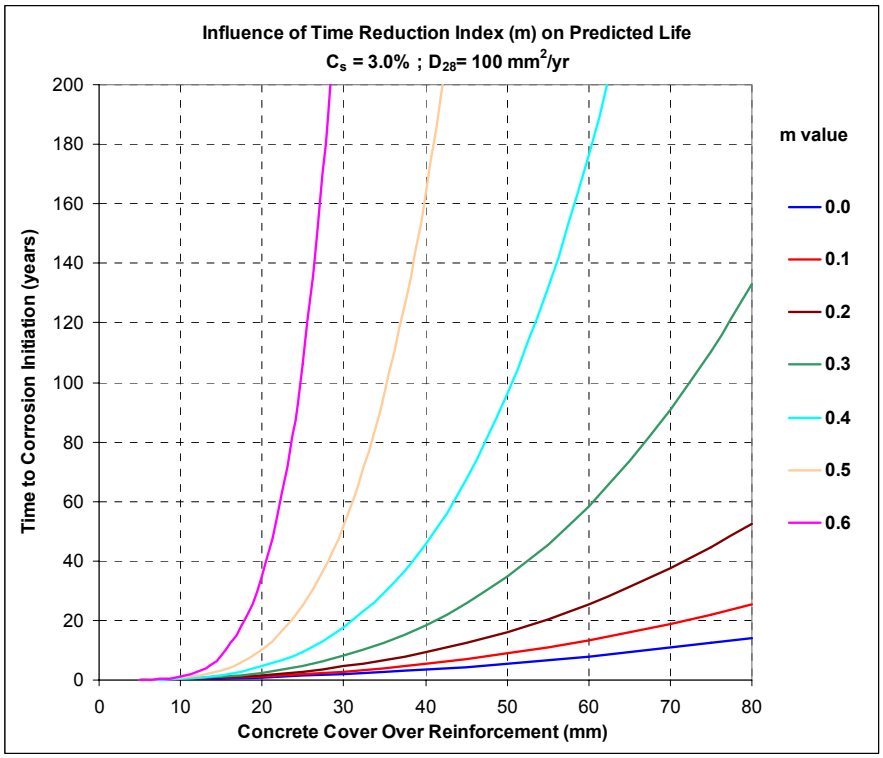

Figure 26: Sensitivity of initiation time to time-reduction index for the Fick's Law solution

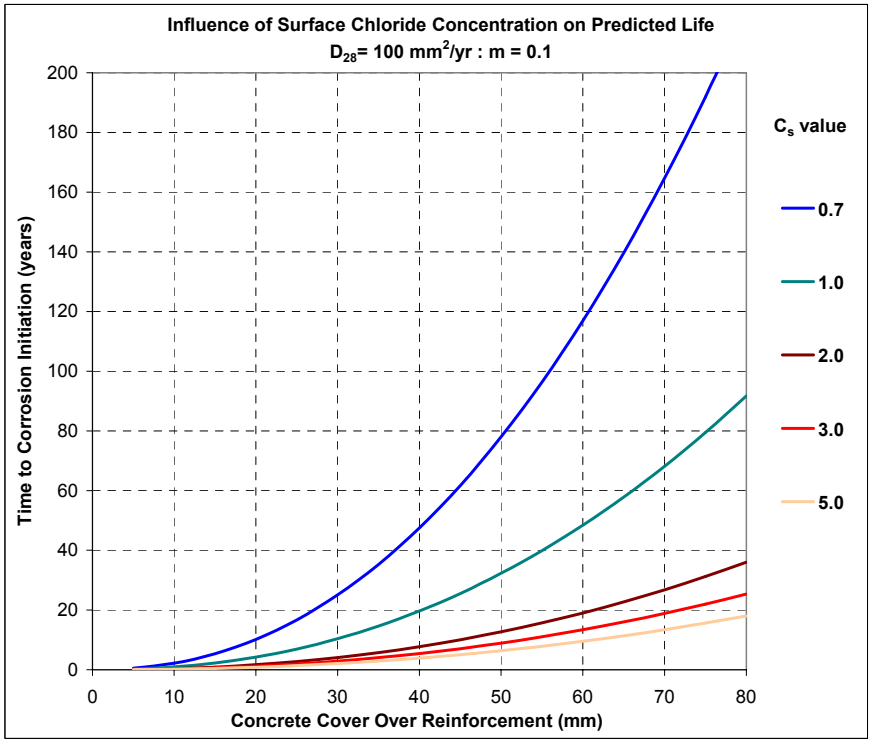

Figure 27: Sensitivity of initiation time to time-reduction index for the Fick's Law solution

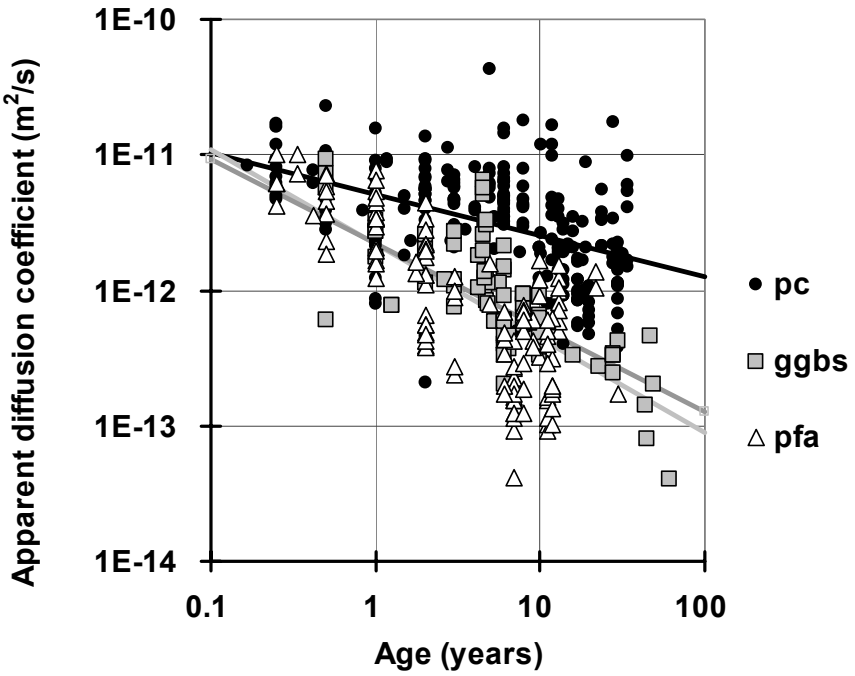

Figure 28: Typical scatter in apparent chloride diffusion coefficients derived from chloride profiles (reproduced from Bamforth). This suggests there is a great deal of uncertainty attached to the values assumed for time-reduction indices

3.6.2 B2 Zone

Calculated covers for a 40 year initiation life in the B2 exposure classification using GP concrete are given in Table 24 and Table 25. Inputs to the models were as for the C Zone calculations, except for the assumption of a reduced surface chloride concentration of 1.0% w/w on cement.

Table 24: Calculated cover (mm) required for a 40 year initiation phase in the B2 Zone. 'X' = no solution with less than 100 mm cover; [(1)] cover > 75 mm not available in model

B2 Zone model covers for 40 year initiation (C_s = 1.0% on cement)					
Model	Specified Compressive Strength f'c				
	30 MPa	40 MPa	50 MPa	60 MPa	70 MPa
AGEDDCA	75	50	30	20	10
CIM	100	75	60	45	35
Life-365	X	X	90	70	60
Microsilica	X	X	> 75 [(1)]	40	30

Table 25: Calculated cover (mm) required for an 80 year initiation phase in the B2 Zone. 'X' = no solution with less than 100 mm cover; [(1)] cover > 75 mm not available in model

B2 Zone model covers for 80 year initiation (C_s = 1.0% on cement)					
Model	Specified Compressive Strength f'c				
	30 MPa	40 MPa	50 MPa	60 MPa	70 MPa
AGEDDCA	X	65	40	25	15
CIM	X	X	80	60	50
Life-365	X	X	X	95	85
Microsilica	X	X	> 75 [(1)]	55	40

3.7 Point-by-point model comparison

<table>
<tr><th colspan="2">Surface Chloride Concentration (C_s)</th></tr>
<tr><td>AGEDDCA</td><td>User inputs the appropriate value. No predefined exposure classes or value limits. Recommended surface chloride levels (mass % on concrete) have been suggested as:
Mix Type — Typical — 90% Confidence
GP — 0.36% — 0.70%
Blended (FA, SL) — 0.51% — 0.85%
Surface coatings are handled as a -0.2% subtraction from C_s. Integral water-proofers reduce C_s by 10% (normal) or 20% (high range).</td></tr>
<tr><td>Holcim CIM</td><td>User-definable from min of C_t+0.1% to max 6% as mass % on cement. Default value is 1.0%. Help suggests the following values (relies on user to change as appropriate):
3101 Exposure Class — GP Only — With SCMs
C Zone — 2.5 – 3.0% — 3.0 – 3.5%
B2 Zone — 0.8 – 1.0% — 1.0 – 1.2%
B1 Zone — 0.4 – 0.5% — 0.5 – 0.6%</td></tr>
<tr><td>Microsilica</td><td>Surface chlorides build-up rapidly to the following predefined exposure levels, as mass % on cement:
Exposure Class — Max Concentration
Splash zone / Low Soffit (C) — 6.0%
Splash zone / Other (C) — 4.0%
Atmospheric (B2) — 2.0%
Near-Coastal (B1) — 1.0%
Upper-Tidal / Lower Splash — 2.0%
Underwater / Lower Tidal — 2.0%</td></tr>
<tr><td>Life-365</td><td>Four predefined exposure classes characterised by a build-up rate and maximum concentration defined as mass % on concrete:
Exposure Class — Build-up Rate — Max Conc — Time to Max
Marine Tidal / Splash — Instantaneous — 0.8% — Immediate
Marine Spray — 0.10% /yr — 1.0% — 10 yr
Within 800 m of Ocean — 0.04% /yr — 0.6% — 15 yr
Within 1500 m of Ocean — 0.02% /yr — 0.6% — 30 yrs
Also user-definable. Cement type does not effect C_s.</td></tr>
<tr><td>NIST CIKS</td><td>No predefined exposure classes. Associated help suggests the following values. Other parts of the CIKS system (prediction of a profile) require exposure severity in units of mol/l.
Exposure Class — Suggested (lb/yd) — In SI Units (kg/m^3) — Mass % Concrete
Low — 3 — 1.78 — 0.07
Moderate — 6 — 3.56 — 0.15
High — 9 — 5.34 — 0.22
Severe — 12.4 — 7.35 — 0.30</td></tr>
</table>

Reference Chloride Diffusion Coefficient (D)	
AGEDDCA	Values derived from exposure profiles in literature. Reference time is t = 20 years. Dependent upon: w/b ratio (separate relationship for each binder type) % addition of SCMs Note there is no link to f'c as in earlier Bamforth work (strength only affects amount of corrosion required to induce cracking).
Holcim CIM	Values derived from exposure profiles. Linked to f'c by default using a semi-log relationship over the range 20 – 90 MPa. End-points for strength are user-definable within limits. Use of SL increases Dce_0 in line with exposure site observations: **f'c** **D_{28}** 20 MPa $200 \cdot X^*$ mm^2/yr 90 MPa $1200 \cdot X^*$ mm^2/yr where $X^* = 1 + 2 \cdot [\%SL / 100]$ Is unaffected by pozzolans (SF, MK etc).
Microsilica	Values are derived from laboratory diffusion cell measurements at 28 days. Tied to w/b ratio by an equation of the form $\log D_{28} = A \cdot (w/b) + B.(w/b)^2$. D_{28} is scaled for incorporation of MS according to an equation with the approximate form: $\text{Log}(D_{MS}) = \text{Log}(D_{GP}) - 0.13 \cdot (\%MS) + 0.04 \cdot (\%MS)^2$.
Life-365	Values are derived from bulk diffusion tests at 28 days, but manual over-rideable. Fundamental value is given by $D_{28} = 1 \times 10^{(-12.06 + 2.4 \cdot w/b)}$ m^2/s i.e. derived from w/b ratio only, not strength or cement content. This is not altered by incorporation of SL or FA (a choice based on contradictory literature results).
NIST CIKS	User to supply apparent bulk diffusion value. Available guidance is: Database of literature values, apparently restricted to GP and undifferentiated by test method. Computer estimation from w/b ratio, SF addition level, vol fraction of aggregate and degree of hydration. Based on a 3-D cellular automata simulation of cement hydration using percolation theory.

<table>
<tr><th colspan="2">Time Reduction Value (m)</th></tr>
<tr><td>AGEDDCA</td><td>Values derived from interpolation of a database of literature data.
Dependent on:
▪ % addition of SCMs for different binder
▪ w/b ratio for SF only (max at low w/b)
▪ has optimum addition values, e.g.
Component | Max m | Addition Level to Achieve Max
SL | 0.62 | 59 to 72%
FA | 0.70 | 30 to 42%
SF | 0.79 at 0.3 w/b | 18 to 22%</td></tr>
<tr><td>Holcim CIM</td><td>Uses a composite index N = Σm′n′ where m′ is the mass fraction of a cement component and n′ is the time-reduction index (i.e. more SL or HRP gives a larger time reduction and their benefit is cumulative).

Component | n′ | n′ default | m′ | m′n′ max
GP | 0.00 – 0.12 | 0.08 | 0.25 – 1.0 | 0.08
SL | 0.6 – 1.0 | 0.95 | 0.3 – 0.75 | 0.71
HRP | 0.6 – 1.40 | 1.0 | 0.0 – 0.13 | 0.13
Max N = Σm′n′ value is ~ 0.74</td></tr>
<tr><td>Microsilica</td><td>Uses a consistent m = (-)0.25 regardless of %MS in binder.

Applies a Factor of Safety (FOS) to the reduction which becomes less conservative as the exposure intensity increases (assuming the sense is the same as for the corrosion threshold (C_t) FOS which is not clear).

FOS = 1.5 in B1 & B2 Zones, 2.0 in C1 (other) and 2.5 in C1 (low soffits).

Exactly how the FOS is applied is not spelt out.</td></tr>
<tr><td>Life-365</td><td>m = 0.2 for GP.

NO allowance made for improvement by SF (still m = 0.2).

For FA or SL, m = 0.2 + 0.4·(%FA/50 + %SL/70), m <=0.6.

Blending seems allowed with max FA = 50%, max SL = 70% and no more than 70% of mix as cement replacement. Effect cumulative with SF addition.</td></tr>
<tr><td>NIST CIKS</td><td>No allowance made for temporal dependence of diffusion for the web options ‘Predict the service life of a reinforced concrete structure exposed to chlorides’ or ‘Predict the chloride-ion penetration profile of a concrete after a specific time’.

The option ‘Predict the chloride-ion penetration profile of concrete after a specific time with temperature effects’ allows a user inputted m value.
A suggested relationship is: m = 2.5·(w/b) – 0.6.</td></tr>
</table>

Corrosion Threshold (C_t)	
AGEDDCA	Dependent on reinforcing type as shown in the table below: **Reinforcement Type** — **C_t (% on cement)** Black Steel — 0.4% Galvanised Steel — 1.0% Stainless Steel (type 316) — 3.0% Corrosion Inhibitor — $C_t=C_{t0}+0.06\cdot I$ (l/m^3)$\cdot$FOS Also dependent on binder type and content (SCMs at normal dosages typically reduce C_t to ca. 0.25 – 0.3%).
Holcim CIM	0.2% – 0.6% on total cementitious material. User-adjustable within this range in steps of 0.05%. 0.4% selected as initial default (and suggested for routine design purposes in help screen).
Microsilica	C_t depends upon w/b ratio, C_3A content of binder. C_t = 0.4% for a base case of 0.5 w/b and 7.5% C_3A. C_t scales linearly from 2 – 14% C_3A, reflecting increasing fraction of total chlorides which are bound and therefore unavailable for corrosion. C_t varies with w/b ratio according to the function $C_t=0.1/(w/b)^2$.
Life-365	User-editable. Default values (**% mass on concrete**) are: **Situation** — **C_t** Black Steel — 0.05% Stainless Steel — 0.50% Calcium Nitrite Inhibitor (30 l/m^3) — 0.4% Not influenced by cement chemistry.
NIST CIKS	Derived from the HETEK model and depends on environment, w/b ratio and cement chemistry: $C_t = k_{Cr}\cdot\exp(-1.5\cdot eqv\{w/b_{Ct}\})$ & $eqv\{w/b_{Ct}\}= w/(GP + f_{FA}\cdot FA + f_{SF}\cdot SF)$ k_{Cr} = 1.25 for atmospheric and splash zones and 3.35 for submerged zones f_{FA} = - 4.7 & f_{SF} = -1.4. Typical values for GP are 6.5 kg/m^3 submerged (0.27%) and 2.4 kg/m^3 (0.1%) in splash. NB addition of FA or SF increases equivalent w/b ratio and C_t.

Temperature Allowance	
AGEDDCA	Reference diffusion coefficient is modified for temperature using an unspecified relationship.
Holcim CIM	No specific functionality to adjust D_{ce} for temperature variation. [Default parameters reflect comprehensive set of exposure profiles measured in the field i.e. are in some sense temperature-adjusted compared with a laboratory bulk diffusion coefficient.]
Microsilica	D_{ce} is modified from the laboratory test values at 20ºC to a temperature appropriate for the structure using a Nernst-Einstein equation (Amey et al): $D_2 = D_1 \frac{T_2}{T_1} e^{q\left(\frac{1}{T_1}-\frac{1}{T_2}\right)}$ where q is an activation coefficient related to w/b ratio and a weighted average annual temperature for the geographic location (7-8x increase over 10º – 50ºC).
Life-365	Temperature-dependent changes in D_{ce} are accounted for using an annual (monthly) temperature profile and the following equation for the dependency: $D_{(T)} = D_{REF} \cdot \exp\left[\frac{U}{R} \cdot \left(\frac{1}{T_{REF}} - \frac{1}{T}\right)\right]$ The initiation solution is carried out by a finite difference implementation of Fick's 2nd Law and so D_{ce} is modified for temperature at every time step. It is not clear with what resolution this takes place (i.e. how small the time steps are).
NIST CIKS	No adjustment for temperature is integrated into the direct 'Predict the service life of a reinforced concrete structure exposed to chlorides' web option. The option 'Predict the chloride-ion penetration profile of concrete after a specific time with temperature effects' allows the user to input a monthly temperature profile. The equation used to correct the diffusion coefficient is not specified.

Safety Margins	
AGEDDCA	Only explicit safety factor is for the effectiveness of corrosion inhibitors raising the corrosion threshold value.
Holcim CIM	'Chloride Capacity Factor, F' allows user to reduce performance predicted by the model. Works by applying a scale factor (1/F) to the time-dependent D_{ce} value. Defaults to F = 1.0 (no reduction). Help-file suggests the following: **Situation** — **F value** Corner bar, square corner — 0.70 – 0.75 Corner bar, rounded or bevelled corner — 0.50 – 0.55 Cracks in cover concrete — 0.20 – 0.50
Microsilica	Applies a Factor of Safety (*FOS*) to value predicted for C_t: $C_t = 0.4 + (C_{tpredict} - 0.4)/FOS$ where FOS is in the range 1.0 – 6.0 Note: this seems to result in less conservative C_t values being used when the model predicts C_t values < 0.4. Assumes a high base chloride level of 0.1% (but note this also works to reduce the driving force). Factor of Safety on time-reduction index (1.5 in B1 to 2.5 submerged).
Life-365	Time-dependent reduction of D_{ce} is assumed to stop after 30 years.
NIST CIKS	Where a reduction factor can be specified for the diffusion coefficient the equation used is of the form: $D=D_{inf}+D_i \cdot t^{(-m)}$ Thus by setting the value for D_{inf} (the diffusion coefficient at infinite time) it is possible to set a limit on the temporal dependence of the diffusion coefficient.

Other Comments	
AGEDDCA	Most comprehensive in range of binders considered (GP, SL, FA, SF, MK). Considers effects of integral water-proofers, controlled permeability formwork, GRC permanent formwork and surface coatings by modification of four standard parameters in the model (i.e. C_s, D_c, C_t, cover). No help built into model. Documentation limited to NZCS 2002 paper.
Holcim CIM	Good in-model help screens offering guidance on appropriate values. Reliant on user to change certain inputs appropriately, i.e. C_s, C_t.
Microsilica	Propagation phase is integral to the model e.g. submerged concrete is assumed to develop a uniform chloride profile almost instantaneously (t_0 = 0 yrs). Sorptivity and time of wetting are important factors, defining an absorption zone penetrating the surface concrete in which diffusion does not apply. This reduces the effective cover (down to zero in the case of completely submerged concrete).
Life-365	Comprehensive manual on disk discusses assumptions behind model, supporting literature, and the test methods used to derive input parameters. No useful help built directly into program. Evaluates effect of surface sealers or membranes, modelled by a reduction in the rate of surface chloride build-up. Effectiveness deteriorates linearly over life of sealant (i.e. rate increases to the same as unprotected concrete). Includes life-cycle costs for different materials choices. Includes 2-d cases (e.g. ingress into piles).
NIST CIKS	Not set up as an integrated model. Life prediction option is simple with no time reduction, temperature effects or predefined exposure classes. Options for predicting chloride profiles after a fixed time are much more flexible and include sophisticated options such as spatial and temporal variations in D_{ce} and temperature, but require unfamiliar inputs (e.g. chloride conc in mol/l).

4. DURABILITY MEASUREMENT

4.1 Introduction

Historically, specifications intended to achieve a more durable concrete have demanded an increase in the concrete compressive strength. Compressive strength and durability are broadly related in the sense that both properties are expected to improve with a reduction in the capillary porosity of a specific concrete, as caused by decreasing w/b ratios for example. However, strength does not always reflect the durability benefit conferred by SCMs, particularly slag and fly-ash. Consequently there is a need for more direct measures of concrete durability. Part of the intent of this research programme was to investigate and develop test methods which directly correlate with the chloride ingress resistance of concrete.

The purpose of test methods to evaluate concrete performance can be categorised into three specific roles, each of which places unique demands on the attributes required from the test:

1. As a tool for concrete mix design

The test needs a direct link to the physio-chemical mechanisms expected to control the durability of the structure in question. For mix development purposes, selection of the most relevant test far outweighs considerations of test duration.

2. As a pre-qualification tool for acceptance of a suggested concrete mix

An acceptable performance criterion can be compiled for the test through rational analysis of existing data without too much trial and error. The test duration must not be too extended.

3. As a quality control tool

The test duration must be short enough for routine application. The test method must be repeatable and robust, with acceptance criteria (including tolerances) established beforehand.

The Concrete Institute of Australia (CIA) publication *Recommended Practice on Performance of Concrete in Marine Environments*[39] evaluated various test methods for their suitability for the above three categories. No test methodology was found to be suitable as a design tool, which mirrors the BRANZ finding that there is no simple link between D_{ce} values characterising concrete performance in-situ and laboratory-measured chloride-ion diffusion coefficients.

Despite the lack of a direct link to durability, the CIA judged compressive strength to be the most suitable single test for prequalification and quality control purposes. Strength has the advantage that acceptance criteria are already established in Table 2.8 of NZS 3104:2003.[40] These are derived from a large statistical base of compressive strength results compiled through the NZ Ready-Mixed Concrete Association's auditing processes.

However, a number of directly durability-related tests were also deemed suitable for prequalification and quality control purposes. Table 26 shows the tests of this nature that were investigated by BRANZ as an important component of this study. A description of these tests and the conclusions drawn about their use follows:

Table 26: Durability test methods investigated for prequalification or quality control purposes

Property	Test Method
Sorptivity	BRANZ in-house test
Rapid Chloride	ASTM C1202
Rapid Migration (RMT)	NT BUILD 492

4.2 Sorptivity

As a simple index test for characterising the resistance of a particular concrete to chloride-ion penetration, the measurement of sorptivity has a number of advantages. The test method is analogous to a recognised ingress process in the field, does not require specialised equipment, and yields relatively rapid results even when considering high performance concrete. However, obtaining meaningful data is dependent on preconditioning the concrete to a consistent and reproducible internal moisture state, which is not necessarily a simple task. This portion of the durability research reviews currently suggested methodologies for sorptivity testing, including the necessary sample preparation. It also presents experimental data which examines the sensitivity of the sorptivity test to variations in concrete quality due to factors such as composition and curing. The aim of the review was to establish an appropriate test procedure and acceptance criteria for use in New Zealand for mix design, pre-qualification and quality control purposes.

4.2.1 Sorptivity theory and practice

For many deleterious processes, the durability of concrete is intimately connected to the ease with which water is able to percolate through it. This has traditionally been characterised by *permeability*, the rate of water flow through saturated concrete under an applied pressure gradient. The technique has some attraction; permeability is an intrinsic material property defined by a well-understood physical theory, but this advantage tends to be outweighed by less favourable considerations. These include both the practical – modern high-performance concretes have permeabilities so low they are difficult to measure accurately – and the theoretical – the high pressure test conditions are not analogous to those experienced by most 'real-world' concrete structures.

Hydraulic *sorptivity*, first applied to building materials by Hall,[41] offers an alternative measure of fluid transport properties of concrete. As the name suggests, it characterises the tendency for a dry, or partially saturated, porous material to absorb water via capillary action. For most structures, which do not become routinely water-saturated, capillary effects are likely to be the dominant transport process. Thus sorptivity is a more appropriate parameter for categorising concrete performance than permeability.

Sorption occurs when water is drawn through the interior of the concrete by capillary forces. These arise from the surface tension of the liquid in contact with the walls of the concrete's capillary pore network. For the simplest case of one-dimensional flow through a plane surface, the water ingress is given by the equation:[42]

$$M_{(t)} = \rho A S \sqrt{t} \qquad [6\text{-}1]$$

where $M_{(t)}$ is the mass of liquid in grams that has been absorbed after time t, ρ is the density of the fluid (neglected for the case of water since ρ = 1.0 g/cm^3 under normal ambient conditions), A is the surface area in mm^2 being exposed to the invading liquid, and S is concrete's 'sorptivity coefficient', which has units of mm/min^{½}.

Equation [6-1] forms the basis of a typical sorptivity experiment, which is shown diagrammatically in Figure 29; Figure 30 is a photograph of a test in practice. Regular prismatic concrete specimens are initially preconditioned by drying to some reproducible moisture state. After cooling they are weighed, then placed in a tray of shallow water and supported such that one face is immersed to a depth of 2 – 3 mm while allowing the water free access across the entire wetted face. At regular intervals the specimens are lifted out, patted with a damp cloth to remove any adhering water droplets, and weighed to an accuracy of 0.1 g or better. At the conclusion of the test, the gain in mass of the specimens at each measured time interval is divided by the area of the exposed face and plotted against the square root of time, as shown in Figure 31.

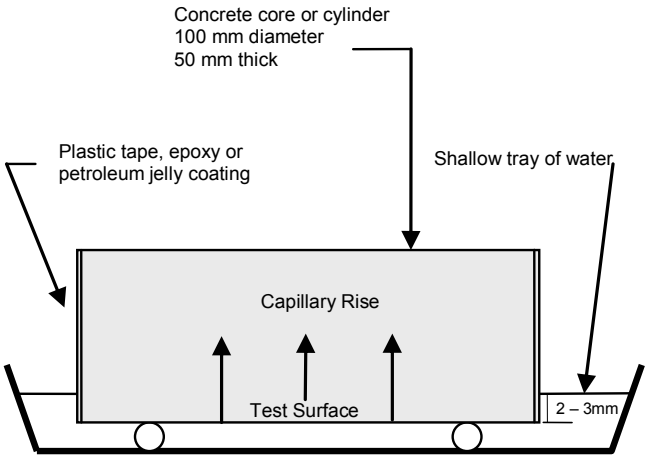

Figure 29: Usual arrangement for a sorptivity test

Figure 30: Sorptivity testing in practice

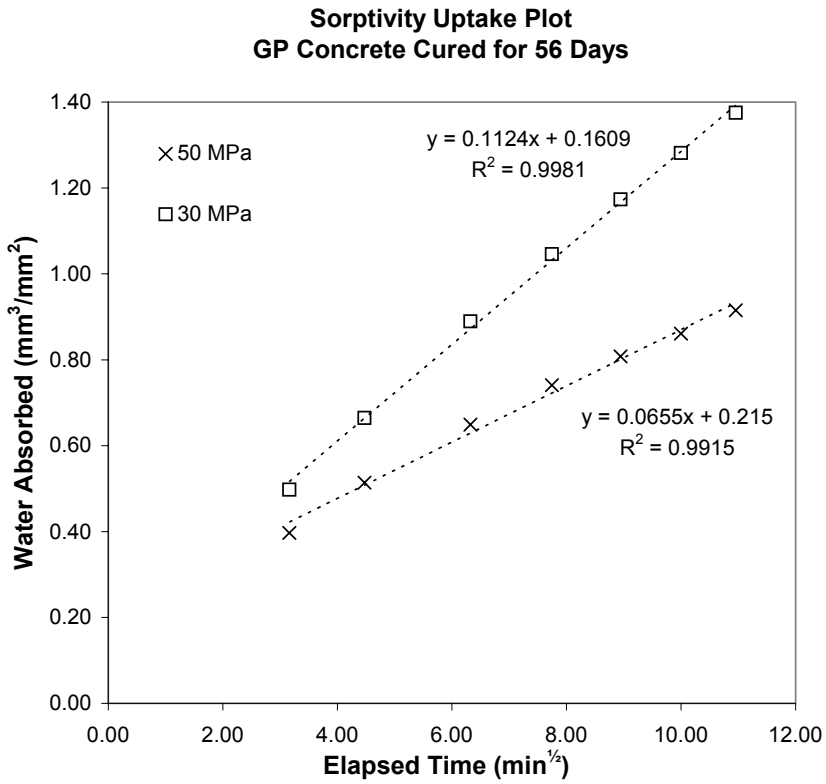

Figure 31: Typical sorptivity results for two different grade concretes

The result should be a straight line whose gradient, determined by least-squares linear regression, defines the sorptivity coefficient of the concrete. Ideally, the linear regression coefficient obtained during the curve fitting procedure should be > 0.98.[43] Plots which show systematic curvature cannot be used to calculate sorptivity. This situation is comparatively rare, but incidences of downward curvature have been associated with materials with coarse pore structures (e.g. concrete masonry) in which the capillary forces are weak and comparable with the gradients of gravitational potential. Curvature may also occur in cases where the preconditioning of the test specimen has produced non-uniform moisture distributions within the concrete.

Sorptivity plots typically show a small positive intercept on the y-axis. This is interpreted to be due to initial filling of pores on the exposed inflow surface and sides of the specimen. For this reason, the initial datum point (the mass uptake between t = 0 and the first weighing) is normally ignored in the calculation of sorptivity.

Sorptivity measurements are usually made over comparatively short periods; Hall suggests two hours is sufficient. It has been claimed[44] that mortars and concretes are characterised by two sorptivity coefficients, represented by a distinct break in gradient on the sorptivity uptake plot. The later-age sorptivity coefficient, for times longer than one day, is attributed to phenomena other than the suction due to the capillary pore network, such as the slow filling of air voids and interactions of the water with cement gel.

Within this broad outline, many variations in the test procedure are possible. For example, a small dam can be built on top of the specimen such that the invading fluid is in contact with the top of the specimen. Under this scheme ('ponding sorptivity'), the capillary forces act in concert with gravity, which may be a more realistic simulation of certain situations (e.g. water on a pavement or bridge deck).

Some investigators[45] prefer to measure the depth of liquid penetration directly rather than monitor the change in mass. This requires the destructive splitting of the sample at the end of the test and a direct measurement of the penetration front (i.e. the height to which the concrete is 'wet'). The sorptivity equation then becomes:

$$d_{(t)} = B\sqrt{t} \qquad [6\text{-}2]$$

where $d_{(t)}$ is the depth of penetration after time t and B is the 'penetration coefficient'. Note that the units of B are length/time^{½} as with the sorptivity coefficient, although they are numerically quite different quantities. This can be a cause for confusion.

BRANZ does not favour direct determination of penetration coefficients because of the difficulty in precisely identifying and measuring the penetration front. The reliance on a single measurement without the benefit of being able to improve precision by fitting the sorptivity coefficient to multiple data points would seem to negate one of the advantages of the test, which is its surprising sensitivity to small changes in concrete quality. Nevertheless, the penetration coefficient *(B)* is conceptually easier to understand than the sorptivity coefficient *(S)*, because it gives the rate of advance of the wetting front directly. The sorptivity and penetration coefficients are theoretically related by the effective porosity of the concrete:

$$Effective \cdot Porosity \approx \frac{S}{B} \qquad [6\text{-}3]$$

This provides an approximate conversion between the values, but it should be noted that the porosity required is that which would be filled by capillarity. This volume would not include entrapped air voids and thus may differ from the porosity determined by an immersed absorption test such as AS1012.21.[46] This difference in definition makes direct comparisons of data from the two sorptivity methods uncertain.

4.2.2 Advantages and disadvantages

The primary advantages of the sorptivity test are:

1. Sorptivity requires no specialised equipment beyond a suitably accurate balance and stopwatch.

2. With a logical weighing sequence in place, multiple specimens (say 10 to 20) can be tested at the same time.

3. The test uses a mechanism relevant to actual deterioration processes in field concrete.

4. The test is sensitive to the overall interconnectivity of the concrete's pore network. In contrast an absorption test such as AS1012.21 is more sensitive to total pore volume, a property more critical to strength than durability.

5. A well-developed mathematical framework is available for capillary flow in unsaturated materials which unites both sorptivity and permeability, and makes explicit their dependence on the water content of the material.

The major problem in the practical application of sorptivity arises from unsaturated flow theory: for a given porous material, sorptivity is found to be strictly a function of the initial and final moisture contents of the test material, θ_0 and θ_1 respectively:

$$S = \int_{\theta_0}^{\theta_1} \phi d\theta \qquad [6\text{-}4]$$

where ϕ gives the dependence of the moisture content on time and position in the sample.

As a consequence of equation [6-4], it is necessary to define a reproducible internal moisture state θ_0 to which test specimens can be conditioned before commencing a sorptivity test (the final state θ_1 is described unambiguously by contact with the invading liquid). It is also necessary to ensure that the moisture distribution is even throughout the specimens. This cannot be taken for granted as steep near-surface moisture gradients are a known feature of capillary drying.[47]

Thus the main disadvantage of the sorptivity test is that the result is very dependent on the moisture state of the specimen before the test, and there is no common internationally recognised drying regime. This means that acceptance criteria must be defined separately for any given drying regime, and results are again not readily comparable between each method variation.

4.2.3 Current use and needed research

For a number of years BRANZ has used sorptivity testing as a simple durability index to rank the performance of concrete mixes. This is the second of the three main tasks required for assuring the long-term durability of a new concrete structure, viz:

1. Define the service environment and performance requirements for the structure.

2. Optimise the concrete mix design in the laboratory by characterising the performance with appropriate index values.

3. Test the in-situ concrete to ensure that the required index values have been achieved in practice.

(after Alexander and Ballim[48]).

BRANZ's experience has given us confidence that sorptivity is a useful test, both reproducible and correlating as expected with mix composition and curing. This suggests that its role could be extended from a laboratory tool (Step 2 above) to include use as a quality assurance test (Step 3). For example, this might include incorporation in a construction specification as an adjunct to compressive strength, or employing the test to determine the effectiveness of site curing.

For this to occur however, it is necessary for a considerable database of sorptivity results to be compiled to allow realistic minimum specifications to be set. In particular, sorptivity values for high performance concrete, comparisons of the influence of different conditioning regimes on the quality of the sorptivity test results, and an assessment of the differences that could be expected between 'lab-crete' and field concrete, do not appear to have been adequately addressed.

4.2.4 Sorptivity conditioning experimental programme

This phase of the experimental programme concentrated on evaluating the practicality of different sorptivity preconditioning methods, and their impact on the effectiveness of the test as a discriminator for degree of curing.

A series of five 100 mm thick concrete slabs were cast into form-ply boxing, compacted with a poker vibrator, and hand-trowelled. The concrete used was a 30 MPa laboratory-produced mix, made with GP cement and Wellington crushed aggregates, and intended to be reasonably representative of a ready-mixed structural grade concrete. The mix design is given in Table 27. Test cylinders (200 mm x 100 mm) were moulded at the same time.

A set of 200 mm x 100 mm cylinders were also cast from a 50 MPa mix (Table 27). A comparison of the two sets of cylinder results was used to assess the sensitivity of the sorptivity test to concrete quality.

Table 27: Concrete mix proportions for sorptivity trials

Mix Constituents (quantity per m^3)		30 MPa mix	50 MPa mix
19 mm	Belmont Chip	638 kg	661 kg
13 mm	Belmont Chip	426 kg	435 kg
Sand	Puketapu	860 kg	684 kg
GP Cement	Golden Bay	290 kg	440 kg
Water Reducer	Sika BV50N	0.7 l	2.0 l
Total Water		175 l	162 l
w/b ratio		0.60	0.37

After 24 hours protected from water loss by black polythene, the slabs were stripped from their formwork. The first slab was allowed to dry immediately in a controlled environment room at 21ºC and 65% RH. The remaining four slabs were moved to a 'fog room' maintained at 100% RH and allowed to cure for 3, 7, 28 and 56 days respectively. At the conclusion of its allocated curing period each slab was placed in the drying room, joining those removed earlier. Fifty-six days after casting, all of the slabs were cored with a 100 mm diameter coring bit to provide specimens for sorptivity testing. Twenty-five cores were taken from each slab allowing for five replicate sorptivity tests using four different conditioning procedures at each curing time. A series of 50 mm cores were also taken to determine the actual (dry) compressive strength of each slab; use of a smaller diameter than permitted by NZS 3112: Part 2 was necessitated by the requirement to maintain a length-to-diameter ratio as close to the 2:1 ideal as possible. All of these cores were tested at 68 days after casting.

The sorptivity specimen cores were trimmed to 50 mm thick for testing. Their orientation was chosen such that the water ingress surface corresponded to the cast face of the slab, both to mimic the likely situation in field concrete elements, and to minimise the influence of finishing technique on the sorptivity result. Concrete cast against a form face often demonstrates heterogeneity in the spatial distribution of the aggregate, with a layer of cement-rich paste at the surface.[49] To avoid the effect of this spatial variation on the test result, approximately 8 mm was trimmed from the outer face of each core. Each suite of cores (sets of five test replicates cured at 1, 3, 7, 28 and 56 days) was then conditioned by one of the methods described below before their sorptivity coefficients were determined.

4.2.5 Conditioning methods

As described earlier, the sorptivity of a concrete correlates strongly with its moisture content and internal relative humidity. All test samples therefore require some form of conditioning to achieve a uniform initial condition, regardless of whether they are saturated (e.g. test cylinders directly after curing) or have experienced some degree of drying. The features of the conditioning regimes chosen for the test programme are compared in Table 28. All of the regimes were selected based on common usage in the literature. ASTM C 1585 – 04 'Standard Test Method for Measurement of Rate of Water Absorption by Hydraulic-Cement Concretes'[50] was introduced shortly after the conclusion of the experimental programme and is not included. However, it largely derives from the NIST sorptivity procedure primarily differing in not requiring a preconditioning step and reducing the drying time from 7 to 3 days.

The conditioning regimes can be subdivided into two groups, based on whether the aim is to produce an artificial 'dry' condition in the test specimens, or to replicate a moisture content typical of field concrete exposed to ambient conditions. Drying at 50º or 105ºC falls into the former category; the NIST and RILEM procedures belong in the latter.

Conditioning specimens at 105ºC in a ventilated oven until an equilibration of mass is achieved has been the norm, and many of the literature values for both sorptivity and permeability have been obtained with this technique. However, it has since been recognised that this temperature can alter the microstructure of the concrete, dehydrating the cement gel and inducing micro-cracking. For this reason BRANZ prefers to carry out the conditioning step at 50ºC. The disadvantage is that the end-point of the drying procedure is not clearly defined as at the higher temperature and that the drying time is naturally longer. By convention we chose to define the sample as dry when the weight loss over 24 hours is less than 0.1%. Once the specimens are dry they are cooled in a desiccator. The subsequent sorptivity testing normally takes place within 18 to 24 hours. It is assumed that the drying procedures are sufficiently aggressive to avoid creating any moisture gradients, at least in the near-surface concrete which influences a sorptivity test.

The NIST procedure, which formed the basis of ASTM C1585, requires test specimens to be conditioned in an environmental chamber maintained at 50 ± 2ºC and 80 ± 3% RH for 7 days.

This is followed by a post-conditioning period of approximately 14 days duration in a sealed container at 23 ± 2ºC, during which the RH in the container is monitored. When the container humidity stabilises it is assumed that the moisture content of the specimens is uniformly distributed (no gradients) and in equilibrium with the measured RH. This should be in the range of 50 – 70%, which is similar to the internal humidity of concrete in field structures.[51]

RILEM conditioning is a more complicated procedure which also aims to ensure initial moisture contents in equilibrium with natural ambient conditions. In addition to the regular sorptivity specimens, additional test concrete is prepared as thin (5 mm) slices or crushed into particles of equivalent diameter. Because of their high surface area, these samples will dry unassisted under ambient conditions relatively quickly. By doing this, the necessary water that must be removed to bring the larger test samples into equilibrium can be calculated. For absolute accuracy, this step must be carried out in a CO_2 free environment to avoid any change in mass associated with carbonation.

Once this weight loss has been determined, the drying of the actual test specimens can be accelerated at 50ºC. This is continued until the calculated loss of water has been attained to within a 5% level of accuracy, which necessitates frequent weighings over small time periods (hours to days). Subsequently, the specimens are sealed to prevent any further moisture loss and returned to the 50ºC environment for a minimum of 14 days. The elevated temperature should accelerate the redistribution of any spatial moisture gradient that has developed.

Table 28: Comparison of conditioning procedures investigated for sorptivity testing

Procedure	Pre-Conditioning	Conditioning	Post-Conditioning
105ºC Drying	None	At 105ºC in ventilated oven until Δmass < 0.1% / 24 hrs	Cool samples in desiccator Test within 18 – 24 hours
50ºC Drying	None	As above but reduce temperature to 50ºC	As above
NIST Procedure[52]	Vacuum saturate samples to SSD conditions Seal sides with tape to minimise formation of radial moisture gradients	Condition at 50ºC & 80% RH for 7 days	Seal into container at 23ºC Test when relative humidity in container stabilises
RILEM Procedure[53]	As Above	Dry sample at 50ºC until: $\Delta m = \frac{\theta_{SSD} - \theta_{65\%RH}}{1 + \theta_{SSD}} \cdot m_{sample}$ where: Θ_{SSD}=moisture content at SSD $\Theta_{65\% RH}$=moisture content at 65% RH Based on desorption experiments carried out under ambient conditions	Seal samples to prevent further moisture exchange Maintain at 50ºC for a minimum of 14 days

4.2.6 Results

Figure 32 shows the mean sorptivity results for each conditioning method, plotted as a function of the curing received by the test cores. The error bars shown are the one standard deviation limit calculated from the variability in the test replicates.

It is apparent that the sorptivity coefficients obtained under different conditioning regimes cannot be directly compared. Coefficients on concrete dried at 105ºC are approximately 1.5 – 2 times greater than those from the samples dried at 50ºC and more than five times greater than the results from NIST or RILEM conditioning.

Conditioning at 50ºC appears to produce the most satisfactory result, with the sorptivity coefficients decreasing in a rational way as the curing period is extended. Statistical analyses (heteroscedastic t-tests) indicate that the differences between the coefficients are significant, that is, they represent a real change in concrete properties rather than random experimental uncertainty.

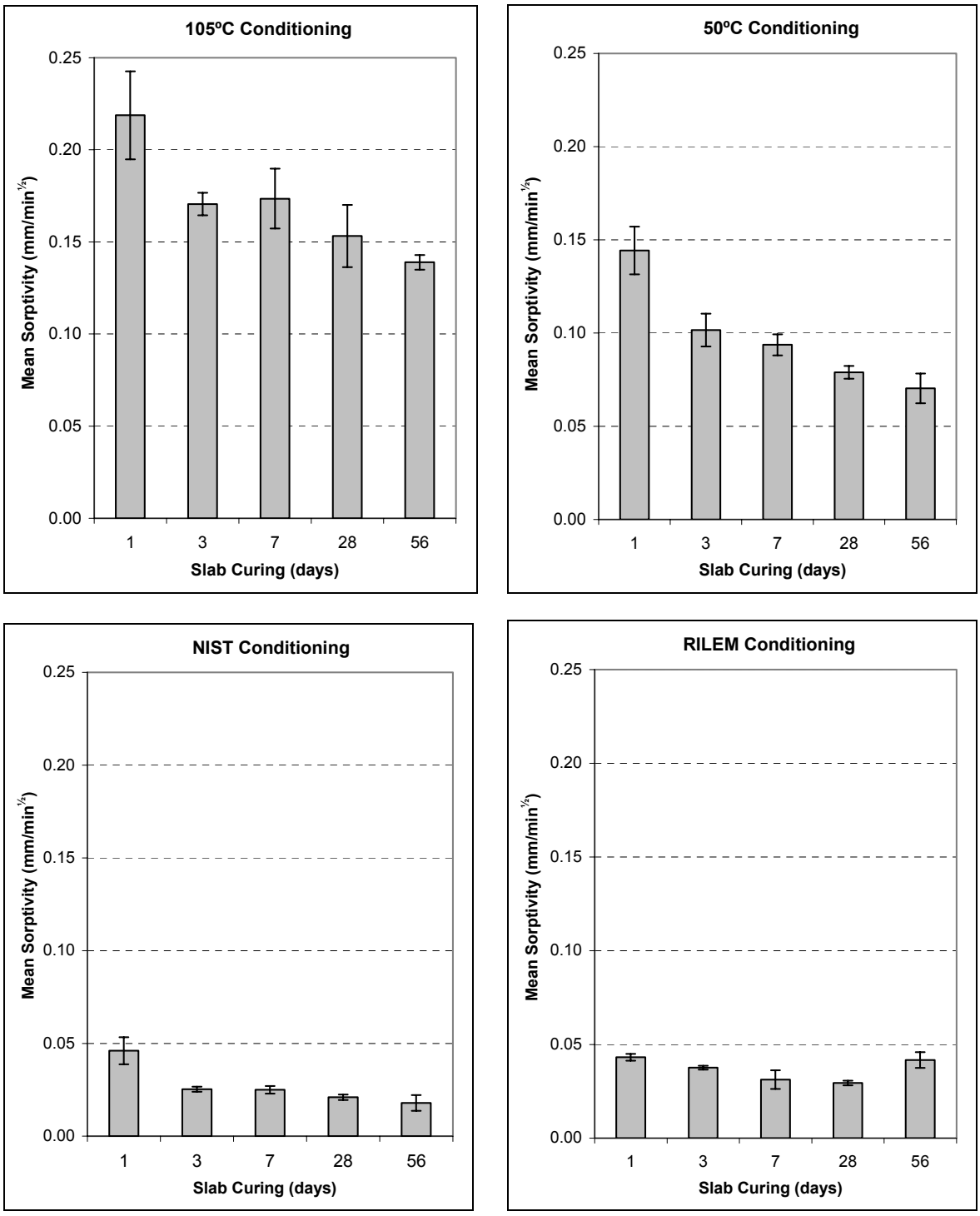

Figure 32: Mean sorptivity results for slab specimens conditioned by the four methods considered

The other three conditioning regimes are less sensitive to the effects of curing. Drying at 105ºC appears to have reduced the improvement in concrete transport parameters expected between 3, 7 and 28 days curing. In the case of NIST and RILEM conditioning, the suppressed sorptivity coefficients resulting from the relatively less dry specimens limit the precision with which differences in concrete quality can be distinguished.

Figure 33 illustrates the difficulty: by 60 minutes into a sorptivity experiment the mean rate of water ingress in a NIST or RILEM conditioned core can be as low as 0.012 g/minute. Thus the cumulative water absorption over a 10 or 20 minute reading interval is comparable with the ± 0.1 g uncertainty typical in a laboratory balance of sufficient load capacity to be used for a sorptivity test.

A consequence of the square root of time dependence in equation [6-1] is that improving the sensitivity of the test requires more frequent early measurements. This imposes practical limitations for the convenient testing of multiple sample replicates.

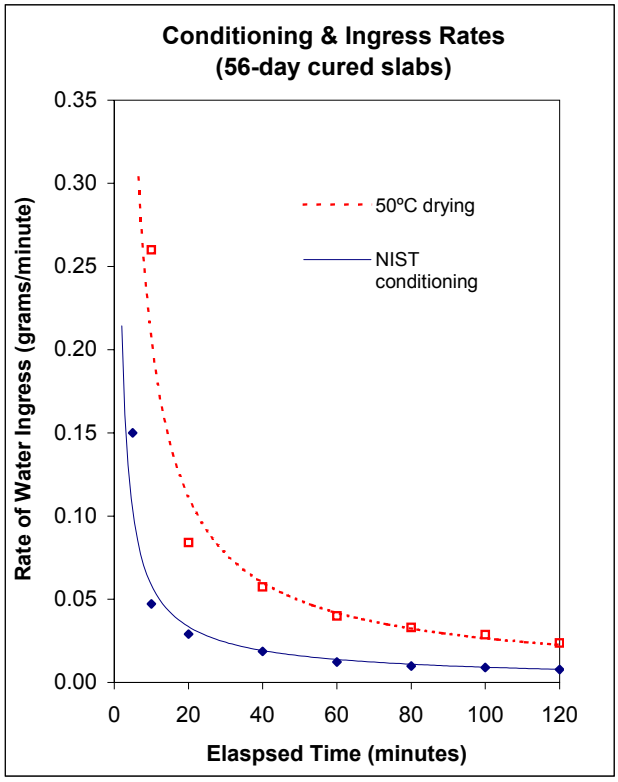

Figure 33: Mean water ingress rates for two different conditioning methods

An indication of the sensitivity of sorptivity and compressive strength as a discriminator of curing effectiveness can be gained from Figure 34. While the sorptivity testing indicates the benefit of extended curing, even up to 56 days, the compressive strength of the slab cured for 56 days is not significantly greater than the 7 day slab. This is a clear demonstration that the achieved compressive strength is not an adequate measure of durability because the bulk concrete, unlike the near-surface layer that controls durability, is generally somewhat insulated from poor curing practice.

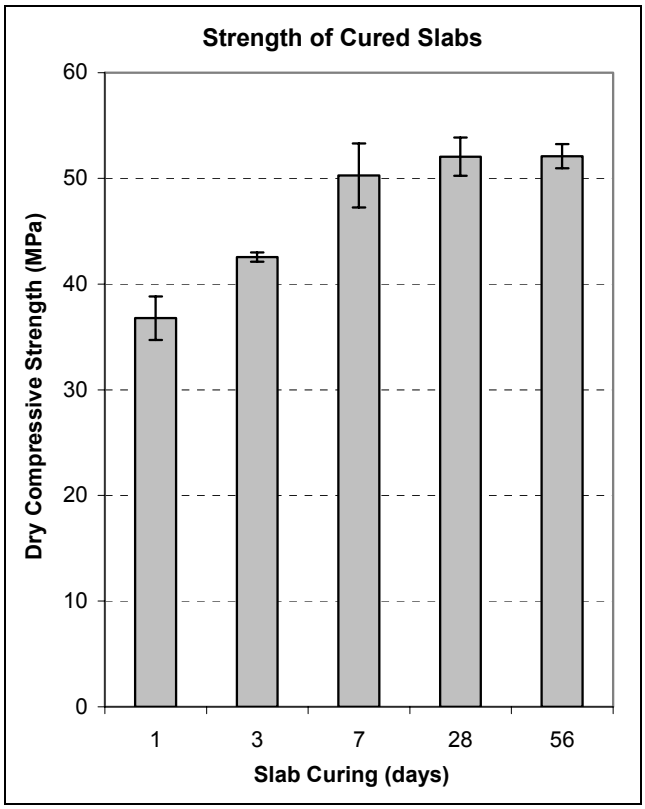

Figure 34: Measured compressive strength of sorptivity test slabs 68 days after casting

4.2.7 Sensitivity of sorptivity to concrete quality

Having established an appropriate conditioning regime, the ability of the sorptivity test to discriminate concrete quality was examined. For this trial, vertically hardened cylinders were produced from both 30 and 50 MPa concrete (Table 27), immersed in water for various curing periods after which time they were removed and placed in a 50% RH and 23ºC drying environment to minimise further hydration until testing at the uniform age of 56 days. The results are shown in Figure 35, and the testing is clearly able to distinguish between the two mixes and the various curing periods for each mix with a high degree of statistically certainty.

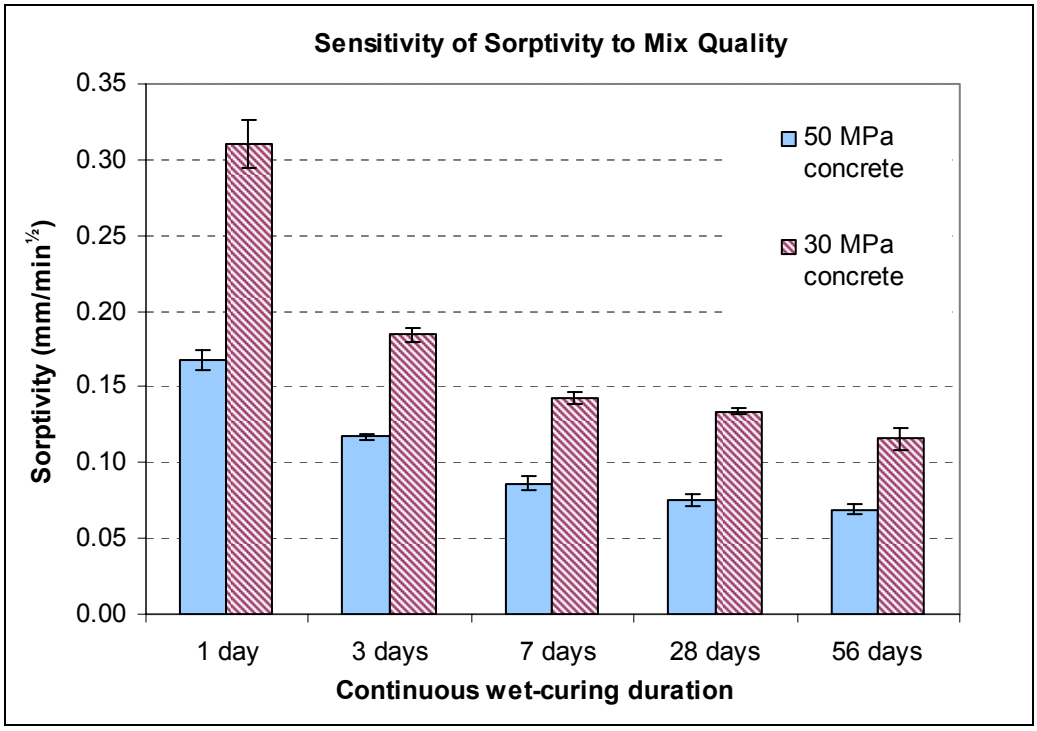

Figure 35: Sorptivity results for cylinder test specimens made from Table 27 concrete mixes

Surprisingly, the sorptivity coefficients determined on the slab series cores were significantly lower than those obtained from cylinders cast from the corresponding mix, as shown in Table 29.

Table 29: Sorptivity comparison between cylinder and cored specimens

Concrete	Sample Type	Mean Sorptivity (mm/min ½)	Standard Deviation (mm/min ½)
30 MPa	cylinder	0.116	0.006
	in-situ core	0.070	0.008
50 MPa	cylinder	0.070	0.002

The 30 MPa cores gave approximately the same result as the 50 MPa grade concrete when cast as a cylinder. The precise reason for this dramatic difference between the sample types is unknown, although the density of the core specimens, at 2,450 kg/m^3, is approximately 40 kg/m^3 denser than the cylinder average, indicating at least some difference in compaction or aggregate distribution between the two. It is probably that this again relates to the tendency for a cement paste enriched zone to form in proximity to cast faces, defined in the case of cylinders by the walls of the mould. Given that cement pastes are more permeable than typical aggregates,

this suggests that water sorptivity through the circumferential edge of a cylinder slice will be greater than that of the interior concrete.

Consequently, if sorptivity is to be used to resolve disputes concerning in-situ concrete quality then it is necessary to have established acceptance criteria based on drilled cores extracted from larger concrete bodies, rather than relying on values derived from cylinders. A more convenient cylinder testing regime is satisfactory for the purposes of mix design and prequalification.

4.2.8 Sensitivity of sorptivity to other factors

In addition to an evaluation of preconditioning methods, BRANZ evaluated the sensitivity of sorptivity to other factors. These studies revealed:

(i) Sorptivity measurements on slices where the direction of water uptake in the test corresponds to the vertical orientation during concrete hardening generally display a lower sorptivity. Thus where acceptable sorptivity limits are specified, for example, as a pre-qualification tool, the sample orientation should be specified.

(ii) Curing of higher grade concrete by total immersion (i.e. a water bath) typically gave lower sorptivity results than those achieved by the same concrete cured for an equivalent length of time in a fog room. This is consistent with a degree of self-desiccation in the internal concrete of low water-to-cement ratio mixes in the less effective curing environment.

(iii) There is a small suggestion that the value of the determined sorptivity coefficient depends on the position that the specimen is taken from the concrete element. In the tests carried out the coefficients typically increased slightly with increasing distance from the cast or form face (Figure 36). However the magnitude of the change appears to be small compared with the sensitivity to the concrete grade or degree of curing

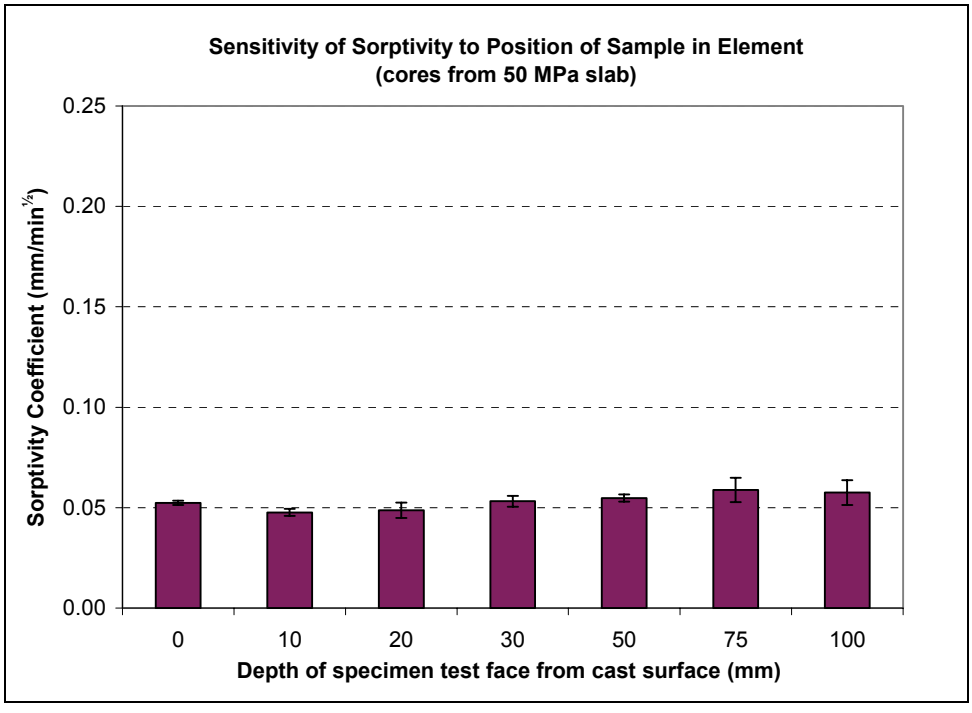

Figure 36: Sorptivity coefficient as a function of distance from formed face

4.2.9 Sorptivity conclusions

Sorptivity is a durability parameter with the virtues of both simplicity and sensitivity to concrete quality. However the influence of moisture content on concrete transport properties is so profound that it is mandatory to know the conditioning history of a test sample before any sense can be made of its sorptivity coefficient.

From the point of view of both ease of testing and sensitivity of results, drying at 50ºC appears to be the most satisfactory conditioning regime. The artificially elevated sorptivity coefficients obtained by this technique offer no real disadvantage to the potential of the test as a simple durability index for characterisation purposes, or as a quality control technique. The need for transport coefficient measurements based on realistic moisture contents (e.g. for multi-mechanistic service-life prediction models) is currently limited. It should be possible to develop empirical equations that scale the 50ºC-conditioned sorptivity coefficients as a function of internal moisture if a demand for these types of values eventuates.

Durability testing as an indicator of potential performance should be carried out 56 days after casting, particularly where SCMs are used in the concrete. Testing at 28 days may be more practical where sorptivity criteria have been specified because of the long lead-in time necessary to condition the samples and achieve a result. In such an instance, a correlation could be established to determine the expected relationship between the 28 and 56 day values. Where sorptivity performance is specified in construction documents, it is important that the method of sample selection and the test methodology are clearly defined. This should cover:

- sample type – cores (from what?) vs cylinders
- casting orientation of the test specimens (horizontal or vertical)
- method of curing (fog or by water bath immersion)
- curing duration and testing age
- method of conditioning to a constant internal moisture content
- method of measurement of sorptivity (by mass or penetration depth).

Cylinders can be used to establish mix designs or for prequalification purposes, but for acceptance of in-situ concrete it is necessary to test core samples and evaluate them against performance specifications that have been established on samples of corresponding type.

The apparent discrepancy between the sorptivity values obtained on cores and cylinders warrants further investigation. It indicates that sorptivity is strongly influenced by factors such as compaction and aggregate distribution, in addition to mix composition and curing. This may make it difficult to use figures derived from laboratory trials as a basis for writing construction specifications that call up absolute sorptivity figures to be achieved in the field. A good example is how to deal with the outer skin of a concrete core extracted from a structure: obtaining a reproducible sorptivity results likely requires testing on a trimmed surface to ensure homogeneity, yet the durability of the structure largely depends on the durability of the discarded layer. A better approach may be a relative sorptivity specification, for example requiring that a curing regime is implemented sufficient that the sorptivity of the outer concrete skin is no larger than a fixed percentage of the interior concrete.

4.3 Laboratory measurements of chloride resistance

The options for measuring the 'chloride penetration resistance' of a concrete mix are not entirely satisfactory. The commentary to NZS 3101[54] indicates that mix performance should be initially proven by a chloride permeability test, but allows for subsequent validation of production batches using a less demanding procedure such as ASTM C1202. As outlined below, both of these solutions have drawbacks. A recent study by the US Federal Highway Authority[55] has suggested a new electrically accelerated method, the rapid migration test. This is claimed to be equally suitable to both initial mix verification and on-going quality control.

4.3.1 Non-steady state diffusion

The most theoretically correct assessment of the 'chloride resistance' of a concrete is to determine its non-steady state chloride-ion diffusion coefficient, D_{ca}. This is most conveniently achieved by an immersion test, in which a completely water-saturated concrete sample, with one exposed plane surface, is submerged in a synthetic seawater solution for a fixed period of time (Figure 37). At the conclusion of the test, the chloride profile that develops is determined by grinding away increments of the exposed concrete face and analysing each ground increment for its chloride content. In this way a concentration vs depth profile is constructed and a chloride diffusion coefficient is calculated by fitting the resulting curve to Crank's solution of Fick's 2nd Law, using a non-linear regression procedure.

Many variations of the methodology exist and there are two published standards NT BUILD 443 and ASTM C 1556. Most authorities agree that this procedure offers the fairest single measure of concrete performance in marine environments. Unfortunately it is better suited to the research environment than routine use by the industry, where constraints of time and money often exist. In particular, the diffusion test is slow, requiring an immersion period of at least 35 days to adequately discriminate between high durability concretes. Combined with the time necessary for curing, sample conditioning and chloride analyses, a diffusion test routinely takes 3 – 4 months to obtain a result. It is also expensive both in terms of labour and the need for multiple precise chloride analyses. This makes it clearly unsuitable for quality control purposes and inconvenient for mix development.

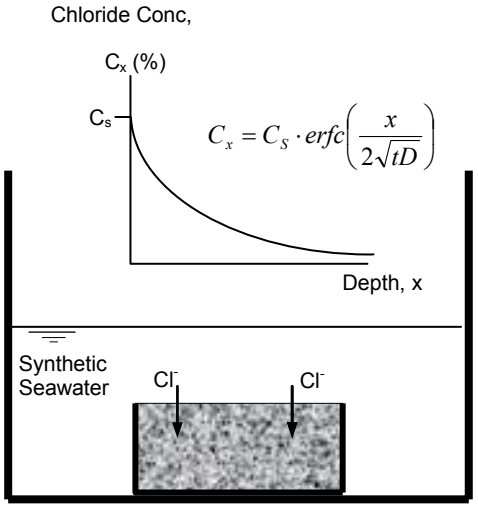

Figure 37: The Chloride Diffusion Test (the diffusion coefficient is 'D' in the equation)

4.3.2 ASTM C 1202 'rapid chloride' permeability

Because of the practical difficulties associated with non-steady state chloride diffusion measurements, the ASTM C1202 'rapid chloride' method has been widely used. The test was developed as a quick quality control method, able to produce results within 48 hours of the nominated test date, but it has often been incorporated into construction specifications or used to trial alternative mix designs in pre-qualification programmes, despite strong criticism of the test's validity[27, 28] when in these roles.

The 'rapid chloride' test set-up is shown schematically in Figure 38. The sample concrete, a 50 mm thick slice of a cylinder or core, is clamped to form a barrier between two fluid reservoirs, one containing sodium chloride solution and the other sodium hydroxide. A 60 V potential is applied across the concrete specimen, causing the chloride-ions to migrate through the concrete and allowing current to flow. The test records the total charge passed in Coulombs over a six hour period. Thus it is a measure of the electrical conductivity of the concrete rather than its ionic diffusivity, as desired. This means the test result reflects not only the connectivity of the pore network, which is the most important determinant of durability, but also the chemistry of the pore solution, which is of little consequence to chloride penetration. As an example of why this can be significant, concretes containing siliceous pozzolans such as silica fume may give exaggeratedly good (low Coulomb) 'rapid chloride' results. This is because the silica reacts with the sodium and potassium ions normally released into the pore solution as the cement hydrates, reducing this contribution to the concrete's overall conductivity. Over the course of test, samples can also become surprisingly hot due to ohmic (i^2R) heating, reaching 80 – 90 ºC in extreme cases, which distorts the result. Poorer quality concretes pass more current and become warmer, increasing their conductivity, leading to a greater Coulomb value than would be obtained if their temperature remained constant.

The test is therefore unsuitable for comparing concrete made with differing binders, but can be effective for monitoring the consistency of production of a single mix. Unlike compressive strength, the 'rapid chloride' result does have a direct correlation with durability.

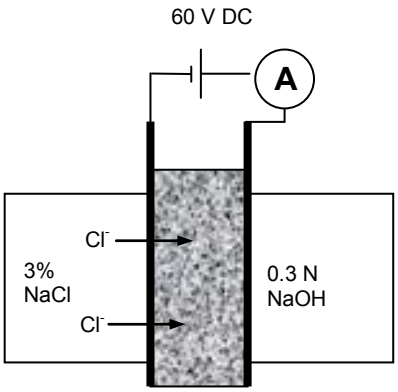

Figure 38: Schematic of an ASTM C1202 'rapid chloride' test (the result is the charge passed in six hours)

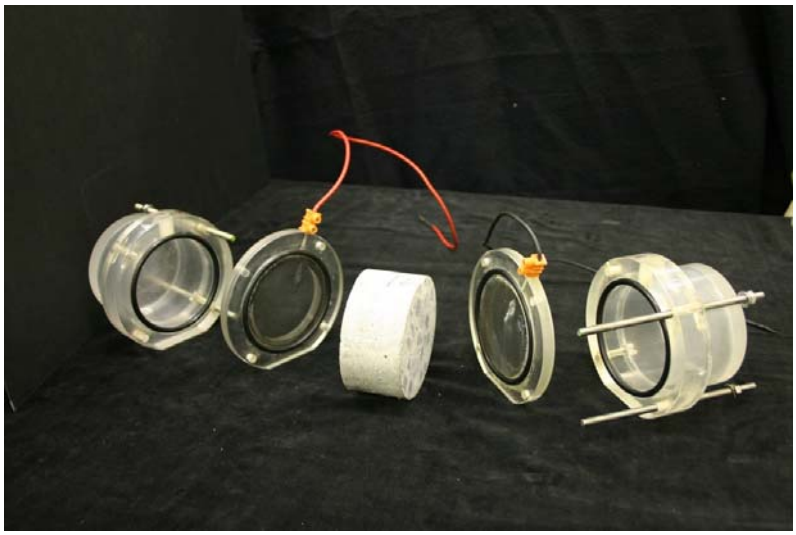

Figure 39: Apparatus for implementing the 'rapid chloride' test

4.3.3 Rapid Migration Test (RMT)

Because of the technical limitations of the 'rapid chloride' test and the impracticality of direct measurements of chloride diffusion, the US Federal Highway Authority sponsored a three year study by the University of Toronto to develop or identify a test method able to predict the chloride penetration resistance of concrete in as short a timeframe as possible. Included in the brief was the requirement that the chosen test would be equally applicable to evaluating new mix designs, accepting or rejecting concrete according to contract specifications, and evaluating the quality of already placed concrete. The test also needed to be immune to distortions due to chemical or mineral admixtures (slag, silica fume, super-plasticisers, corrosion inhibitors etc), not be affected by the presence of reinforcing steel, and give valid results over a w/c range of 0.25 – 0.5. The success of the test methods was gauged by how closely their results correlated with long-term (90 and 365 day) Actual Diffusion tests.

After a literature review, laboratory evaluation of 10 different methods and inter-laboratory trials a 'rapid migration test' (RMT) was developed. This was a slight variation on an existing methodology by Tang & Nilsson[56] that has subsequently been adopted as NordTest standard NT Build 492. The basic principle of the RMT is similar to the 'rapid chloride' test with an electrical potential being applied to cause migration of chloride-ions from solution into the test sample (Figure 40). The critical differences are:

(i) The chloride resistance of the sample is measured directly in NT Build 492, rather than by an indirect inference from the current passed. At the conclusion of the test, the sample is split open and sprayed with silver nitrate solution, which reacts to give white insoluble silver chloride on contact with chloride-ions. This gives a simple physical measurement of the degree to which the sample has been penetrated and, unlike ASTM C 1202, is unaffected by the chemistry of pore solution within the concrete.

(ii) The temperature of the sample is effectively constant under the NT Build 492 test regime. Through immersion in a large volume (18 litres) of chloride solution the concrete is greatly buffered against temperature changes due to ohmic heating that can distort a 'rapid chloride' test result.

These changes address the major criticisms levelled at the 'rapid chloride' test methodology while retaining its principal virtue of a quick result.

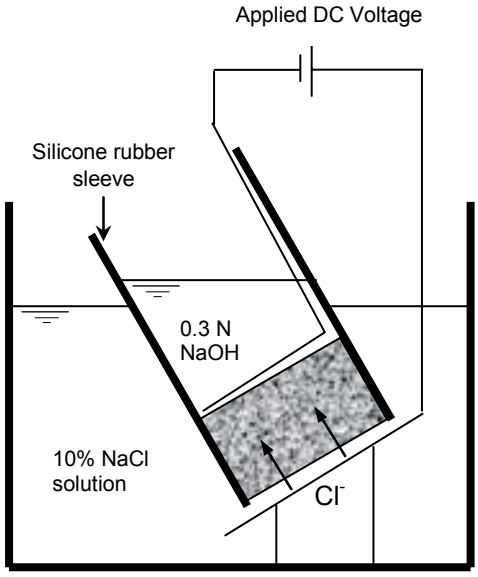

Figure 40: Schematic for a 'rapid migration test' (the specimen is broken open and the penetration measured at the end of test)

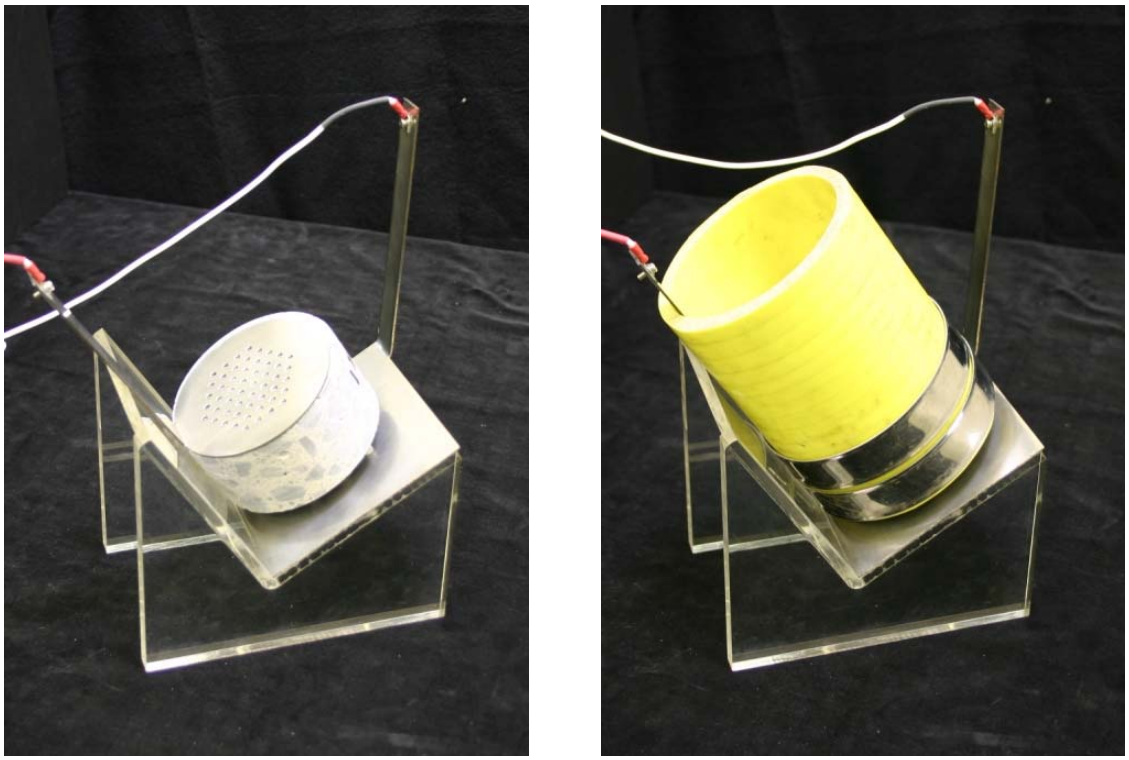

Figure 41: Apparatus for implementing the 'rapid migration test'

In an RMT, the applied voltage and test duration are varied, according to the initial current which flows when the potential is applied. This ensures that the chloride front does not penetrate completely through the sample before the conclusion of the test. For most concretes, testing is completed within 24 hours (plus 1 to 2 days for sample preparation). Using electrochemical theory, the measured chloride penetration can be converted to a non-steady state diffusion coefficient. However, for a variety of reasons this will not exactly correspond with the equivalent immersion test value. Providing all the test data is obtained at the same temperature the results are more conveniently expressed in the arbitrary units of mm/V.hr (mm per volt-hour). This is the convention adopted by the Federal Highway Authority.

4.3.4 BRANZ RMT results

BRANZ carried out comparative testing on cores taken from exposure blocks on the B2 (Oteranga Bay) site after 48 months exposure examining the correlation between RMT values and non-steady state diffusion results. All the test specimens were taken from the interior of the block, in the interval 100 – 150 mm below the exposed surface, to avoid the possibility of environmental chloride contamination. As shown in Figure 42 the determined RMT values correlate well with D_{ca} (actual chloride diffusion coefficient) measurements, with a correlation coefficient (r^2) value above 0.95. In contrast, previous attempts to correlate between 'rapid chloride' values and diffusion coefficients gave very poor results. Figure 43 shows a typical example for the characterisation cylinders produced at the time of block casting; the r^2 value is only 0.56. This would appear to provide strong support for favouring the RMT methodology over 'rapid chloride' testing where a reasonable approximation to the chloride-ion diffusivity of the concrete is required.

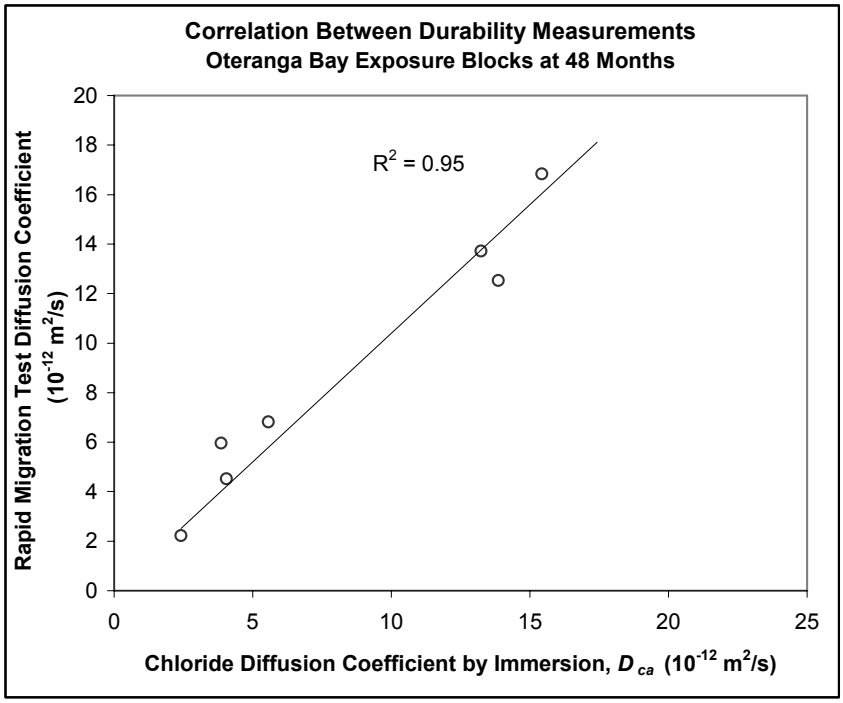

Figure 42: Correlation between measured chloride diffusion coefficients and the NT Build 492 'rapid migration test'

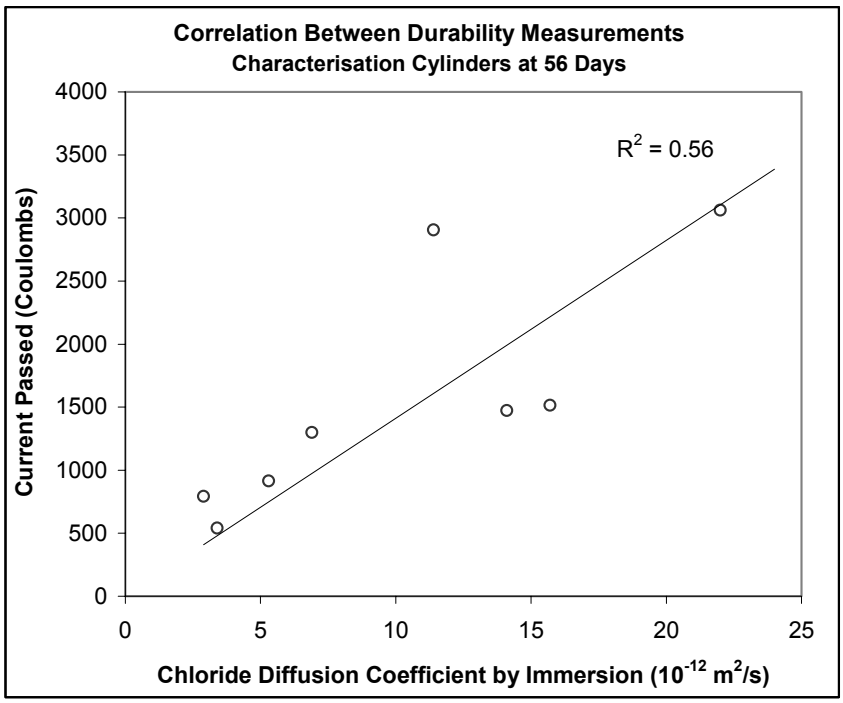

Figure 43: Correlation between measured chloride-ion diffusion coefficients and the ASTM C1202 'rapid chloride test'

4.4 Durability measurement conclusions

BRANZ prefers the RMT methodology over the ASTM C1202 'rapid chloride' technique for the specification or prequalification of durable concrete mixes intended for use in marine environments. It offers the compelling speed and convenience of the latter method with the advantage of a sounder theoretical footing. However further validation is required, particularly for the application of the procedure to cores from field structures rather than laboratory-cast cylinders. The relatively more variable compaction encountered in field concrete typically gives rise to a less well-defined chloride penetration front that can be troublesome to measure accurately. For pure quality control purposes, where a firm correlation can be established between the electrical conductivity of the concrete and its chloride-ion diffusion coefficient, the ASTM C1202 test may be used and the choice of method is largely due to personal preference. However it should also be remembered that numerically equal 'rapid chloride' Coulomb values do not always translate to the same resistance to chloride-ion penetration where concretes with different binder compositions are being considered.

A more wide-ranging assessment of potential test methods relevant to marine durability performance has been undertaken by RILEM Committee TC 178 'Chloride Penetration into Concrete', employing a 'round-robin' of international laboratories including BRANZ. The results are currently in press[57] and should provide further clarity about the most appropriate techniques to adopt for various purposes.

BRANZ believes that sorptivity is the best available method for assessing the capillary absorption of a particular concrete mix. Sorptivity is a significant transport mechanism for chloride-ions through partially-saturated concrete in marine environments, and optimisation and control of this property is an important facet of adequate durability performance. However users are cautioned to carefully specify the sample preconditioning regime. The sensitivity of the test method to specimen compaction and orientation suggest that its use is best restricted to indexing the durability of alternative mix designs produced in the laboratory under controlled conditions. Care should also be exercised in the interpretation of absolute sorptivity results, particularly on cores taken from field structures with unknown curing and placement histories.

Based on the experience gained here, one of the most effective approaches to guaranteeing the quality of delivered concrete for a contract-specified marine durability requirement is by monitoring concrete performance through the course of the project relative to performance levels established by a pre-contract trial placement. This necessitates careful pre-planning because lead times of at least three months are required if chloride diffusion parameters are to be measured. A possible approach is outlined below:

1. Carry out a trial placement of concrete in the form of a slab or other project-appropriate shape to confirm the workability and general placement qualities of the desired mix.

2. Determine the intrinsic chloride-ion diffusion coefficient of the as-supplied trial concrete using NT BUILD 443, ASTM C 1556 or similar, and correlate this value with the result of an electrically-accelerated migration test such as NT BUILD 492. Confirm that the chloride diffusion coefficient is sufficiently low to provide the required durability based on reference to published literature, including this report. Note that, as discussed in Section 2.4, there is no simple relationship between the effective diffusion coefficient of the in-situ structure, which is linked to design life, and the actual diffusion coefficient determined in the laboratory and that the exposure environment and cement type used need to be considered.

3. Establish the specified compressive strength to be used for quality control purposes during construction to meet the above durability requirement. Monitor the concrete quality supplied over the course of the contract by routine compressive strength testing, evaluated against the criteria specified in Table 2.8 of NZS 3104:2003. A testing frequency needs to be established that takes into consideration the historical performance data available on the mix being used. An initially high sampling frequency can be reduced once positive compliance trends are observed. Rapid migration tests should be carried out occasionally to verify satisfactory ongoing durability performance, with acceptance based on comparison with the results achieved in the pre-contract trial. The appropriate margin for variability in these parameters will need to be established for each different contract. A minimum of 85% of the performance achieved in the trial has been used as the acceptance level in some recent contracts.

4. Carry out rapid migration and compressive strength tests on concrete cores removed from the trial placement. If, in the course of the contract, a dispute arises about the performance of concrete placed in-situ, these results can be used to establish acceptable test results that could be expected for cores removed from the main body of the structure in question. These reference values can be used without concern that the results are influenced by different site placement, compaction and curing practices as might be the case if reference values derived from laboratory-produced cylinder specimens were benchmarked instead.

5. SUMMARY

Given the difficulty involved in a sound theoretical treatment of the processes governing chloride ingress into concrete, the current most practical approach to service life prediction is empirical modelling of the development of concentration profiles using a Fick's Law-derived model. Little direct correlation is observed between chloride-ion diffusivity measured in the laboratory and the diffusion coefficients that describe the performance of corresponding concrete in the field because of the dominance of environmental factors. Consequently the empirical approach is only feasible if an extensive database of appropriate model input parameters exists for well-characterised concrete under realistic exposure conditions.

To completely specify the performance of concrete for chloride resistance in a particular environment, three parameters are necessary: a surface chloride concentration, C_s, quantifying the stress imposed by the environment; an effective diffusion coefficient, D_{ce}, characterising the concrete's response to the environmental stress; and an index, m, representing any observed change in the chloride-ion diffusivity through the concrete with time.

These parameters have derived for four types of cement binder used in New Zealand by modelling the rate of chloride ingress through concrete blocks placed on marine exposure sites of varying severity [Section 2.4]. A statistically-significant time-dependent decrease in chloride-ion diffusivity was measured for concrete produced with Duracem, Microsilica and Micropoz binders. This decrease was mostly strongly evident in the Duracem concrete samples, but the greater potential durability benefit was counteracted somewhat by their tendency to develop higher surface chloride loads than the other concrete types. Concrete made with GP cement showed no such improvement in chloride resistance and is not adequately durable when used in combination with mild steel reinforcing under severe (C Zone) marine exposure conditions.

While this data provides confidence in the durability enhancement conferred by the use of Duracem, Micropoz and Microsilica, it appears too imprecise to be relied upon absolutely for durability design purposes. Therefore, the apparent improvement in chloride resistance with time demonstrated should not be used in combination with service-life prediction models to

justify reducing covers over reinforcement, or to decrease the binder content or increase the w/b ratio of concrete, from the values specified in NZS 3101 *Concrete structures* for marine environments.

The temporal dependence of effective chloride-ion diffusivity was only observed for concrete placed on the most severe C Zone exposure, where the blocks were in direct contact with seawater. This phenomenon cannot be adequately explained by ongoing hydration refining the concrete's pore structure, as confirmed by relatively static measurements of intrinsic diffusivity made on the interior concrete. It is most likely to be due to a combination of effects, including a transition between absorption and diffusion as the predominant chloride-ion transport mechanism, pore-blocking reactions due to ion exchange with seawater, and a spatial variation in the distribution of cement paste and aggregate through the concrete.

Given the uncertainty surrounding the causes of time-dependent diffusivity and its potentially dominant effect on predicted rates of chloride ingress, it is important that service-life prediction models are not used uncritically. No individual implementation of the empirical Fick's Law type model should be absolutely relied upon. Users should compare the predictions obtained with a number of implementations from different sources when evaluating potential durability solutions. This will help to minimise the influence of any bias present in the models due to differences in their underlying assumptions [Section 3].

BRANZ recommends that the choice of a durable marine concrete mix should primarily be guided by the results of early-age characterisation tests that have a direct link to the physiochemical mechanisms expected to control the durability of the structure in question. Consideration should also be given to the ease with which the mix can be placed and compacted on site: achieving an adequate quality of workmanship is crucial to satisfactory durability performance.

The most significant physiochemical mechanisms that should be addressed by characterisation tests for marine durability are absorption and diffusion. These represent the transport mechanism for a chloride-enriched solution in contact with an unsaturated and totally saturated concrete respectively. BRANZ suggests that a hydraulic sorptivity test is the most satisfactory means of determining absorption characteristics [Section 4.2] and that a 'rapid migration test' should be preferred as the most satisfactory accelerated laboratory test for chloride-ion diffusion [Section 4.3].

Obtaining meaningful sorptivity data is dependent on preconditioning the concrete to a consistent and reproducible internal moisture state. BRANZ prefers that sorptivity tests are performed by conditioning test specimens to a constant mass at 50ºC in a ventilated oven, before measuring their unidirectional water uptake through a defined plane surface by mass. Drying at higher temperatures is undesirable because of the potential to dehydrate the cement gel and introduce micro-cracking, physically altering the structure of the concrete. At the opposite end of the scale, conditioning to replicate a moisture content typical of field concrete under ambient conditions is difficult to execute correctly and introduces problems of moisture gradients and poor test sensitivity.

A non-steady diffusion test is the most theoretically correct method of assessing chloride resistance of concrete. However, the 3 – 4 months necessary to complete a test renders it unsuitable for quality control purposes and inconvenient for mix development and prequalification. In these situations, the NT Build 492 'rapid migration test' was found to correlate well with measured chloride-ion diffusion coefficients and offers the speed of the well-known ASTM C1202 'rapid chloride' test without the limitations of sensitivity to binder type and ohmic heating distortions.

Analysis of the durability performance of in-situ structures by mathematically fitting their chloride ingress profiles to diffusion parameters is a relatively recent development amongst concrete technologists. The value and sophistication of empirical service-life prediction models employing this technique should improve as more comprehensive databases of appropriate parameters are compiled for various combinations of cement binder type, exposure environment and concrete grade. However, such models will always be constrained by the fact that they reflect only a statistical average of the available performance data for a particular concrete in a particular environment. This is satisfactory for comparing the performance of one binder type with another; however, there will always be an inherent risk in using these tools for design purposes because the environment-specific factors may result in chloride ingress behaviour departing from the expected statistical mean.

This limitation will only be overcome by a comprehensive durability model that addresses from first principles the multi-mechanistic transport processes to which cracked and uncracked concrete can be subject to. Acquiring the fundamental data necessary to construct and validate such models would necessitate the development and routine incorporation of embedded sensors into reinforced concrete structures to non-destructively monitor their performance. This is a challenge for the future.

APPENDIX: CHLORIDE PROFILE DATA

Table 30: Chloride profiles developed on GP concrete at the Weka Bay exposure site

325 GP Weka Bay 'C' zone															
6 months' exposure			**12 months' exposure**			**18 months' exposure**			**30 months' exposure**			**60 months' exposure**			
Depth	**Chloride** (% concrete)		**Depth**	**Chloride** (% concrete)		**Depth**	**Chloride** (% concrete)		**Depth**	**Chloride** (% concrete)		**Depth**	**Chloride** (% concrete)		
(mm)	replicate 1	replicate 2	(mm)	replicate 1	replicate 2	(mm)	replicate 1	replicate 2	(mm)	replicate 1	replicate 2	(mm)	replicate 1	replicate 2	replicate 3
1.0	0.307	0.234	1.5	0.254	0.269	1.0	0.336	0.365	2.5	0.185	0.206	2.5	0.220	0.282	0.282
3.0	0.200	0.173	4.5	0.181	0.175	6.0	0.210	0.197	7.5	0.125	0.154	7.5	0.149	0.202	0.198
5.0	0.160	0.129	7.5	0.147	0.156	11.0	0.157	0.183	12.5	0.089	0.127	12.5	0.143	0.176	0.193
7.5	0.132	0.104	10.5	0.143	0.165	16.0	0.131	0.145	17.5	0.060	0.102	17.5	0.129	0.159	0.166
10.5	0.130	0.075	13.5	0.117	0.139	21.0	0.104	0.116	22.5	0.035	0.067	22.5	0.100	0.128	0.138
13.5	0.103	0.048	16.5	0.078	0.103	26.0	0.071	0.073	27.5	0.018	0.039	27.5	0.087	0.091	0.110
16.5	0.068	0.030	19.5	0.063	0.086	31.0	0.037	0.046	32.5	0.010	0.025	32.5	0.072	0.082	0.100
						36.0	0.020	0.022	37.5	0.005	0.011	37.5	0.045	0.063	0.077
						41.0	0.012	0.012				42.5	0.039	0.051	0.062
						46.0	0.005	0.007							
400 GP Weka Bay 'C' zone															
6 months' exposure			**12 months' exposure**			**18 months' exposure**			**30 months' exposure**			**60 months' exposure**			
Depth	**Chloride** (% concrete)		**Depth**	**Chloride** (% concrete)		**Depth**	**Chloride** (% concrete)		**Depth**	**Chloride** (% concrete)		**Depth**	**Chloride (% concrete)**		
(mm)	replicate 1	replicate 2	(mm)	replicate 1	replicate 2	(mm)	replicate 1	replicate 2	(mm)	replicate 1	replicate 2	(mm)	replicate 1	replicate 2	replicate 3
1.0	0.316	0.205	1.5	0.279	0.299	1.0	0.306	0.276	2.5	0.285	0.240	2.5	0.318	0.299	0.287
3.0	0.207	0.130	4.5	0.170	0.217	6.0	0.163	0.142	7.5	0.203	0.159	7.5	0.208	0.172	0.185
5.0	0.156	0.089	7.5	0.149	0.181	11.0	0.125	0.117	12.5	0.160	0.137	12.5	0.182	0.151	0.159
7.5	0.146	0.064	10.5	0.126	0.141	16.0	0.084	0.066	17.5	0.134	0.110	17.5	0.149	0.116	0.123
10.5	0.089	0.041	13.5	0.091	0.124	21.0	0.037	0.028	22.5	0.089	0.062	22.5	0.107	0.091	0.080
13.5	0.058	0.022	16.5	0.053	0.093	26.0	0.021	0.014	27.5	0.056	0.035	27.5	0.089	0.055	0.050
16.5	0.033	0.009	19.5	0.033	0.056	31.0	0.005	0.007	32.5	0.038	0.023	32.5	0.060	0.036	0.035
						36.0	0.003	0.005	37.5	0.020	0.011	37.5	0.042	0.023	0.022
						41.0	0.004	0.004				42.5	0.031	0.012	0.014
						46.0	0.005	0.005							

Table 31: Chloride profiles developed on Duracem concrete at the Weka Bay exposure site

280 DC Weka Bay 'C' zone

6 months' exposure			12 months' exposure			18 months' exposure			30 months' exposure			60 months' exposure			
Depth	**Chloride** (% concrete)		**Depth**	**Chloride** (% concrete)		**Depth**	**Chloride** (% concrete)		**Depth**	**Chloride** (% concrete)		**Depth**	**Chloride** (% concrete)		
(mm)	replicate 1	replicate 2	**(mm)**	replicate 1	replicate 2	**(mm)**	replicate 1	replicate 2	**(mm)**	replicate 1	replicate 2	**(mm)**	replicate 1	replicate 2	replicate 3
1.0	0.428	0.523	1.5	0.472	0.461	1.5	0.441	0.410				2.5	0.498	0.490	0.566
3.0	0.325	0.399	4.5	0.351	0.350	4.5	0.317	0.325				7.5	0.389	0.351	0.307
5.0	0.249	0.281	7.5	0.249	0.293	7.5	0.284	0.326				12.5	0.331	0.284	0.272
7.5	0.195	0.182	10.5	0.190	0.238	10.5	0.270	0.284				17.5	0.239	0.186	0.193
10.5	0.160	0.110	13.5	0.149	0.162	13.5	0.202	0.227	No measurements made			22.5	0.111	0.096	0.076
13.5	0.110	0.059	16.5	0.081	0.099	16.5	0.113	0.163				27.5	0.042	0.040	0.030
16.5	0.059	0.031	19.5	0.036	0.042	19.5	0.056	0.101				32.5	0.022	0.023	0.018
												37.5	0.018	0.018	0.017
												42.5	0.019	0.016	0.018

325 DC Weka Bay 'C' zone

6 months' exposure			12 months' exposure			18 months' exposure			30 months' exposure			60 months' exposure			
Depth	**Chloride** (% concrete)		**Depth**	**Chloride** (% concrete)		**Depth**	**Chloride** (% concrete)		**Depth**	**Chloride** (% concrete)		**Depth**	**Chloride** (% concrete)		
(mm)	replicate 1	replicate 2	**(mm)**	replicate 1	replicate 2	**(mm)**	replicate 1	replicate 2	**(mm)**	replicate 1	replicate 2	**(mm)**	replicate 1	replicate 2	replicate 3
1.0	0.540	0.591	1.5	0.612	0.631	1.5	0.456	0.456	1.5	0.461	0.442	2.5	0.565	0.502	0.616
3.0	0.402	0.422	4.5	0.429	0.395	4.5	0.366	0.353	4.5	0.370	0.377	7.5	0.380	0.354	0.360
5.0	0.326	0.275	7.5	0.293	0.264	7.5	0.264	0.273	7.5	0.310	0.310	12.5	0.170	0.186	0.187
7.5	0.209	0.150	10.5	0.151	0.166	10.5	0.152	0.214	10.5	0.230	0.203	17.5	0.036	0.048	0.043
10.5	0.091	0.063	13.5	0.089	0.073	13.5	0.053	0.112	13.5	0.118	0.110	22.5	0.013	0.012	0.013
13.5	0.038	0.035	16.5	0.033	0.025	16.5	0.019	0.051	16.5	0.044	0.061	27.5	0.009	0.010	0.012
16.5	0.022	0.022	19.5	0.022	0.009	19.5	0.012	0.022	19.5	0.016	0.031	32.5	0.012	0.008	0.008
												37.5	0.010	0.010	0.010
												42.5	0.013	0.009	0.009

400 DC Weka Bay 'C' zone

6 months' exposure			12 months' exposure			18 months' exposure			30 months' exposure			60 months' exposure			
Depth	**Chloride** (% concrete)		**Depth**	**Chloride** (% concrete)		**Depth**	**Chloride** (% concrete)		**Depth**	**Chloride** (% concrete)		**Depth**	**Chloride** (% concrete)		
(mm)	replicate 1	replicate 2	**(mm)**	replicate 1	replicate 2	**(mm)**	replicate 1	replicate 2	**(mm)**	replicate 1	replicate 2	**(mm)**	replicate 1	replicate 2	replicate 3
1.0	0.483	0.474	1.5	0.527	0.522	1.5	0.392	0.417	1.5	0.469	0.435	2.5	0.645	0.688	0.650
3.0	0.359	0.278	4.5	0.331	0.314	4.5	0.237	0.301	4.5	0.360	0.338	7.5	0.365	0.350	0.372
5.0	0.263	0.170	7.5	0.174	0.190	7.5	0.127	0.206	7.5	0.295	0.243	12.5	0.208	0.195	0.169
7.5	0.195	0.100	10.5	0.080	0.116	10.5	0.062	0.116	10.5	0.211	0.151	17.5	0.069	0.053	0.047
10.5	0.105	0.051	13.5	0.038	0.043	13.5	0.026	0.060	13.5	0.119	0.085	22.5	0.017	0.014	0.013
13.5	0.037	0.052	16.5	0.017	0.017	16.5	0.026	0.029	16.5	0.060	0.040	27.5	0.011	0.010	0.011
16.5	0.016	0.012	19.5	0.007	0.011	19.5	0.026	0.021	19.5	0.023	0.014	32.5	0.010	0.011	0.014
												37.5	0.012	0.013	0.011
												42.5	0.011	0.010	0.010

Table 32: Chloride profiles developed on Micropoz concrete at the Weka Bay exposure site

325 MP Weka Bay 'C' zone													
6 months' exposure			**12 months' exposure**			**18 months' exposure**			**30 months' exposure**			**60 months' exposure**			
Depth	**Chloride** (% concrete)		**Depth**	**Chloride** (% concrete)		**Depth**	**Chloride** (% concrete)		**Depth**	**Chloride** (% concrete)		**Depth**	**Chloride** (% concrete)		
(mm)	replicate 1	replicate 2	**(mm)**	replicate 1	replicate 2	**(mm)**	replicate 1	replicate 2	**(mm)**	replicate 1	replicate 2	**(mm)**	replicate 1	replicate 2	replicate 3
1.0	0.251	0.251	1.5	0.282	0.306	1.5	0.376	0.390	1.5	0.429	0.419	2.5	0.542	0.523	0.450
3.0	0.137	0.167	4.5	0.149	0.170	4.5	0.270	0.251	4.5	0.306	0.303	7.5	0.250	0.242	0.202
5.0	0.097	0.112	7.5	0.100	0.094	7.5	0.219	0.168	7.5	0.237	0.200	12.5	0.220	0.157	0.145
7.5	0.054	0.077	10.5	0.061	0.059	10.5	0.120	0.118	10.5	0.179	0.140	17.5	0.117	0.103	0.096
10.5	0.026	0.043	13.5	0.035	0.028	13.5	0.078	0.075	13.5	0.128	0.105	22.5	0.071	0.058	0.049
13.5	0.011	0.026	16.5	0.012	0.015	16.5	0.045	0.042	16.5	0.093	0.073	27.5	0.031	0.026	0.023
16.5	0.010	0.021	19.5	0.012	0.008	19.5	0.016	0.013	19.5	0.058	0.038	32.5	0.014	0.011	0.011
												37.5	0.005	0.005	0.009
												42.5	0.006	0.004	0.007
400 MP Weka Bay 'C' zone															
6 months' exposure			**12 months' exposure**			**18 months' exposure**			**30 months' exposure**			**60 months' exposure**			
Depth	**Chloride** (% concrete)		**Depth**	**Chloride** (% concrete)		**Depth**	**Chloride** (% concrete)		**Depth**	**Chloride** (% concrete)		**Depth**	**Chloride** (% concrete)		
(mm)	replicate 1	replicate 2	**(mm)**	replicate 1	replicate 2	**(mm)**	replicate 1	replicate 2	**(mm)**	replicate 1	replicate 2	**(mm)**	replicate 1	replicate 2	replicate 3
1.0	0.373	0.407	1.5	0.387	0.352	1.5	0.279	0.283	1.5	0.305	0.286	2.5	0.517	0.531	0.463
3.0	0.263	0.299	4.5	0.239	0.207	4.5	0.192	0.189	4.5	0.220	0.168	7.5	0.234	0.234	0.246
5.0	0.181	0.193	7.5	0.138	0.112	7.5	0.118	0.115	7.5	0.171	0.151	12.5	0.190	0.129	0.159
7.5	0.124	0.109	10.5	0.079	0.065	10.5	0.068	0.069	10.5	0.126	0.141	17.5	0.132	0.081	0.097
10.5	0.062	0.055	13.5	0.042	0.031	13.5	0.041	0.039	13.5	0.086	0.099	22.5	0.077	0.036	0.052
13.5	0.028	0.023	16.5	0.025	0.021	16.5	0.020	0.017	16.5	0.075	0.069	27.5	0.032	0.016	0.024
16.5	0.017	0.019	19.5	0.011	0.011	19.5	0.008	0.010	19.5	0.045	0.038	32.5	0.012	0.009	0.008
												37.5	0.009	0.006	0.007
												42.5	0.004	0.004	0.005

Table 33: Chloride profiles developed on Microsilica concrete at the Weka Bay exposure site

325 MS Weka Bay 'C' zone														
6 months' exposure			**12 months' exposure**			**18 months' exposure**			**30 months' exposure**			**60 months' exposure**			
Depth	**Chloride** (% concrete)		**Depth**	**Chloride** (% concrete)		**Depth**	**Chloride** (% concrete)		**Depth**	**Chloride** (% concrete)		**Depth**	**Chloride** (% concrete)		
(mm)	replicate 1	replicate 2	**(mm)**	replicate 1	replicate 2	**(mm)**	replicate 1	replicate 2	**(mm)**	replicate 1	replicate 2	**(mm)**	replicate 1	replicate 2	replicate 3
1.0	0.455	0.418	1.5	0.391	0.363	1.5	0.304	0.351	1.5	0.405	0.372	2.5	0.451	0.426	0.362
3.0	0.285	0.254	4.5	0.249	0.206	4.5	0.199	0.281	4.5	0.282	0.281	7.5	0.250	0.245	0.234
5.0	0.207	0.184	7.5	0.183	0.154	7.5	0.150	0.239	7.5	0.239	0.234	12.5	0.201	0.191	0.190
7.5	0.163	0.127	10.5	0.141	0.118	10.5	0.116	0.200	10.5	0.211	0.226	17.5	0.136	0.140	0.110
10.5	0.108	0.077	13.5	0.090	0.066	13.5	0.081	0.111	13.5	0.162	0.186	22.5	0.063	0.056	0.056
13.5	0.058	0.042	16.5	0.056	0.030	16.5	0.047	0.073	16.5	0.130	0.136	27.5	0.028	0.024	0.020
16.5	0.035	0.028	19.5	0.031	0.018	19.5	0.029	0.040	19.5	0.076	0.096	32.5	0.009	0.012	0.008
												37.5	0.004	0.009	0.007
												42.5	0.005	0.006	0.005

400 MS Weka Bay 'C' zone														
6 months' exposure			**12 months' exposure**			**18 months' exposure**			**30 months' exposure**			**60 months' exposure**			
Depth	**Chloride** (% concrete)		**Depth**	**Chloride** (% concrete)		**Depth**	**Chloride** (% concrete)		**Depth**	**Chloride** (% concrete)		**Depth**	**Chloride** (% concrete)		
(mm)	replicate 1	replicate 2	**(mm)**	replicate 1	replicate 2	**(mm)**	replicate 1	replicate 2	**(mm)**	replicate 1	replicate 2	**(mm)**	replicate 1	replicate 2	replicate 3
1.0	0.348	0.358	1.5	0.262	0.299	1.5	0.299	0.294	1.5	0.375	0.308	2.5	0.334	0.440	0.438
3.0	0.178	0.195	4.5	0.116	0.132	4.5	0.150	0.142	4.5	0.227	0.182	7.5	0.158	0.163	0.207
5.0	0.096	0.099	7.5	0.065	0.066	7.5	0.072	0.070	7.5	0.159	0.105	12.5	0.078	0.079	0.108
7.5	0.035	0.041	10.5	0.021	0.050	10.5	0.029	0.026	10.5	0.083	0.065	17.5	0.022	0.021	0.035
10.5	0.013	0.017	13.5	0.013	0.011	13.5	0.013	0.010	13.5	0.035	0.034	22.5	0.009	0.010	0.013
13.5	0.015	0.009	16.5	0.005	0.019	16.5	0.010	0.006	16.5	0.014	0.013	27.5	0.011	0.011	0.009
16.5	0.012	0.008	19.5	0.009	0.004	19.5	0.011	0.015	19.5	0.012	0.011	32.5	0.011	0.010	0.010
												37.5	0.009	0.008	0.010
												42.5	0.010	0.008	0.010

Table 34: Chloride profiles developed on GP concrete at the Oteranga Bay exposure site

280 GP Oteranga Bay 'B2' zone											
6 months' exposure			**18 months' exposure**			**48 months' exposure**			**60 months' exposure**		
Depth	**Chloride** (% concrete)		**Depth**	**Chloride** (% concrete)		**Depth**	**Chloride** (% concrete)		**Depth**	**Chloride** (% concrete)	
(mm)	replicate 1	replicate 2	(mm)	replicate 1	replicate 2	(mm)	replicate 1	replicate 2	(mm)	replicate 1	replicate 2	replicate 3
1.0	0.037		1.0	0.095	0.079	4.0	0.042		2.5	0.075	0.074	0.089
3.0	0.027		3.0	0.086	0.073	9.0	0.033		7.5	0.057	0.057	0.075
5.0	0.023	Not	5.0	0.069	0.055	14.0	0.029	Not	12.5	0.051	0.042	0.065
7.5	0.023	Determined	7.0	0.063	0.050	19.0	0.021	Determined	17.5	0.036	0.033	0.049
10.5	0.023		9.0	0.051	0.042	24.0	0.019		22.5	0.031	0.029	0.038
13.5	0.020		11.0	0.042	0.032	29.0	0.016		27.5	0.020	0.021	0.029
						34.0	0.013		32.5	0.018	0.019	0.020
325 GP Oteranga Bay 'B2' zone											
6 months' exposure			**18 months' exposure**			**48 months' exposure**			**60 months' exposure**		
Depth	**Chloride** (% concrete)		**Depth**	**Chloride** (% concrete)		**Depth**	**Chloride** (% concrete)		**Depth**	**Chloride** (% concrete)	
(mm)	replicate 1	replicate 2	(mm)	replicate 1	replicate 2	(mm)	replicate 1	replicate 2	(mm)	replicate 1	replicate 2	replicate 3
1.0	0.037		1.0	0.088	0.073	4.0	0.033		2.5	0.124	0.118	0.123
3.0	0.030		3.0	0.073	0.055	9.0	0.021		7.5	0.074	0.081	0.071
5.0	0.023	Not	5.0	0.038	0.046	14.0	0.020	Not	12.5	0.062	0.068	0.061
7.5	0.021	Determined	7.0	0.029	0.036	19.0	0.014	Determined	17.5	0.043	0.039	0.045
10.5	0.018		9.0	0.027	0.030	24.0	0.011		22.5	0.027	0.032	0.027
13.5	0.019		11.0	0.021	0.024	29.0	0.010		27.5	0.023	0.017	0.020
						34.0	0.006		32.5	0.014	0.013	0.016

Table 35: Chloride profiles developed on Duracem concrete at the Oteranga Bay exposure site

280 DC Oteranga Bay 'B2' zone											
6 months' exposure			**18 months' exposure**			**48 months' exposure**			**60 months' exposure**		
Depth	**Chloride** (% concrete)		**Depth**	**Chloride** (% concrete)		**Depth**	**Chloride** (% concrete)		**Depth**	**Chloride** (% concrete)	
(mm)	replicate 1	replicate 2	(mm)	replicate 1	replicate 2	(mm)	replicate 1	replicate 2	(mm)	replicate 1	replicate 2	replicate 3
			1.0	0.045	0.051	4.0	0.111		2.5	0.126	0.129	
			3.0	0.069	0.070	9.0	0.115		7.5	0.109	0.127	
			5.0	0.072	0.066	14.0	0.057	Not	12.5	0.075	0.117	Not
No Measurements Made			7.0	0.058	0.055	19.0	0.019	Determined	17.5	0.031	0.044	Determined
			9.0	0.038	0.032	24.0	0.016		22.5	0.022	0.020	
			11.0	0.029	0.023	29.0	0.014		27.5	0.018	0.016	
						34.0	0.016		32.5	0.020	0.019	

325 DC Oteranga Bay 'B2' zone											
6 months' exposure			**18 months' exposure**			**48 months' exposure**			**60 months' exposure**		
Depth	**Chloride** (% concrete)		**Depth**	**Chloride** (% concrete)		**Depth**	**Chloride** (% concrete)		**Depth**	**Chloride** (% concrete)	
(mm)	replicate 1	replicate 2	(mm)	replicate 1	replicate 2	(mm)	replicate 1	replicate 2	(mm)	replicate 1	replicate 2	replicate 3
1.0	0.037		1.0	0.104	0.097	4.0	0.087		2.5	0.087	0.088	0.085
3.0	0.030		3.0	0.078	0.064	9.0	0.034		7.5	0.043	0.049	0.040
5.0	0.022	Not	5.0	0.041	0.034	14.0	0.011	Not	12.5	0.016	0.014	0.012
7.5	0.021	Determined	7.0	0.018	0.018	19.0	0.007	Determined	17.5	0.011	0.008	0.008
10.5	0.022		9.0	0.011	0.010	24.0	0.009		22.5	0.014	0.010	0.008
13.5	0.025		11.0	0.012	0.007	29.0	0.007		27.5	0.010	0.010	0.007
						34.0	0.010		32.5	0.010	0.009	0.008

Table 36: Chloride profiles developed on Micropoz concrete at the Oteranga Bay exposure site

280 MP Oteranga Bay 'B2' zone									
18 months' exposure			**48 months' exposure**			**60 months' exposure**			
Depth	**Chloride** (% concrete)		**Depth**	**Chloride** (% concrete)		**Depth**	**Chloride** (% concrete)		
(mm)	replicate 1	replicate 2	(mm)	replicate 1	replicate 2	(mm)	replicate 1	replicate 2	replicate 3
1.0	0.135	0.135	4.0	0.055		2.5	0.090	0.088	0.100
3.0	0.111	0.111	9.0	0.051		7.5	0.061	0.074	0.103
5.0	0.098	0.098	14.0	0.034	Not	12.5	0.061	0.064	0.079
7.0	0.072	0.072	19.0	0.026	Determined	17.5	0.047	0.048	0.060
9.0	0.064	0.064	24.0	0.016		22.5	0.030	0.032	0.036
11.0	0.043	0.043	29.0	0.011		27.5	0.021	0.017	0.020
			34.0	0.011		32.5	0.018	0.011	0.016
325 MP Oteranga Bay 'B2' zone									
18 months' exposure			**48 months' exposure**			**60 months' exposure**			
Depth	**Chloride** (% concrete)		**Depth**	**Chloride** (% concrete)		**Depth**	**Chloride** (% concrete)		
(mm)	replicate 1	replicate 2	(mm)	replicate 1	replicate 2	(mm)	replicate 1	replicate 2	replicate 3
1.0	0.138	0.117	4.0	0.094		2.5	0.093	0.117	0.135
3.0	0.110	0.083	9.0	0.056		7.5	0.057	0.074	0.069
5.0	0.077	0.061	14.0	0.034	Not	12.5	0.034	0.047	0.051
7.0	0.060	0.036	19.0	0.014	Determined	17.5	0.023	0.031	0.027
9.0	0.042	0.031	24.0	0.007		22.5	0.013	0.017	0.016
11.0	0.025	0.025	29.0	0.010		27.5	0.010	0.011	0.010
			34.0	0.008		32.5	0.008	0.007	0.007

Table 37: Chloride profiles developed on Microsilica concrete at the Oteranga Bay exposure site

280 MS Oteranga Bay 'B2' zone								
18 months' exposure			**48 months' exposure**			**60 months' exposure**		
Depth	**Chloride** (% concrete)		**Depth**	**Chloride** (% concrete)		**Depth**	**Chloride** (% concrete)	
(mm)	replicate 1	replicate 2	(mm)	replicate 1	replicate 2	(mm)	replicate 1	replicate 2	replicate 3
1.0	0.073	0.070	4.0	0.051		2.5	0.097	0.095	0.096
3.0	0.058	0.074	9.0	0.052		7.5	0.073	0.075	0.090
5.0	0.054	0.053	14.0	0.037	Not	12.5	0.066	0.067	0.066
7.0	0.045	0.042	19.0	0.025	Determined	17.5	0.045	0.049	0.052
9.0	0.040	0.031	24.0	0.016		22.5	0.026	0.029	0.030
11.0	0.025	0.025	29.0	0.015		27.5	0.019	0.019	0.024
			34.0	0.008		32.5	0.014	0.014	0.013
325 MS Oteranga Bay 'B2' zone								
18 months' exposure			**48 months' exposure**			**60 months' exposure**		
Depth	**Chloride** (% concrete)		**Depth**	**Chloride** (% concrete)		**Depth**	**Chloride** (% concrete)	
(mm)	replicate 1	replicate 2	(mm)	replicate 1	replicate 2	(mm)	replicate 1	replicate 2	replicate 3
1.0	0.138	0.137	4.0	0.062		2.5	0.108	0.100	0.114
3.0	0.092	0.099	9.0	0.048		7.5	0.080	0.083	0.082
5.0	0.062	0.069	14.0	0.029	Not	12.5	0.053	0.057	0.055
7.0	0.039	0.053	19.0	0.017	Determined	17.5	0.026	0.026	0.026
9.0	0.039	0.038	24.0	0.012		22.5	0.016	0.015	0.012
11.0	0.022	0.029	29.0	0.011		27.5	0.013	0.009	0.010
			34.0	0.009		32.5	0.010	0.005	0.006

Table 38: Chloride profiles developed on GP concrete at the Judgeford exposure site

250 GP Judgeford 'B1' zone					
18 months' exposure			**60 months' exposure**		
Depth (mm)	**Chloride** (% concrete) replicate 1	replicate 2	**Depth** (mm)	**Chloride** (% concrete) replicate 1	replicate 2
1.0	0.022	0.016	1.0	0.019	
3.0	0.010	0.020	3.0	0.020	
5.0	0.017	0.020	5.0	0.016	Not
7.0	0.012	0.015	7.0	0.016	Determined
9.0	0.020	0.018	9.0	0.015	
			11.0	0.013	
325 GP Judgeford 'B1' zone					
18 months' exposure			**60 months' exposure**		
Depth (mm)	**Chloride** (% concrete) replicate 1	replicate 2	**Depth** (mm)	**Chloride** (% concrete) replicate 1	replicate 2
1.0	0.011	0.018	1.0	0.022	
3.0	0.008	0.011	3.0	0.019	
5.0	0.004	0.005	5.0	0.016	Not
7.0	0.004	0.007	7.0	0.012	Determined
9.0	0.006	0.008	9.0	0.012	
11.0	0.007	0.015	11.0	0.010	

6. REFERENCES

[1] Verbeck, G.J. (1975). 'Mechanisms of corrosion in concrete'. In *Corrosion of Metals in Concrete*. ACI SP-49. American Concrete Institute, Detroit, United States, pp 21 – 38.

[2] Tuutti, K. (1982). *Corrosion of Steel in Concrete*. Report No. 4. Swedish Cement and Concrete Research Institute, Stockholm, Sweden.

[3] *The NZ Building Code and Approved Documents*. (1992). Building Industry Authority, Wellington, New Zealand.

[4] NZS 3101:1995 *Concrete structures*. *Part 1 – The design of concrete structures*. Standards New Zealand, Wellington.

[5] Chisholm, D.H. (1997). *Factors Influencing Reinforced Concrete Durability Design in New Zealand's Marine Environment.* Proceedings of the Fourth Canmet /ACI International Durability Conference. ACI SP 170, pp 797 – 822.

[6] Crank, J. (1976). *The Mathematics of Diffusion*. Oxford University Press, Oxford, England.

[7] RILEM TC 178-TMC. (2002). 'RILEM Recommendation of Analysis of Total Chloride in Concrete'. *Materials and Structures* 35: 583 – 585.

[8] Andrade, C., Diez, J.M. and Alonso, C. (1997). 'Mathematical Modelling of a Concrete Surface Skin Effect on Diffusion in Chloride Contaminated Media'. *Advanced Cement Based Materials* 6.

[9] NT BUILD 443. (1995). *Concrete, Hardened: Accelerated Chloride Penetration*. NordTest, Espoo, Finland.

[10] ASTM C1556 – 03. (2003). *Standard Test Method for Determining the Apparent Chloride Diffusion Coefficient of Cementitious Mixtures by Bulk Diffusion*. American Society for Testing and Materials, Philadelphia, United States.

[11] Kropp, J. (1995). 'Chlorides in Concrete'. In *Performance Criteria for Concrete Durability*. RILEM Report No 12, Kropp, J. and Hilsdorf, H.K. (ed). E & FN Spon, London, United Kingdom.

[12] Kropp, J. (1995). 'Chlorides in Concrete'. In *Performance in Concrete*. Kropp, J. and Hilsdorf H. K. (eds). E & FN Spon, London.

[13] Boddy, A., Bentz, E., Thomas, M.D.A. and Hooton, R.D. (1999). 'An Overview and Sensitivity Study of a Multi-mechanistic Chloride Transport Model'. *Cement and Concrete Research* 29: 827 – 837.

[14] Glass, G.K. and Beunfeld, N.R. (2000). 'The Influence of Chloride Binding on the Chloride Induced Corrosion Risk in Reinforced Concrete'. *Corrosion Science* 42: 329 – 344.

[15] Glass, G.K., Reddy, B. and Buenfeld, N.R. (2000). 'The Participation of Bound Chloride in Passive Film Breakdown on Steel in Concrete'. *Corrosion Science* 42: 2013 – 2021.

[16] Schieβl, P. (ed). (1988). *Corrosion of Steel in Concrete.* Report of RILEM Technical Committee 60 – CSC. Chapman & Hall, London.

[17] Collepardi, M., Marcialis, A. and Turriziani R. (1972). 'Penetration of Chloride-ions into Cement Pastes and Concrete'. *Journal of the American Ceramic Society* 55.

[18] Takewaka, K. and Mastumoto, S. (1988). *Quality and Cover Thickness of Concrete Based on the Estimation of Chloride Penetration in a Marine Environment*. ACI SP 109. American Concrete Institute, Detroit, United States.

[19] Maage, M., Helland, S. and Carlsen J.E. (1999). *Chloride Penetration into Concrete with Lightweight Aggregates.* Brite EuRam Report BE96-3942/R3. www.sintef.no, accessed 5 August 2003.

[20] Mangat, P.S. and Molloy, B.T. (1994). 'Prediction of Long-term Chloride Concentration in Concrete'. *Materials and Structures* 27: 338 – 346.

[21] Bamforth, P.B. (1999). 'The Derivation of Input Data for Modelling Chloride Ingress from Eight-year UK Coastal Exposure Trials'. *Magazine of Concrete Research* 51(2): 87 – 96.

[22] NZS 3112:1986. *Methods of test for concrete. Part 2 – Determination of the strength of concrete*. Standards New Zealand, Wellington.

[23] AS 1012.13. (1992). *Methods of testing concrete. Part 13 – Determination of drying shrinkage of concrete*. Standards Australia, Sydney.

[24] Hall, C. (1989). 'Water Sorptivity of Mortars and Concretes: A Review'. *Magazine of Concrete Research* (June 1989) 147: 51 – 61.

[25] ASTM C1202. (1997). *Standard method for electrical indication of concrete's ability to resist chloride-ion penetration.* American Society for Testing and Materials, Philadelphia, United States.

[26] Bamforth, P.B. (1990). *Minimising the Risk of Chloride Induced Corrosion by Selection of Concreting Materials.* 3rd International Symposium on Corrosion of Reinforcement in Concrete Construction, Wishaw, United Kingdom, May 1990.

[27] Geiker, M., Thaulow, N. and Andersen, P.J. (1990). 'Assessment of Rapid Chloride-ion Permeability Test of Concrete With and Without Mineral Admixtures'. In *Durability of Building Materials*. J.M. Baker, P.J. Nixon, A.J. Majumdar and H. Davis (eds). E & FN Spon, London, pp 493 – 502.

[28] Trinh Cao, H. and Meck, E.A. (1996). 'Review of the ASTM C 1202 Standard Test and its Applicability in the Assessment of Concrete's Resistance to Chloride-ion Penetration'. *Concrete in Australia* (October 1996) 23 – 26.

[29] NT BUILD 492. (1999). *Concrete, Mortar and Cement-based Repair Materials: Chloride Migration Coefficients From Non-steady-state Migration Experiments*. NordTest, Espoo, Finland.

[30] Bamforth, P.B. (2002). 'Concrete Durability by Design: Limitations of the Current Prescriptive Approach and Alternative Methods for Durability Design'. *Concrete 2002: Enduring Concrete*. New Zealand Concrete Society Technical Report TR27, Auckland.

[31] Carlsen, J.E. (2000). 'Chloride Penetration into Concrete with Lightweight Aggregates'. In *Testing and Modelling the Chloride Ingress into Concrete.* Proceedings of the 2nd International RILEM Workshop. C. Andrade and J. Kropp (eds). RILEM, Paris, pp 429 – 440.

[32] Andrade, C., Diez, J.M. and Alonso, C. (1997). 'Mathematical Modelling of Concrete's Surface "Skin Effect" on Diffusion in Chloride Contaminated Media'. *Advances in Cement-Based Materials* 6: 39 – 44.

[33] Higgins, D.D. (1995). 'The Effect of some Test Variables on Chloride Profiles'. In *Chloride Penetration into Concrete*. Proceedings of the International RILEM Workshop, L.O. Nilsson and J.P. Ollivier (eds). RILEM, Paris, pp 234 – 242.

[34] Bentz, D.P., Feng, X. and Hooton, R.D. (2000). 'Time-dependent Diffusivities: Possible Misinterpretation Due to Spatial Dependence'. In *Testing and Modelling the Chloride Ingress into Concrete*. Proceedings of the 2nd International RILEM Workshop. C. Andrade and J. Kropp (eds). RILEM, Paris, pp 225 – 233.

[35] Nilsson, L.O. (2000). 'A Numerical Model for Combined Diffusion and Convection of Chloride in Non-saturated Concrete'. In *Testing and Modelling the Chloride Ingress into Concrete*. Proceedings of the 2nd International RILEM Workshop. C. Andrade and J. Kropp (ed). RILEM, Paris, pp 261 – 275.

[36] Cochet, G. and Jésus, B. (1991). *Diffusion of Chloride-ions in Portland Cement-filler Mortars*. International Conference on Blended Cements in Construction, Sheffield 1991. Elsevier Science, Oxford, United Kingdom, pp 365 – 76.

[37] Thomas, M.D.A. and Bamforth, P.B. (1999). 'Modelling Chloride Diffusion in Concrete: Effect of Fly-ash and Slag'. *Cement and Concrete Research* 29: 487 – 495.

[38] BRANZ Appraisal Certificate 417. (2003). *Holcim Coastal Concrete Durability Design Method*. BRANZ Ltd, Wellington, New Zealand.

[39] Concrete Institute of Australia. (2001). *Performance Criteria for Concrete Marine Environments: Recommended Practice z13.* Sydney, Australia.

[40] NZS 3104:2003 *Specification for concrete production*. Standards New Zealand, Wellington.

[41] Hall, C. (1977). 'Water Movement in Porous Building Materials – I. Unsaturated Fluid Flow and Its Applications'. *Building Environment* 12: 117 – 125.

[42] Martys, N.S. (1995). *Survey of Transport Properties and Their Measurements*. NISTIR 5592, US Department of Commerce.

[43] ASTM Sub-committee C09.66. (2001). *ASTM Draft Test Method for Measurement of Rate of Absorption of Water by Hydraulic-cement Mortars or Concretes*. American Society for Testing and Materials, Philadelphia, United States.

[44] Martys, N. and Ferraris, C. (1997). 'Capillary Transport in Mortars and Concrete'. *Cement and Concrete Research* 27(5): 747 – 760.

[45] Ho, D.W.S. and Lewis, R.K. (1987). 'The Water Sorptivity of Concretes: The Influence of Constituents Under Continuous Curing'. *Durability of Building Materials* 4: 241 – 252.

[46] AS 1012.21. (1999). *Determination of Water Absorption and Apparent Volume of Permeable Voids in Hardened Concrete.* Standards Australia, Sydney, Australia.

[47] Quénard, D. and Sallée, J. (1988). *The Transport of Condensable Water Vapour Through Microporous Building Materials*. IDS '88 International Drying Symposium, Versailles, September 1988.

[48] Alexander, M.A. and Ballim, Y. (1993). *Experiences with Durability Testing of Concrete: A Suggested Framework Incorporating Index Parameters and Results from Accelerated Concrete Durability Tests*. Proceedings of the Third Canadian Symposium on Cement and Concrete, pp 248-263.

[49] Bentz, D.P., Garboczi, E.J. and Lagergren, E.S. (1998). 'Multi-scale Micro-structural Modelling of Concrete Diffusivity: Identification of Significant Variables'. *Cement, Concrete and Aggregates* 20(1): 129 – 138.

[50] ASTM C1585 – 04. (2004). *Standard Method for Measurement of Rate of Absorption of Water by Hydraulic-cement Concretes.* American Society for Testing and Materials, Philadelphia, United States.

[51] DeSouza, S.J., Hooton, R.D. and Bickley, J.A. (1997). 'Evaluation of Laboratory Drying Procedures Relevant to Filed Conditions for Concrete Sorptivity Measurements'. *Cement, Concrete and Aggregates* 19(2): 59 – 63.

[52] Bentz, D.P., Ehlen, M.A., Ferraris, C. and Garboczi, E.J. (2001). *Sorptivity-based Service Life Predictions for Concrete Pavements.* 7th International Conference on Concrete Pavements, Orlando, Florida, pp 181 – 193.

[53] Recommendations of TC 116-PCD. (1999). 'Preconditioning of Concrete Test Specimens for the Measurement of Gas Permeability and Capillary Absorption of Water'. *Materials and Structures* 32: 174 – 176.

[54] NZS 3101:1995 *Concrete structures standard. Part 2: Commentary*. Standards New Zealand, Wellington.

[55] Hooton, R.D., Thomas, M.D.A. and Stanish, K. (2001). *FHWA-RD-00-142: Prediction of Chloride Penetration in Concrete.* U.S. Department of Transportation – Federal Highway Authority. McLean, Virginia, USA.

[56] Tang, L. and Nilsson, L.O. (1991). 'Rapid Determination of the Chloride Diffusivity in Concrete by Applying an Electrical Field'. *ACI Materials Journal* 89(1): 49 – 53.

[57] Castellote, Marta. (2005). pers. comm. Institute of Construction Science, 'Eduardo Torroja', CSIC, Madrid, Spain.